Ecole Centrale Marseille

THESE

en vue d'obtenir le grade de **Docteur**
de l'Ecole Centrale Marseille

Discipline : Mathématiques

Sur un couplage Krigeage/Schémas de subdivision pour la modélisation de données localement non régulières.

soutenue publiquement le **9 Octobre** par

Xiaoyun SI

Ecole Doctorale : Mathematiques et informatique, ED 184

Membres du jury:

Rapporteurs :	B. IOOSS, Ingénieur-recherche, EDF, MRI
	S. MEIGNEN, MCF, Université de Grenoble, LJK
Examinateurs :	F. ARANDIGA, Prof., Univ. de Valencia (Espagne)
	F. GAMBOA, Prof., Univ. de Toulouse, IMT
Directeur de thèse:	J. LIANDRAT, Prof., Centrale Marseille, LATP
Co-encadrant:	J. BACCOU, Ingénieur-recherche, IRSN, Cadarache

---

Laboratoire d'Analyse, Topologie, Probabilités, UMR-7353, Marseille, France

Acknowledgements

As what you all know, I have spent three years of research time in the south of this beautiful country–France. My major is applied mathematics.

To begin with my work, I'd like to, first of all, give my deepest thankfulness to my dear supervisor, Mr Jacques LIANDRAT. Thank him for leading me to this wonderful mathematical worlds patiently and considerately. He is so professional, intelligent and humorous that makes me like mathematics very much. Secondly I should say many many thanks to our co-worker, Mr Jean BACCOU. Thanks for giving me lots of ideas, advices and deducing helps. I should be honest to declare that without their academic direction, I can not finish my subject so well. Furthermore, they not only help me with ph.d studies, but also impress me as the nicest, the most educated and the most modest persons I have seen. It's a great pleasure to work with them.

I want to thank Prof F.ARANDIGA, Prof F.GAMBOA, Doctor S.MEIGNEN and Doctor B.IOOSS for their interests in this thesis, the reading of my manuscript, their advices and having made a long journey to Marseille.

Thanks to all the Chinese students studying for their Ph.D degree in Ecole Centrale de Marseille. They are ZHANG Ting, XIAO Zhiyong, SONG Ningning, RUAN Yi, LIU Yan, ZHANG Yuan, GAO Di, ZHU Mingxuan, LIN Tao, YANG Guowei, LIU Zubin, SHU Da..... We spent together these three years here, we shared all the funny, sad, and encouraging things. Thanks to CSC, who gives my scholarship during three years. Many thanks to all the Ph.Ds, post-doctorates and Profs in LATP: Clothilde, Bruno, Benjamin, Leyuan, Weiwei DING, Vi, Zen, Hichen, Whael, Claire, Valentin... the seminars are always wonderful. Thanks to all the persons we go to lunch together: Thomas A, Thomas Z, Bien, Nguen... Thanks to all the kindhearted secretaries: Dominique, Nathalie, Marie, Valerie, Augustino, Julien....

Last but the biggest thanks for my dear family, Mom, dad, my sisters, my brother, my sister-in-law, my brothers-in-law, my nieces, my nephews. And immense kisses for my

husband WANG Xiao, you are my spirit!

Salut, la France! Tu me manques!

Contents

Notations

S	Subdivision scheme
j	scale or level
S^j	j iterations of a subdivision scheme S
$S_1 : (df_k^j)_{k\in\mathbb{Z}} \mapsto (df_k^{j+1})_{k\in\mathbb{Z}}$	subdivision for the differences
$S_m : (d^m f_k^j)_{k\in\mathbb{Z}} \mapsto (d^m f_k^{j+1})_{k\in\mathbb{Z}}$	subdivision for the m-th derivative
$S_{l,r}$	Subdivision with a stencil of l left points and r right points
$X^j = (x_k^j)_{k\in\mathbb{Z}}$	grid points at scale j: $x_k^j = k2^{-j}$
$(f_n^0)_{n\in\mathbb{Z}}$	initial sequence
$(f_n^j)_{n\in\mathbb{Z}}$	sequence at level j
$(df^j)_k = f_{k+1}^j - f_k^j$	difference between two neighboring points
f^0	the initial set of points
f^j	the set of points at level j
$(a_m^{j,k})_{m\in\mathbb{Z}}$	subdivision mask at position $k2^{-j}$
$a(z) = \sum a_k z^k$	Laurent polynomial associated to a stationary uniform scheme S
$a_1(z) = \sum a_k^{(1)} z^k$	Laurent polynomial associated to S_1
$(l_{j,2k+1}, r_{j,2k+1})$	reconstruction stencil parameters at position $(2k+1)2^{-j}$
$L_m^{l,r}(x) = \Pi_{n=-l,n\neq m}^{r-1} \frac{x-n}{m-n}$	Lagrange polynomial associated to the stencil (l, r)
$(y_i)_{i\in I}$	segmentation points

$A_{0,j}, A_{1,j}$	refinement matrices associated to S
$A^{(1)}_{0,j}, A^{(1)}_{1,j}$	refinement matrices associated to S_1
$A^{+}_{2,0}, A^{+}_{2,1}, A^{-}_{2,0}, A^{-}_{2,1}$	edge matrices associated to a 4-point stencil S
$A^{(1),+}_{2,0}, A^{(1),+}_{2,1}, A^{(1),-}_{2,0}, A^{(1),-}_{2,1}$	edge matrices associated to a 4-point stencil S_1
ϕ_m	B_m-spline function of order m
μ	Lagrange multiplier
$\mathcal{C}$	error variance or penalization vector
$P(x)$	polynomial function
$\mathcal{F}(x)$	random process
$\mathcal{F}(x_i)$	random variables
$\gamma(h)$	semi-variogram
$\mathcal{G}^*_{OD}, \mathcal{G}^*_{ED}$	Sets of semi-variograms with different behaviors at the origin
$\mathcal{X}_\omega$	characteristic function of ω: $\begin{cases} \mathcal{X}x = 1 \text{ if } x \in \omega \\ \mathcal{X}x = 0 \text{ if } x \notin \omega \end{cases}$

Abstract

This work is devoted to the definition, analysis and test of new subdivision algorithm adapted to signal exhibiting inhomogeneous properties such as noise or discontinuities. The global framework is based on position/zone dependent subdivision schemes on one hand and stochastic prediction schemes of Kriging type on the other hand.

After a review on non homogeneous/non stationary subdivision schemes with the emphasis on the advantages of zone dependent implementations and a description of Kriging type subdivision scheme, the second part of the thesis is devoted to the integration of Kriging approach into the subdivision framework; interpolatory and non interpolatory schemes are derived. A family of 4 points stencil schemes is analyzed. A zone dependent strategy is applied that leads to a family of new schemes combining the advantages of Kriging (evaluation of error variance, local flexibility) and of non homogeneous subdivision schemes (adaption to a zone segmentation of a signal). Applications and tests on univariate and bivariate data are provided.

The third part of this work deals with the definition and analysis of new subdivision schemes called penalized Lagrange. Their construction is based on an original reformulation for the construction of the coefficients of the mask associated with the classical 4-point Lagrange interpolatory subdivision scheme: these coefficients can be formally interpreted as the solution of a linear system similar to the one resulting from the constrained minimization problem in Kriging theory. Following this idea, we propose to penalize the 4-point Lagrange system in order to transform the interpolatory schemes into approximating ones with specific properties suitable for locally noisy or strongly oscillating data. Various applications are provided.

Open questions, among others, concern the generalization of the second and third parts to stencils of any length.

Chapter 1

Résumé de la thèse en français

Introduction générale

L'objectif de la thèse est la définition et l'analyse de nouveaux schémas de subdivision adaptés à des données localement discontinues (forts gradients) ou localement bruitées. On s'intéresse à des schémas linéaires dyadiques en dimension 1: ils sont dérivés à partir du couplage de techniques de subdivision avec l'approche par Krigeage utilisée en géostatistiques. Après une revue des techniques de subdivision classiques et de différentes implémentations ainsi qu'une présentation du Krigeage et de ses différentes variantes, la thèse propose trois avancées: l'implémentation de schémas dite zone-dépendante, la famille de schémas de subdivision de type Krigeage avec variance d'erreur et une nouvelle famille de schémas dits schémas de Lagrange pénalisés. Certains d'entre eux sont complétement analysés et implémentés.

Le corps de la thèse est organisé en 3 chapitres: Le chapitre 2 effectue des rappels sur les schémas de subdivision, les outils d'analyse et leur implémentation. Une attention particulière est portée au phénomène de Gibbs qui apparaît naturellement pour les schémas interpolants sur des données présentant de forts gradients. Le chapitre 3 présente le Krigeage et ses variantes avec ou sans variance d'erreur ainsi que les schémas de subdivision associés. Les résultats sur la convergence des schémas de type Krigeage sans variance d'erreur sont rappelés. Le chapitre 4 introduit une nouvelle famille de schémas de type Krigeage avec variance d'erreur: ces schémas sont non interpolants et ne produisent pas d'oscillation du type phénomène de Gibbs en présence de forts gradients. Une analyse complète de schémas à 4 points est réalisée. Une implémentation de type zone dépendante

est définie, analysée et testée. Le dernier chapitre est dédié à un nouveau schéma dit de Lagrange pénalisé. Un coefficient local de pénalisation est introduit dans une nouvelle formulation de définition des coefficients des schémas de subdivision de Lagrange. Ce coefficient permet, quand il n est pas nul, de transformer le schéma classique de Lagrange en un schéma non interpolant. La famille des schémas obtenus pour des stencils à 4 points est complétement analysée. La conclusion ouvre de nombreuses perspectives vers des généralisations ou des applications

1.1 Schémas de subdivision (Chapitre 2)

Après une introduction sur les notions de schémas de subdivision et de décimation (avec en particulier un rappel sur les notions de schémas uniforme ou stationnaire) et un rappel de la notion de convergence de schémas de subdivision, différents outils d'analyse sont rappelés. La notion de polynômes de Laurent associés à un schéma de subdivision uniforme est rappelée ainsi que l'analyse de la convergence qu'elle permet. L'approche matricielle est ensuite décrite; cette approche se généralise à des schémas non uniformes. Pour l'analyse de schémas non stationnaires, un théorème permettant d'analyser un schéma non stationnaire dont les coefficients convergent vers ceux d'un schéma stationnaire est rappelé. Après un rapide retour sur le phénomène de Gibbs pour les schémas de subdivision, 2 schémas de base (Lagrange et B-spline) et différentes implémentations sont présentés en insistant sur les problèmes d'oscillations des fonctions limites générant le phénomène de Gibbs. La notion d'implémentation "zone-dépendante" est en particulier introduite et analysée pour le cas Lagrange/B-spline.

1.2 Krigeage et schémas de subdivision associés (Chapitre 3)

Ce chapitre présente une famille de schémas de subdivision non stationnaires résultant du couplage de l'approche subdivision avec la prédiction par Krigeage. Une première section est dédiée à la description de la théorie du Krigeage et sa formulation en terme d'optimisation. Plusieurs familles de semi-variogramme permettant de modéliser la structure spatiale associée aux données sont présentées. La section 3.2.3 introduit la notion de Krigeage avec variance d'erreur qui sert de base au chapitre 4 et inspire le chapitre 5.

Quelques résultats numériques sont présentés.

1.3 Schémas de subdivision à base de Krigeage avec variance d'erreur (Chapitre 4)

Ce chapitre présente une nouvelle famille de schémas de subdivision basés sur la prédiction par Krigeage avec variance d'erreur. Cette prédiction n' est pas interpolante et est contrôlée localement par un vecteur de variance d'erreur. Grâce à l'étude du comportement asymptotique des coefficients de ces schémas, une analyse de convergence des schémas est proposée. Elle dépend de la taille des stencils, des semis variogrammes et des vecteurs de variances d'erreur. Une analyse théorique complète est réalisée pour des stencils à 4 points, différents types de semi variogrammes et différents vecteurs de variance d'erreur. Elle permet de conclure sur la convergence d'implémentations "zone dépendante" de cette famille de schémas de subdivision. Des applications en dimension 1 sur des courbes localement bruitées et discontinues ainsi qu'un premier exemple en deux dimensions pour l'approximation de la réponse d'un code de calcul en présence d'incertitudes (pour lesquelles les schémas sont généralisés par produit tensoriel) sont fournies

1.4 Schémas de Lagrange pénalisés (Chapitre 5)

Ce chapitre reproduit dans sa majorité un article soumis au journal Computer Aided Geometric Design.

Le point de départ de cette construction originale est l'analyse menée au chapitre précèdent qui d'une part fait apparaître le schéma de subdivision interpolant de Lagrange comme limite des schémas de Krigeage pour une certaine classe de semi-variogramme et d'autre part permet d'interpréter le vecteur de variance d'erreur comme un vecteur de pénalisation des oscillations des coefficients de subdivision par Krigeage.

Une reformulation du calcul des coefficients du schéma de subdivision interpolant de Lagrange à 4 points utilisant un vecteur de pénalisation est proposée. On construit alors un schéma de subdivision non stationnaire qui, pour un vecteur de pénalisation nul converge vers le schéma de Lagrange quand le paramètre d'échelle tend vers l'infini. Une étude complète est réalisée pour plusieurs configurations du vecteur de pénalisation. Ce chapitre se termine par la définition de schémas du type "zone dépendant" où le vecteur

de pénalisation varie en fonction des zones traversées.

Conclusions et perspectives

Après un résumé des principaux résultats de la thèse (implémentation zone dépendante, schémas de subdivision de type Krigeage avec variance d'erreur, schémas de Lagrange pénalisés) plusieurs perspectives sont mentionnées, entre autres: la généralisation des résultats théoriques sur le Krigeage avec variance d'erreur et le schéma de Lagrange pénalisé à des stencils de taille quelconque, l'utilisation des schémas de type Krigeage dans le cadre de décompositions multirésolution, le couplage segmentation/subdivision, la construction de schémas non linéaires ainsi que plusieurs applications à la compression d'images et à l'approximation de codes de calculs en présence d'incertitudes.

General introduction

This work is devoted to the coupling of some computer graphics tools with Geo-statistical ones in the framework of data reconstruction from a set of discrete values in presence of segmentation points, local noise or discontinuities.

Reconstruction of signals or surfaces is a very active scientific domain with many connections in functional analysis, signal processing, numerical analysis, modeling, animation, risk analysis,... Geo-statistics are classical approaches used by the environmental community for the analysis of spatial data: the reconstruction is based on a stochastic modelling that allows one to get besides the predicted values, the associated precision from a statistical point of view.

For the majority of the tools used in these fields, it is assumed that the phenomenon underlying the data is regular; this is not the case in practice, as in risk analysis for instance: local noise can appear, discontinuities or zone segmentations can blow up naturally.

In this thesis, we will discuss subdivision schemes (one of the basic tools of computer graphics) and Kriging (a stochastic tool coming from Geo-statistics). A first attempt to couple these two techniques has been performed in [1]. Here, our goal is to go a step further, exploiting the advantages and degrees of freedom of the two approaches in the framework of non-regular data.

Position-dependent subdivision schemes, local error variance for Kriging, segmentation of data and multi-resolution will therefore be revisited. A first output of our work is a family of new Kriging-based subdivision schemes integrating local error variance allowing one to combine interpolatory and non-interpolatory predictions. Some of them are analyzed and tested. The flexibility of the Kriging theory is then extended to the deterministic framework of Lagrange subdivision leading to locally non-interpolatory and non-oscillating schemes called penalized Lagrange schemes. Some of them are also analyzed and tested.

The organization of the manuscript is as follows: first linear subdivision schemes are reviewed with emphasis on different possible implementations, mainly uniform, position dependent or zone dependent. The properties of different classical schemes with different implementations are analyzed focussing on the reconstruction of locally discontinuous data, i.e on the Gibbs phenomenon.

In Chapter 3, an overview on Kriging theory is provided with an emphasis to non-interpolatory predictions resulting from the introduction of error variance. Then, the original work performed in [1] on interpolatory Kriging-based subdivision schemes is recalled.

Chapter 4 is devoted to the construction and analysis of a new class of Kriging-based subdivision schemes integrating error variance. As for interpolatory Kriging-based schemes, the notion of asymptotically equivalent schemes is the key notion that allows one to prove the convergence of this new tool.

In Chapter 5, we focus on a new approach of Lagrange subdivision schemes. Mimicking the introduction of error variance in Kriging prediction and exploiting the proof of convergence derived in the previous chapter, the so-called penalized Lagrange scheme is introduced: this scheme uses penalization parameters that allow one to locally transform the classical Lagrange interpolatory scheme in an approximating (non-interpolatory) one. This scheme reveals to be particularly suitable to zone segmented data or locally discontinuous data.

The last chapter is devoted to conclusions and to the description of various future works linked to the generalization and the derivation of non linear schemes as well as their applications on real problems.

Chapter 2

Subdivision schemes

2.1 Introduction

Subdivision schemes have been introduced ([2]) historically in the framework of curve and surface storage. Nowadays as all the class of multi-resolution analysis algorithms they are working horses in many fields of applied mathematics including computer aided geometric design, signal compression, approximation and modeling, animation, data reconstruction, numerical solutions of partial differential equations... In all these fields the question of the convergence as well as the question of stability of the subdivision scheme is a basic key point. The behavior of the scheme on initial data sets presenting strong variations is also an important aspect since, generally, smooth interpolating schemes lead to oscillating limit functions that are not desirable.

In this thesis, we focus on binary subdivision on the real line and therefore consider dilation factor 2, scales $2^{-j}, j \in \mathbb{Z}$ and grid points $x_k^j = k2^{-j}, j \in \mathbb{Z}, k \in \mathbb{Z}$.

Linear subdivision schemes are defined as:

$$S : \begin{cases} l^\infty(\mathbb{Z}) \to l^\infty(\mathbb{Z}) \\ (f_k^j)_{k\in\mathbb{Z}} \mapsto S(f_k^j)_{k\in\mathbb{Z}} \end{cases}$$

with

$$Sf_k^j = \sum_{l\in\mathbb{Z}} a_{k-2l}^{j,k} f_l^j \tag{2.1}$$

where $((a_l^{j,k})_{l\in\mathbb{Z}})_{(k,j)\in Z}$are the masks of the subdivision scheme. The coefficients of the masks are zero but a finite number of them whose indices define the associated stencil and

stencil length. If the scale parameter j is associated with the sequence $f^j = (f_k^j)_{k\in\mathbb{Z}}$, the scale parameter corresponding to Sf^j is $j+1$. Note that the coefficients of the masks may depend on the scale parameter j as well as on the position parameter k. The notation S^p refers to p applications of S, keeping in mind that the coefficients of S may change at each application following the increment of the scale parameter.

Schemes are said to be uniform if the masks do not depend on k and stationary if the mask does not depend on j. All the schemes considered here are linear since they are linear operators; non linear (also called semi non linear) schemes relate to schemes where the mask depend on the sequence to which it is applied.

This section is devoted to a review on linear subdivision schemes focusing on their convergence, stability and behavior in presence of locally discontinuous data (Gibbs phenomenon). We first give several tools for the analysis of these properties. Two families of schemes, interpolatory Lagrange schemes and B-Spline schemes, are recalled and various implementations of these schemes, uniform (also called translation-invariant), position-dependent and zone-dependent are investigated. The behavior of these schemes and their different implementations in presence of initial data presenting strong variations are tested.

2.2 Definitions and Tools

We provide in this section the definitions and several tools useful to analyze the convergence property.

2.2.1 Convergence and stability

Note that in fact, subdivision involves independently two families $(a_{2k'}^{j,k})$ and $(a_{2k'+1}^{j,k})$, $k' \in \mathbb{Z}$. They control the shape of the reconstructed points and the regularity of the limit function if the scheme is convergent. We recall the following definitions:

Definition 2.2.1 *Convergence of a subdivision scheme:*
A subdivision scheme S is said to be L^∞-convergent if for any sequence $f^0 = \{f_k^0\}_{k\in\mathbb{Z}}$ there exists a continuous function $f = S^\infty f^0$ such that:

$\forall\epsilon, \exists J,$ *such that* $\forall j \geq J$*:*

$$||S^j f^0 - f(\frac{\cdot}{2^j})||_\infty \leq \epsilon.$$

Definition 2.2.2 *Stability of a subdivision scheme:*
A subdivision S is said to be stable if there exist a constant M such that, for any sequence $f^0 = (f^0_k)_{k\in\mathbb{Z}}$:

$$||S^j f^0||_\infty \leq M||f^0||_\infty$$

The stability property is essential for all the applications of subdivisions. However, for linear subdivision schemes the stability is a consequence of the convergence and we therefore focus on the convergence analysis.

A simple necessary condition for S to be convergent is the reproduction of constants that reads:

$$\forall j,k \ \sum_{l\in\mathbb{Z}} a^{j,k}_{2l} = 1, \ \sum_{l\in\mathbb{Z}} a^{j,k}_{2l+1} = 1. \tag{2.2}$$

In the sequel we assume that (2.2) is satisfied.

The convergence of subdivision scheme is directly connected to the analysis of the behavior of the differences $d^j_k = (S^j f^0)_{k+1} - (S^j f^0)_k$ when j goes to infinity. More precisely, the convergence of the subdivision scheme is equivalent to the convergence (when j goes to ∞) of d^j_k towards 0 for any initial sequence. The analysis of the behavior of the differences can be performed using various tools depending on the properties of the scheme.

2.2.2 Analysis tools

a) **Convergence analysis for linear, uniform and stationary schemes:**

For such schemes, as soon as (2.2) is satisfied, the evolution of d^j_k is controlled by a linear, uniform and stationary scheme S_1. The convergence of the initial subdivision scheme S is equivalent to the convergence of $||(S_1)^L||_\infty$ towards 0 when L goes to infinity ([3]).

The definition and analysis of S_1 can be performed using two basic tools: the Laurent polynomials and the matrix approach ([3]).

a.1) Characterization of S_1 using Laurent polynomials

For linear uniform stationary schemes, the unique mask $(a_l)_{l\in\mathbb{Z}}$ can be associated with a generalized polynomial $a(z) = \sum_{l\in\mathbb{Z}} a_l z^l$, remembering that nonzero a_l are in a finite number.

If one associates to each sequence $(f_k^j)_{k\in\mathbb{Z}}$ its Laurent polynomial $F^j(z) = \sum_{k\in\mathbb{Z}} f_k^j z^k$ then the subdivision relation is equivalent to

$$F^{j+1}(z) = a(z)F^j(z^2). \tag{2.3}$$

Moreover, the reproduction of constants leads to $a(-1) = 0$ and therefore to the factorization of $a(z)$ as $a(z) = (z+1)\tilde{a}_1(z)$. It is a simple calculation to see that if $D^j(z) = \sum \delta_k^j z^k$ is the Laurent polynomial associated to the differences then $D^{j+1}(z) = z\tilde{a}_1(z)D^j(z^2)$.

Therefore, $a_1(z)$, the polynomial associated to S_1 is defined by

$$a_1(z) = \frac{z}{1+z}a(z),$$

and the analysis of S_1 is then reachable. Moreover we have the following theorem:

Theorem 2.2.1 *If $a(z)$ the Laurent polynomial of a subdivision scheme S can be written as:*

$$a(z) = (\frac{1+z}{z})^p q(z)$$

where q is a Laurent polynomial, then if the subdivision scheme S_p associated to the polynomial q is uniformly convergent, the subdivision scheme S also uniformly converges to a function

$$\phi \in C^{p-1}$$

a.2) Characterization of S_1 using the matrix approach

Due to the finiteness of the number of non zero coefficients of $(a_l)_{l\in\mathbb{Z}}$, one can define for any value $(j,k) \in \mathbb{Z}^2$ the minimal set of points at level j that determines all the values of (f_m^l) with $l \geq j+1$ and $m2^{-l} \in [k2^{-j}, (k+1)2^{-j}]$. If one call N the number of these points and $F_k^j \in \mathbb{R}^N$ the corresponding vector of N values of the sequence $(f_k^j)_{k\in\mathbb{Z}}$ there exist two matrices A_0 and A_1 called the refinement matrices such that

$$\forall k \in \mathbb{Z},\ F_{2k}^{j+1} = A_0 F_k^j,\ F_{2k+1}^{j+1} = A_1 F_k^j.$$

Denoting $A_0^{(1)}$ and $A_1^{(1)}$ the refinement matrices associated to S_1, the uniform convergence to zero of S_1 which is necessary and sufficient for the uniform convergence of S, can be reformulated as follows [3]:

Theorem 2.2.2 *A necessary and sufficient condition for the uniform convergence of S is the existence of a positive integer L such that,*

$$||A_{i_1}^{(1)} A_{i_2}^{(1)} \cdots A_{i_L}^{(1)}||_\infty < 1, \quad \forall (i_1, i_2, \cdots, i_L) \in \{0,1\}^L.$$

b) **Convergence analysis for linear, non uniform, stationary schemes:**

For such schemes the evolution of $(\delta_k^j)_{k\in\mathbb{Z}}$ is controlled by a linear, non uniform and stationary scheme S_1. The convergence is analyzed at each point using the matrix approach. In non uniform schemes, there exist two sets of refinement matrices such that

$$\forall k \in \mathbb{Z},\ F_{2k}^{j+1} = A_{0,k} F_k^j,\ F_{2k+1}^{j+1} = A_{1,k} F_k^j,$$

where $A_{0,k}, A_{1,k}$ are dependent on the position k.

Denoting $A_{0,k}^{(1)}$ and $A_{1,k}^{(1)}$ the two sets of refinement matrices associated to S_1, the convergence at any dyadic point can be studied by the infinite product of the matrices of differences involved in the computation of the differences at this point. An example of application is given in Section 2.3.5:

c) **Convergence analysis for linear, non stationary schemes:**

For such schemes the evolution of $(\delta_k^j)_{k\in\mathbb{Z}}$ is controlled by a linear, non stationary scheme $S_{j,1}$. The convergence of such a subdivision scheme can be established as soon as its mask converges, when j goes to infinity, towards the mask of a convergent stationary subdivision scheme called the asymptotical subdivision scheme. This result is recalled in the following theorem ([4]):

Theorem 2.2.3 *Let S be a non-stationary subdivision scheme defined by its masks $\{a_m^{j,k}\}_{m\in\mathbb{Z}}$, $(j,k) \in \mathbb{Z}^2$. We suppose that there exists two constants $K < K'$, independent of j and k such that $a_m^{j,k} = 0$ for $m > K'$ or $m < K$. If there exists a convergent stationary subdivision scheme SS of masks $\{a_m^k\}_{m\in\mathbb{Z}}$, $k \in \mathbb{Z}$ with $a_m^k = 0$ for $m > K'$ or $m < K$ and such that*

$$\lim_{j\to+\infty} ||a^{j,k} - a^k||_\infty = 0\ ,$$

then S is convergent.

2.3 Gibbs phenomenon for linear subdivision schemes

This section is devoted to the description of two basic schemes, Lagrange interpolatory scheme and B-spline scheme as well as three possible implementations, uniform, position dependent and zone dependent. These schemes and implementations are described focussing on the generation of Gibbs oscillations that occurs usually when the initial data exhibit strong gradients.

According to D.Gottlieb and C.W.Shu [5], given a punctually discontinuous function g and its sampling g^h defined by $g^h_k = g(kh)$, the Gibbs phenomenon deals with the convergence of $S^\infty(g^h)$ towards g when h goes to 0. It can be characterized by two features ([5]):

- Away from the discontinuity the convergence is rather low and for any point x,

$$|g(x) - S^\infty(g^h)(x)| = O(h).$$

- There is an overshoot, close to the discontinuity, that does not diminish with the reduction of h. Thus

$$max|g(x) - S^\infty(g^h)(x)| \text{ does not tend to zero with } h.$$

The key situation is then given by the initial sequence $(g^0_k)_{k\in\mathbb{Z}}$ with $g^0_k = 1$ if $k \leq 0$ and $g^0_k = 0$ if $k > 0$. Since all the scheme studied here are linear, if one calls δ_k the limit function reached after convergence starting from the initial sequence $\delta^j_k = \delta_{k,j}, k \in \mathbb{Z}$ it is well known that the limit function reached starting from the sequence $(f^0_k)_{k\in Z}$ is $S^\infty f^0 = \sum_{k\in\mathbb{Z}} f^0_k \delta_k$.

For the specific case of $g^0 = (g^0_k)_{k\in\mathbb{Z}}$ we get $G(x) = \sum_{k\leq 0} \delta_k$. Since $\sum_{k\in\mathbb{Z}} \delta_k = 1$ due to the reproduction of constants and since δ_k has compact support of length uniformly bounded by a constant K, for $x \leq -K$, $G(x) = 1$ and for $x \geq K$, $G(x) = 0$. The behavior of $G(x)$ for $-K \leq x \leq K$ is directly linked to the shapes of $(\delta_k)_{-K\leq x\leq K}$ and, more precisely to their oscillations. Reducing these oscillations directly reduces the Gibbs oscillations associated to the scheme.

2.3.1 Lagrange interpolatory subdivision scheme

Lagrange subdivisions constitute a classical family of interpolatory schemes. In interpolatory schemes, values at the grid points $(x^j_k)_{k\in\mathbb{Z}}$ are kept while, locally, several values at

level j are used to predict a 'middle' point at level $j+1$, doubling in this way the number of points. Supposing we take $l_{j,2k+1}$ points on the left and $r_{j,2k+1}$ points in the right to reconstruct the value at position x^j_{2k+1} at the middle of interval $[x^{j-1}_k, x^{j-1}_{k+1}]$, and denoting by $S_{l_{j,2k+1},r_{j,2k+1}}$ the corresponding reconstruction stencil and by D the degree of Lagrange polynomial (i.e. $D = l_{j,2k+1} + r_{j,2k+1} - 1$), then the subdivision operator is defined as: $\forall k \in \mathbb{Z}$

$$\begin{cases} (Sf^j)_{2k} = f^j_k, \\ (Sf^j)_{2k+1} = \sum_{m=-l_{j,2k+1}+1}^{r_{j,2k+1}} L_m^{l_{j,2k+1},r_{j,2k+1}}(\frac{1}{2}) f^j_{k+m}, \end{cases} \tag{2.4}$$

where $L_m^{l_{j,2k+1},r_{j,2k+1}}(x) = \Pi_{n=-l_{j,2k+1}+1, n\neq m}^{r_{j,2k+1}} \frac{x-n}{m-n}$.

The corresponding masks $(a^{j,k}_k)_{k\in\mathbb{Z}}$ satisfy:

$$\begin{cases} a^{j,k}_{2k} &= \delta_{k,0}\ , \\ a^{j,k}_{2k+1-2m} &= L_m^{l_{j,2k+1},r_{j,2k+1}}(\frac{1}{2})\ ,\ -l_{j,2k+1}+1 \leq m \leq r_{j,2k+1}. \end{cases}$$

General results are given for specific sets of couples $(l_{j,2k+1}, r_{j,2k+1})$:

- for $l_{j,2k+1} = r_{j,2k+1}$, the scheme is said to be centered and necessarily corresponds to an even degree D of interpolation. When $l_{j,2k+1} = r_{j,2k+1} = l = r$ one gets a uniform, stationary and centered scheme. Such schemes have been first studied by G.Deslaurier and S. Dubuc in [6] who proved the convergence of the schemes and established the regularity of the limit function, see Figure 2.1. More precisely they established the following

  Theorem 2.3.1 *All the Lagrange subdivision schemes with centered-stencil $S_{l,l}$ are convergent.*

  Moreover, the limit function is $C^{\alpha-}$ with $\alpha \approx 0.4l$.

- for $l_{j,2k+1} = l, r_{j,2k+1} = r$ and $l \neq r$, the scheme is said to be uniform and non-centered. It has been proved in ([7]) that for any value of $(l-r) \neq 0$ there exists a degree D_{max} such that for any non-centered scheme of degree $D \geq D_{max}$ the scheme diverges. Moreover these schemes appear to have a reduced regularity compared to centered ones, see Figure 2.2. The centered scheme seems to have the highest regularity among all the Lagrange schemes.

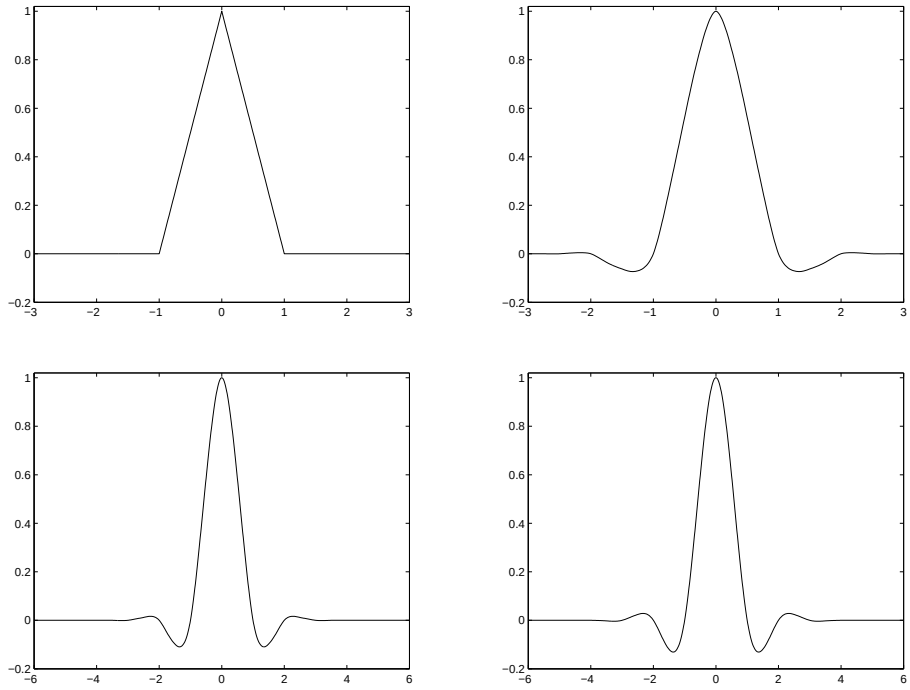

Figure 2.1: Examples of limit functions of centered Lagrange subdivision scheme for the initial control points $f^0 = (\delta_{n,0})_n$: top left $S_{1,1}$, top right $S_{2,2}$, bottom left $S_{3,3}$, bottom right $S_{4,4}$.

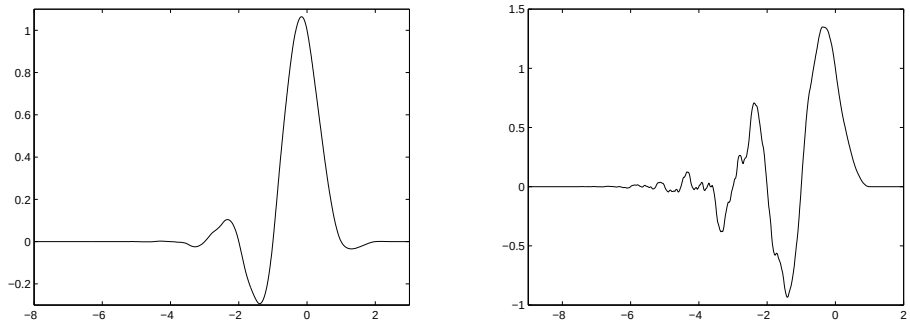

Figure 2.2: Examples of limit functions of non-centered Lagrange subdivision for the initial control points $f^0 = (\delta_{n,0})_n$: left $S_{2,4}$, right $S_{1,5}$.

- for $l_{2k+1} = 0$ or $r_{2k+1} = 0$, one gets a uniform extrapolatory scheme that diverges for any degree.

As examples, we consider the Lagrange interpolatory subdivision scheme using a four-point centered stencil i.e. $l = 2, r = 2$ and a four-point non-centered stencil i.e. $l = 3, r = 1$. These schemes will appear in many parts of the thesis.

- 4-point centered stencil:
  The prediction operator is written as: $\forall k \in \mathbb{Z}$,

$$\begin{cases} (Sf^j)_{2k} = f^j_k, \\ (Sf^j)_{2k+1} = -\frac{1}{16} f^j_{k-1} + \frac{9}{16} f^j_k + \frac{9}{16} f^j_{k+1} - \frac{1}{16} f^j_{k+2}. \end{cases}$$

  The Laurent polynomial associated to this scheme is given by the formula:

$$a(z) = -\frac{1}{16} \frac{(z+1)^4}{z^3} (z^2 - 4z + 1).$$

  The Laurent polynomial associated to S_1 is then:

$$a_1(z) = -\frac{1}{16} z^3 + \frac{1}{16} z^2 + \frac{1}{2} z + \frac{1}{2} + \frac{1}{16} z^{-1} - \frac{1}{16} z^{-2},$$

  and a direct calculation gives

$$||S_1||_\infty = |\frac{1}{2} + \frac{1}{16} + \frac{1}{16}| < 1.$$

  Similarly one can get the Laurent polynomial associated to S_2:

$$a_2(z) = -\frac{1}{8} \frac{(z+1)^2}{z} (z^2 - 4z + 1).$$

  The L^∞ norm of this scheme is equal to 1 and we can not go further now. One must study the schemes $(S_2)^2$ and $(S_2)^3$. The Laurent polynomial associated to $(S_2)^3$ is $\frac{1}{8} a_2(z) a_2(z^2) a_2(z^3)$ and we find that

$$||(S_2)^3||_\infty < 1.$$

  Since $\forall m, ||(S_3)^m||_{L^\infty} > 1$, we deduce that the 4-point Lagrange interpolatory centered scheme is convergent and its limit function $\tilde{\phi}_0 \in C^1(R)$ (Figure 2.1, top, right).

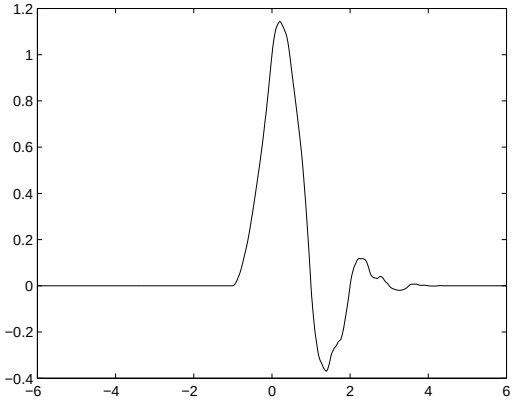

Figure 2.3: The limit function of non-centered scheme $S_{3,1}$.

- 4-point non-centered stencil: $l = 3, r = 1$
  In this situation, the subdivision scheme is written as: $\forall k \in \mathbb{Z}$

$$\begin{cases} (Sf^j)_{2k} = f_k^j, \\ (Sf^j)_{2k+1} = \frac{1}{16} f_{k+1}^j - \frac{5}{16} f_k^j + \frac{15}{16} f_{k-1}^j + \frac{5}{16} f_{k-2}^j. \end{cases}$$

  Its Laurent polynomial is

$$a(z) = \frac{1}{16} z^5 - \frac{5}{16} z^3 + \frac{15}{16} z + \frac{5}{16} z^{-1} + 1.$$

  We deduce the Laurent polynomial associated to S_1

$$a_1(z) = \frac{1}{16} z^5 - \frac{1}{16} z^4 - \frac{1}{4} z^3 + \frac{1}{4} z^2 + \frac{11}{16} z + \frac{5}{16},$$

  we can get that $||S_1||_{L^\infty} = 1$, but also

$$||(S_1)^2||_{L^\infty} < 1.$$

  The same calculation for S_2 gives that

$$\forall m,\ ||(S_2)^m||_{L^\infty} > 1.$$

  The non-centered scheme converges but its limit function $\tilde{\phi}_0$ is only in $C^0(R)$. The limit function of the scheme $S_{3,1}$ is plotted in Figure 2.3.

2.3.2 B-spline subdivision scheme

B-spline subdivision appeared in the framework of curve storage as a consequence of the existence of the B_m-spline functions that turns out to be the associated limit functions.

For any $m \geq 1$ the basic spline function of order m, ϕ_m, is defined by:

$$\phi_0 = \chi_{[-\frac{1}{2},\frac{1}{2}]},\ \phi_m(x) = \int_{x-\frac{1}{2}}^{x+\frac{1}{2}} \phi_{m-1}(t)dt.$$

For any $m \geq 1$, ϕ_m is a compact support function ($supp(\phi_m) = \lfloor -[2^{-1}m] - 1, m - [2^{-1}m] \rfloor$), $\phi_m \in C^{m-1}(\mathbb{R})$ with, moreover the restriction of ϕ_m to any interval $[k - \frac{1}{2}, k + \frac{1}{2}], k \in \mathbb{Z}$ is a polynomial of degree m. The set $\{\phi_m(x-k), k \in \mathbb{Z}\}$ is a Riesz basis of the spline functions of order m associated with the segmentation $(k + \frac{1}{2})_{k\in\mathbb{Z}}$[1]. It satisfies the following induction relation:

$$\phi_m(x) = \phi_{m-1} * \phi_0(x).$$

Any function f that satisfies:

$$\exists (f_k^0)_{k\in\mathbb{Z}} |\ f = \sum f_k^0 \phi_m(x-k)$$

can be written as: $f = \sum f_k^1 \phi_m(2x-k)$ with

$$f_k^1 = \sum a_{k-2l} f_l^0. \tag{2.5}$$

Relation (2.5) defines the B-spline subdivision scheme of order m. By construction it is a convergent scheme of regularity C^{m-1} and the limit functions δ_k satisfy $\delta_k = \phi_m(x-k)$.

The only interpolatory B-spline scheme is the B-spline scheme of order 1. Indeed, for $m = 1$ one gets:

$$\begin{cases} f_{2k}^{j+1} = f_k^j \\ f_{2k+1}^{j+1} = \frac{1}{2} f_k^j + \frac{1}{2} f_{k-1}^j \end{cases}.$$

The B-spline subdivision scheme of order $m = 2$ is also known as the Chaikin scheme or corner cutting scheme. It is written as:

$$\begin{cases} f_{2k}^{j+1} = \frac{3}{4} f_k^j + \frac{1}{4} f_{k+1}^j \\ f_{2k+1}^{j+1} = \frac{1}{4} f_k^j + \frac{3}{4} f_{k+1}^j \end{cases}.$$

[1] Spline functions of order m associated to a segmentation $y_k, k \in \mathbb{Z}$ are functions globally C^{m-1} which restriction on $[y_k, y_{k+1}]$ are polynomials of degree $m-2$

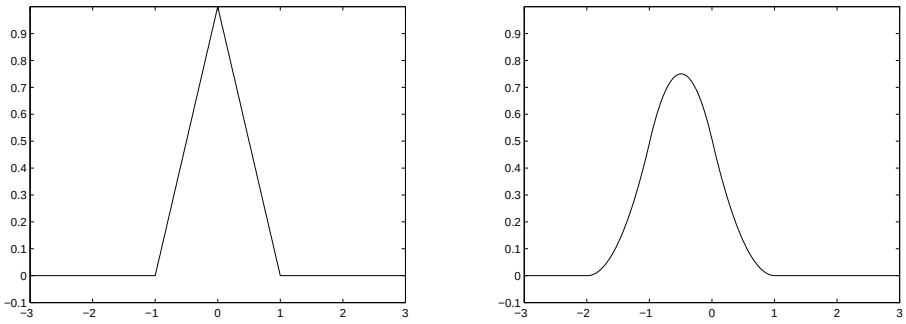

Figure 2.4: Limit function of B_m-spline schemes for the initial points $f^0 = (\delta_{n,0})_n$: left $m = 1$, right $m = 2$.

When used for curve subdivision the plot of the control polygon[2] at each iteration (see Figure 2.5) clearly reveals the origin of the corner cutting name. In the plane, starting from a family of points $M_k^0 = (x_k^0, y_k^0)$, the curve subdivision consists in generating the family of points $M_k^j = (x_k^j, y_k^j)$ with $(x_k^{j+1})_{k\in\mathbb{Z}} = S(x_k^j)_{k\in\mathbb{Z}}$, $(y_k^{j+1})_{k\in\mathbb{Z}} = S(y_k^j)_{k\in\mathbb{Z}}$.

By construction, the B-spline function ϕ_m does not oscillate in connection to the positivity of the coefficients $(a_k)_{k\in\mathbb{Z}}$. This property (see next section) is essential for the behavior of the limit function generated by initial data exhibiting strong gradients.

2.3.3 Uniform implementation

By translation invariance, if $\phi(x) = S^\infty\delta_0$ then $S^\infty\delta_n = \phi(x-n)$ and $S^\infty f = \sum_{k\in\mathbb{Z}} f_k^0\phi(x-k)$. As soon as ϕ oscillates, the limit function associated to the initial sequence

$$\begin{cases} H_k^0 = 1 & \text{if} \quad k \leq 0 \\ H_k^0 = 0 & \text{if} \quad k > 0 \end{cases}$$

is oscillating and therefore the Gibbs phenomenon is observed.

As an example, Figure 2.6 exhibits this phenomenon for the Lagrange subdivision scheme $S_{2,2}$. On the left the functions $\phi(x-k), k \leq 0$ are plotted and their sum is shown on the right. On Figure 2.7 the same plots are provided for the B_3 subdivision scheme. Observe that the non oscillating property of ϕ leads to the absence of Gibbs oscillations.

[2]The control polygon at scale j is the polygon obtained connecting the successive values at scale j using straight lines

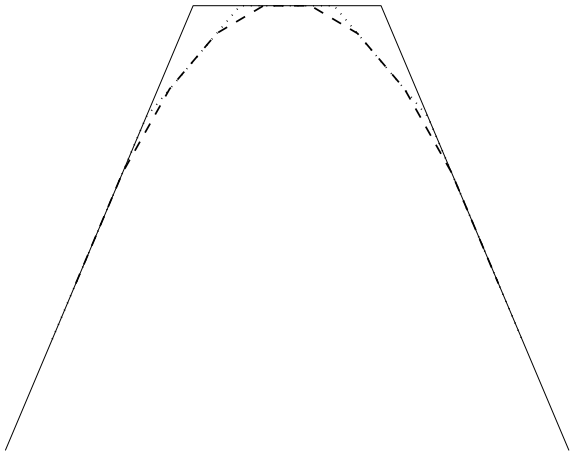

Figure 2.5: Curve subdivision by B_2-spline scheme. Solid line: initial control polygon, dotted line: control polygon at first iteration, dashed line: control polygon at second iteration.

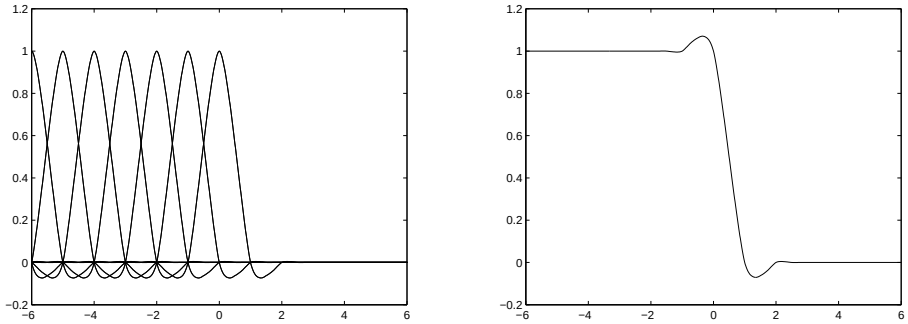

Figure 2.6: Limit function of the translation-invariant Lagrange interpolatory scheme. Left, limit functions starting from $(\delta_{n,m})_n, m \in \{\mathbb{Z}^- \text{ and } 0\}$; right, the Gibbs phenomenon near the discontinuity $x = 0$.

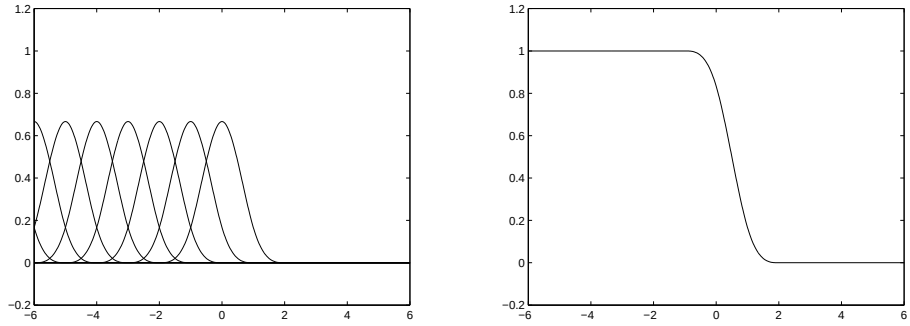

Figure 2.7: Limit function of the translation-invariant B_3 non-interpolatory scheme. Left, limit functions starting from $(\delta_{n,m})_n, m \in \{\mathbb{Z}^- \text{ and } 0\}$; right, the smooth curve near the discontinuity $x = 0$.

2.3.4 Position-dependent implementation

In some situations one gets a set P of subdivision schemes reproducing constants characterized by a fixed stencil length but different values of the stencils parameter (l, r). This is the case for instance for Lagrange interpolatory scheme of fixed degree D with $l \geq 0, r \geq 0$ and $l + r = D + 1$. Each of the $(D + 2)$ different schemes corresponding to all the values of (l, r) exhibits an oscillating limit function. For $D = 3$, the different limit functions are displayed on Figure 2.1 ($S_{2,2}$) and Figure 2.3 ($S_{3,1}$), while for $D = 4$ they are depicted by Figure 2.1 ($S_{3,3}$) and Figure 2.2 ($S_{2,4}, S_{1,5}$). With the same arguments as previously, the limit function associated to $(H^0_k)_{k\in\mathbb{Z}}$ is oscillating for each of the schemes implemented in a uniform way.

The position dependent implementation is a non stationary scheme derived from the set P that allows to erase the Gibbs phenomenon at a fixed position called a segmentation point. This construction can be easily generalized to any finite set of segmentation points but we provide a full description for a single segmentation point $y_0 = 0$. The goal is to construct a scheme such that $S^\infty\delta_0$ is not oscillating. This means that the scheme is perfectly fitted for a discontinuity at position y_0. The scheme is derived as follows:

Starting from an a priori choice (l_0, r_0), the stencil used to predict a value of index (j, k) is chosen such that the couple $(l_{j,k}, r_{j,k})$ chosen among the stencils of the set P is as close as possible to (l_0, r_0) with the constraint that the point y_0 does not belong to the interval $[x^{j-1}_{-l_0+k}, x^{j-1}_{r_0-1+k}]$, the distance being $d((l, r), (l', r')) = |l - l'|$. Practically, it means that far from the point y_0 the stencil parameters are (l_0, r_0) while, close to y_0, the

stencil is shifted so that the subdivision formula does not involve points from both sides of y_0. Figure 2.8 exhibits the corresponding choices for $(l_0, r_0) = (2, 2)$.

As soon as the uniform scheme based on the stencil (l_0, r_0) converges, convergence analysis of position dependent scheme defined using the previous strategy is reached if the convergence at the point y_0 is proved. Indeed it is clear that at any position $y \neq y_0$ and any value $M > 0$ there exists a value j_y such that for any $j \geq j_y$ the subdivision of the M points of the grid X^j closest to y is performed using the scheme (l_0, y_0). The use of the matrix formalism therefore ensures that the scheme converges at the point y. The situation at the point y_0 is more involved even if, at that point, the matrix formalism involves a quasi stationary set of matrices depending on y. Indeed, as shown on Figure 2.8 the stencil distribution in the vicinity of y depends on the dyadic development of y. More precisely, writing $y = \sum_{j \in N} k_j 2^{-j}$ with $k_j \in \{0, 1\}$, the stencil distribution (a) corresponds to all the values of j with $k_{j+1} = 0$ while the stencil distribution (b) corresponds to all the values of j with $k_{j+1} = 1$.

If we call $A_0^{(1),+}, A_1^{(1),+}$ (resp. $A_0^{(1),-}, A_1^{(1),-}$) the matrices for the differences on the right (resp. left) side of y_0, we then have the following theorem:

Theorem 2.3.2 *If there exists $L > 0$ such that*

$$||A_{2,i_1}^{(1),-} \cdots A_{2,i_L}^{(1),-}||_\infty \leq \mu_1 < 1, \tag{2.6}$$

$$||A_{2,i_1}^{(1),+} \cdots A_{2,i_L}^{(1),+}||_\infty \leq \mu_2 < 1, \tag{2.7}$$

for all $(i_1, \cdots, i_L) \in \{0, 1\}^L$, then the position-dependent subdivision scheme is punctuality convergent at $y = y_0$.

A general result for a set P of stencil derived for Lagrange interpolatory schemes has been described in [8]. It provides the eigen values of the refinement matrices at point y_0 that, except for the eigen value 1 are the eigenvalues of the refinement matrices for the differences. The fact that all these eigenvalues are strictly less then 1 allows one to get the convergence using a local version of theorem 2.2.2. It reads with $l_0 = r_0 = r$:

Theorem 2.3.3 *For any $j \geq 0$, $y_0 \in [x_{k_j}^j, x_{k_j+1}^j]$, then the four edge-matrices $A_{2,0}^-, A_{2,1}^-, A_{2,0}^+$ and $A_{2,1}^+$ are the $2r \times 2r$-matrices of the form:*

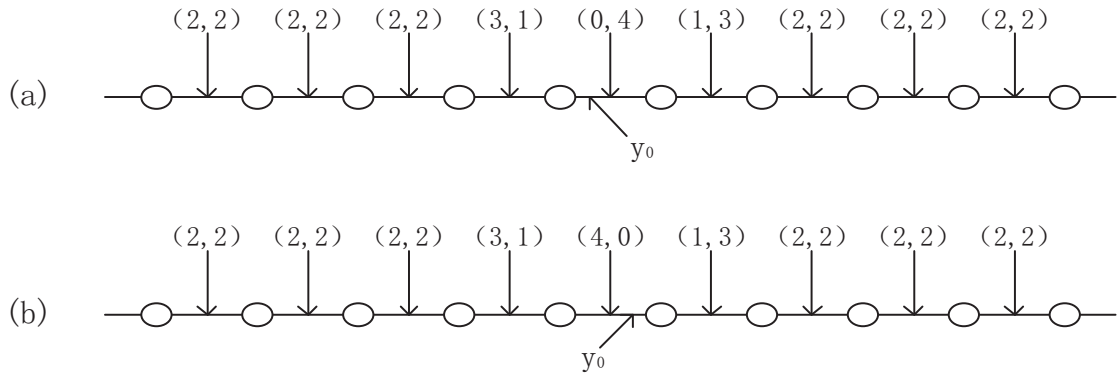

Figure 2.8: Example of a 4-point stencil position-dependent strategy in the vicinity of a segmentation point y_0.

- *if* $y_0 \in [x_{2k_j}^{j+1}, x_{2k_j+1}^{j+1}]$,

$$A_{2,0}^{-} = \begin{bmatrix} L_{-r}^{r,r} & \cdots & \cdots & L_{0}^{r,r} & \cdots & L_{r-1}^{r,r} \\ 0 & \cdots & \cdots & 1 & 0 & \cdots \\ L_{-r-1}^{r+1,r-1} & \cdots & \cdots & \cdots & \cdots & L_{r-2}^{r+1,r-1} \\ \cdots & \cdots & \cdots & \cdots & \cdots & \cdots \\ \cdots & \cdots & \cdots & \cdots & \cdots & \cdots \\ L_{-2r+1}^{2r-1,1} & \cdots & \cdots & \cdots & \cdots & L_{0}^{2r-1,1} \\ 0 & \cdots & \cdots & \cdots & \cdots & 1 \end{bmatrix},$$

$$A_{2,0}^{+} = \begin{bmatrix} L_{0}^{0,2r} & \cdots & \cdots & \cdots & L_{2r-1}^{0,2r} \\ 1 & 0 & \cdots & \cdots & 0 \\ \cdots & \cdots & \cdots & \cdots & \cdots \\ \cdots & \cdots & \cdots & \cdots & \cdots \\ \cdots & \cdots & \cdots & \cdots & \cdots \\ L_{-r+1}^{r-1,r+1} & \cdots & L_{0}^{r-1,r+1} & \cdots & L_{r}^{r-1,r+1} \\ \cdots & \cdots & 1 & \cdots & 0 \end{bmatrix}.$$

- *if* $y_0 \in [x^{j+1}_{2k_j+1}, x^{j+1}_{2k_j+2}]$,

$$A^-_{2,1} = \begin{bmatrix} 0 & \cdots & 1 & \cdots & 0 \\ L^{r+1,r-1}_{-r-1} & \cdots & L^{r+1,r-1}_{0} & \cdots & L^{r+1,r-1}_{r-2} \\ \cdots & \cdots & \cdots & \cdots & \cdots \\ \cdots & \cdots & \cdots & \cdots & \cdots \\ 0 & \cdots & \cdots & \cdots & 1 \\ L^{2r,0}_{-2r} & \cdots & \cdots & \cdots & L^{2r,0}_{-1} \end{bmatrix},$$

$$A^+_{2,1} = \begin{bmatrix} 1 & 0 & \cdots & \cdots & 0 \\ L^{1,2r-1}_{-1} & \cdots & \cdots & \cdots & L^{1,2r-1}_{2r-2} \\ \cdots & \cdots & \cdots & \cdots & \cdots \\ \cdots & \cdots & \cdots & \cdots & \cdots \\ \cdots & \cdots & 1 & \cdots & 0 \\ L^{r,r}_{-r} & \cdots & L^{r,r}_{0} & \cdots & L^{r,r}_{r-1} \end{bmatrix}.$$

with $Sp(A^+_{2,i}) = Sp(A^-_{2,i}) = \{1, \frac{1}{2}, \frac{1}{2^2}, \cdots, \frac{1}{2^{2r-1}}\}, 0 \leq i \leq 1$ *in both case.*

To our knowledge there is no general proof for non centered scheme, keeping in mind that, according to [7], for any decentering value ($l_0 - r_0 = p, p \neq 0$) there exists a degree $D = l_0 + r_0 + 1$ such that the uniform Lagrange interpolatory scheme (l_0, r_0) diverges.

A conjecture is that if each scheme of the set P converges then the position dependent scheme defined previously converges but we don't know any proof of this result.

Concerning the Gibbs oscillations the situation is simpler. Starting from the initial sequence $(H^0_k)_{k\in\mathbb{Z}}$, the reproduction of constants by each of the subdivision schemes of P and the distribution of the stencils imply that the limit function associated to $(H^0_k)_{k\in\mathbb{Z}}$ is the characteristic function of $\mathbb{R}^-$. This function does not oscillate and the Gibbs phenomenon does not appear.

The situation is however different as soon as the discontinuity point of the initial sequence and the segmentation point y_0 don't coincide. Unfortunately, this can be the case if the detection procedure for discontinuity miss the correct point. In such a situation, since oscillations appears in the limit functions associated to each initial sequence $\delta^0(\cdot - n)$, as soon as the families $(\delta^0(\cdot - n))_{n\leq 0}$ or $(\delta^0(\cdot - n))_{n>0}$ are not complete, oscillations appear. This situation is illustrated on Figure 2.9. On the first line the segmentation point $y_0 = 0$ coincides with the discontinuity point of the sequence (H^0) while on the second line

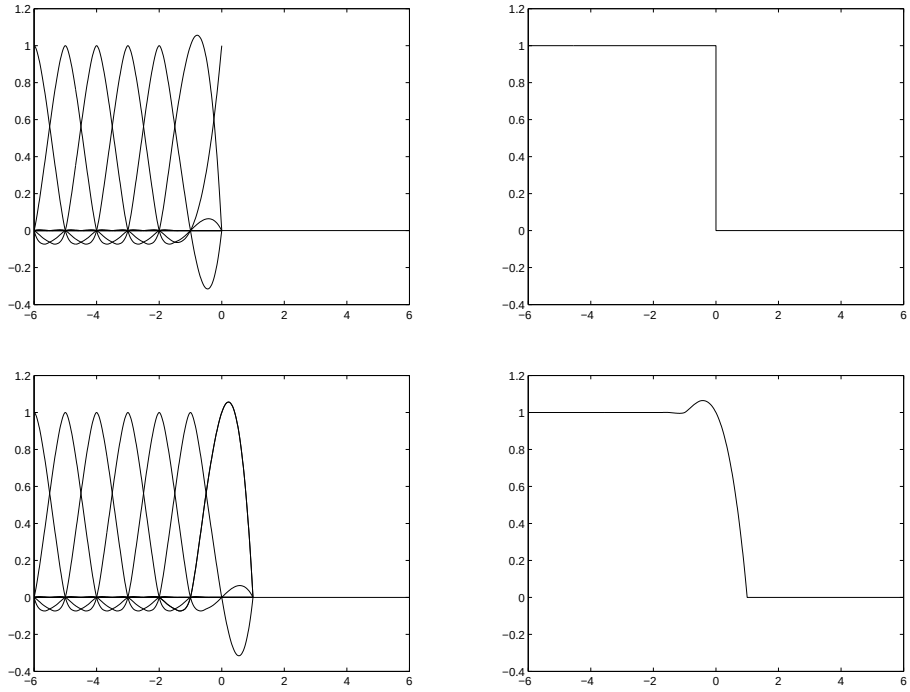

Figure 2.9: limit function of the position-dependent Lagrange interpolatory scheme. Top left, the limit functions caused by $(\delta_{n,m})_n, m \in \{\mathbb{Z}^- \text{ and } 0\}$; Top right, no Gibbs phenomenon; bottom left, the limit functions caused by $(\delta_{n,m})_n, m \in \{\mathbb{Z}^- \text{ and } 0, 1\}$; bottom right, the Gibbs phenomenon near the discontinuity $x = 0$.

$y_0 = 0$ but the initial sequence is $H^0(\cdot + 1)$. On the second line the most right function that contributed to the limit step function has disappeared, that generates oscillations.

This discussion on the Gibbs phenomenon for the position dependent implementation shows that the advantage of this implementation is under the control of the fitting between the data and the segmentation. This weakness has been observed in [8] devoted to image compression using position dependent implementation. The real efficiency of the position dependent multi-resolution on geometric images (where the detection of discontinuities leading to the segmentation is easy) contrasts with a modest efficiency on real images. This behavior was originally the main motivation for the derivation of zone dependent implementation.

2.3.5 Zone dependent implementation

The goal of zone dependent implementation is to weaken the dependency of the previous construction on the segmentation. Instead of constructing a scheme able to manage a discontinuity at a fixed point this construction aims to derive a scheme free of Gibbs oscillations as soon as the discontinuity appears in closed sub interval of fixed open zones. The practice of image analysis indeed leads to think that it will be easier to determine a zone for possible discontinuities than to determine the exact position. Without loss of generality we consider the case of a single zone $]y_0, y_1[$.

According to Section 2.3.3 uniform non oscillating scheme will be affected to the subdivision in the interior of the zone $]y_0, y_1[$ (this interior, depending on the scale, corresponds to the points where the subdivision can be performed with all the stencil points included in $]y_0, y_1[$) while eventually oscillating schemes will be used outside. Since isolated discontinuities are supposed to appear only in a closed sub interval $]y_0, y_1[$, the subdivision around the edge points y_0, y_1 can be treated using the position dependent strategy described previously. Again, a specific analysis of the convergence must be provided.

As an example we describe the implementation that will be used in our numerical experiments. It is based on Lagrange $D = 3$ interpolation schemes for the zone $]-\infty, y_0] \cup [y_1, +\infty[$ and on B-spline $m = 3$ non-interpolatory schemes for the interior of the zone $]y_0, y_1[$.

Construction

The construction of zone-dependent strategies relies on three essential ingredients that are fully specified in the sequel:

- Segmentation of the data:

  The real line is supposed to be split in three zones separated by the segmentation points $y_0 < y_1$ belonging to the coarse grid ($(y_0, y_1) \in \mathbb{N}^2$). The zones $]-\infty, y_0]$ and $[y_1, +\infty[$ are called regular zones and it is assumed that there is no discontinuities or noisy data, while $[y_0 + 1, y_1 - 1]$ corresponds to a non-regular zone in which discontinuities or noisy data may exist (Figure 2.10, top).

- Local subdivision:

  Local subdivision predictors are constructed independently in each zone. In the interior of the regular zone, a degree 3 centered Lagrange interpolatory scheme is

applied formally as:

$$\begin{cases} f_{2k}^{j} = f_{k}^{j-1} \\ f_{2k+1}^{j} = -\frac{1}{16} f_{k-1}^{j-1} + \frac{9}{16} f_{k}^{j-1} + \frac{9}{16} f_{k+1}^{j-1} - \frac{1}{16} f_{k+2}^{j-1}, \end{cases} , \tag{2.8}$$

while in the interior of non-regular zone, a B_3-spline non-interpolatory scheme is performed as:

$$\begin{cases} f_{2k}^{j} = 1/8 f_{k-1}^{j-1} + 3/4 f_{k}^{j-1} + 1/8 f_{k+1}^{j-1} \\ f_{2k+1}^{j} = 1/2 f_{k}^{j-1} + 1/2 f_{k+1}^{j-1} \end{cases} .$$

- Adaption at the boundaries of the zones:

  These schemes can not be applied close to the boundaries of the zone and a specific adaption is required. For the sake of clarity, we describe this adaption around the segmentation point y_0 which is written for any j, $y_0 = k_{j-1} 2^{-(j-1)}$. The adaption close to y_1 is performed similarly. We consider necessarily each side of the point y_0:

  Regular zone: the adaption is performed using the position dependent strategy. Here it involves a non-centered Lagrange interpolation with stencil index ($l_{j,k} = 3, r_{j,k} = 1$).

  Non-regular zone: the interior scheme can not be used to predict the first two points of the zone at positions $(2k_{j-1})2^{-j}, (2k_{j-1}+1)2^{-j}$ (Figure 2.10, bottom, right). We propose to estimate the first two points by a polynomial extrapolation of degree 3 from the regular zone.

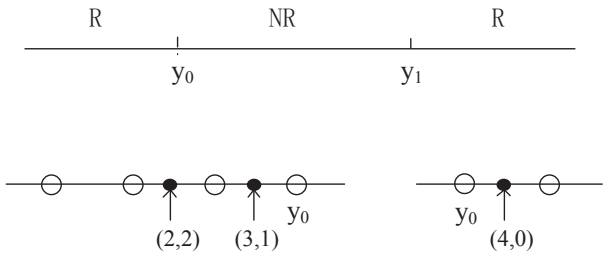

Figure 2.10: Top: segmentation of the line (R:Regular zone; NR: Non-Regular zone); Left bottom: adaption at the edge area y_0^-; Right bottom: adaption at the edge area y_0^+.

Convergence analysis for a zone dependent implementation using degree 3 Lagrange and B_3-spline subdivision scheme

Again we focus on the convergence and regularity analysis at the zone $]-\infty, y_0]$ and $]y_0, y_1[$.

- In $]-\infty, y_0]$, a degree-3 Lagrange interpolation is applied as follows:
  - if $y_0 \geq 2^{-(j-1)}(k+1)$, then $l_{j,2k+1} = r_{j,2k+1} = 2$, and the centered Lagrange interpolation is used.
  - if $y_0 < 2^{-(j-1)}(k+1)$, then $l_{j,2k+1} = 3, r_{j,2k+1} = 1$, and the scheme reads:

$$\begin{cases} f_{2k}^j = f_k^{j-1} \\ f_{2k+1}^j = \frac{1}{16} f_{k-2}^{j-1} - \frac{5}{16} f_{k-1}^{j-1} + \frac{15}{16} f_k^{j-1} + \frac{5}{16} f_{k+1}^{j-1}, \end{cases} , \tag{2.9}$$

  The convergence of such a subdivision scheme in the interior of the zone has already been studied in [8]. According to [3], the scheme is C^1 convergent in $]-\infty, y_0[$. For any $j \in \boldsymbol{N}$, the four values $(f_{k_j-3}^j, f_{k_j-2}^j, f_{k_j-1}^j, f_{k_j}^j)$ satisfy:

$$\begin{cases} f_{k_j-3}^j = P_0((k_j-3)2^{-j}) \\ f_{k_j-2}^j = P_0((k_j-2)2^{-j}) \\ f_{k_j-1}^j = P_0((k_j-1)2^{-j}) \\ f_{k_j}^j = P_0(k_j 2^{-j}) \end{cases}$$

  where P_0 is the polynomial of degree 3 interpolating $(f_{k_0-3}^0, f_{k_0-2}^0, f_{k_0-1}^0, f_{k_0}^0)$. Therefore the regularity at the point y_0^- is C^∞.

- For any j, the first two values $f_{k_j}^j, f_{k_j+1}^j$ in zone $]y_0, y_1[$ $(k_j 2^{-j} = y_0)$ are defined extrapolating by P_0 from zone $]-\infty, y_0]$ as:

$$\begin{cases} f_{k_j}^j = P_0(k_j 2^{-j}) \\ f_{k_j+1}^j = P_0((k_j+1)2^{-j}) \end{cases}$$

  The next values $f_k^j, k > k_j + 2$ are predicted using the B_3-spline subdivision relation. The convergence and regularity of B-spline is well known and B_3-spline generates a C^2 continuous limit function. For any point $y \in]y_0, y_1[$, there exist a scale j'

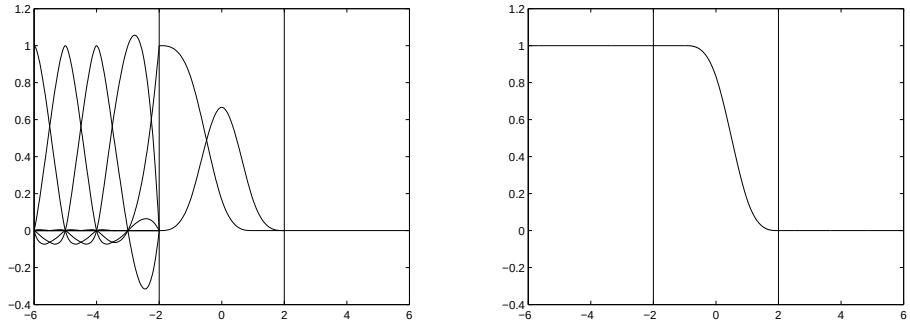

Figure 2.11: Limit function of the translation-invariant Lagrange interpolatory scheme. Left, limit functions starting from $(\delta_{n,m})_n, m \in \{\mathbb{Z}^-\}$ with the non-regular zone set to be $]-2,2[$ and the adaption near the edge areas; right, no Gibbs phenomenon but a smooth curve near the discontinuity $x = 0$.

such that for $j > j'$ the prediction at scale j is performed by the B-spline scheme. Therefore, the convergence occurs towards a C^2 continuous limit function. At y_0^+ the limit function is C^∞.

Finally the limit function is globally C^1.

Concerning the Gibbs oscillations, gathering the results obtained in the previous section it appears that no oscillations appears as soon as the discontinuity in the data is localized in a closed sub interval of $]y_0, y_1[$ such that at any scale (in fact at scale $j = 0$) the adaptation at the edges does not interact with this sub interval. This is illustrated for degree 3 Lagrange / B_3-spline schemes on Figure 2.11.

2.4 Applications to univariate data

We provide an example of univariate data where three subdivision schemes are compared. We test three schemes on the regular sampling $(x_i = i * h, i \in \mathbb{Z})$ of the following function:

$$f = \begin{cases} 5 * sin(\pi * (x - 0.1) + \frac{1}{6}) & \text{if } x \in [0, 0.65] \\ 5 - 5 * sin(\pi * (x - 0.1) + \frac{1}{6}) & \text{if } x \in [0.65, 1] \end{cases}$$

with one discontinuity at $x_0 = 0.65$.

In the tests, it is assumed that the segmentation procedure has led to an inaccurate estimation of the segmentation point $(y_0 \neq x_0)$. We take $y_0 = 0.68$.

The three schemes are defined as follows:

In ZDLB (Zone dependent Lagrange/B-spline) , two regular zones ($[0, 0.6]$ and $[0.7, 1]$) and one non-regular zone ($]0.6, 0.7[$) are defined. In PDL (Position dependent Lagrange) it is assumed that the segmentation position is located at $y_0 = 0.68$ while in TIL (Translation invariant Lagrange) no particular information for discontinuity is provided and a uniform Lagrange interpolatory scheme is applied. Figure (2.12) displays the reconstructed results after 10 iterations of subdivision. Table (2.1) gathers the resulting l_2-errors between the different limit functions and the original function f for different values of the sampling parameter h.

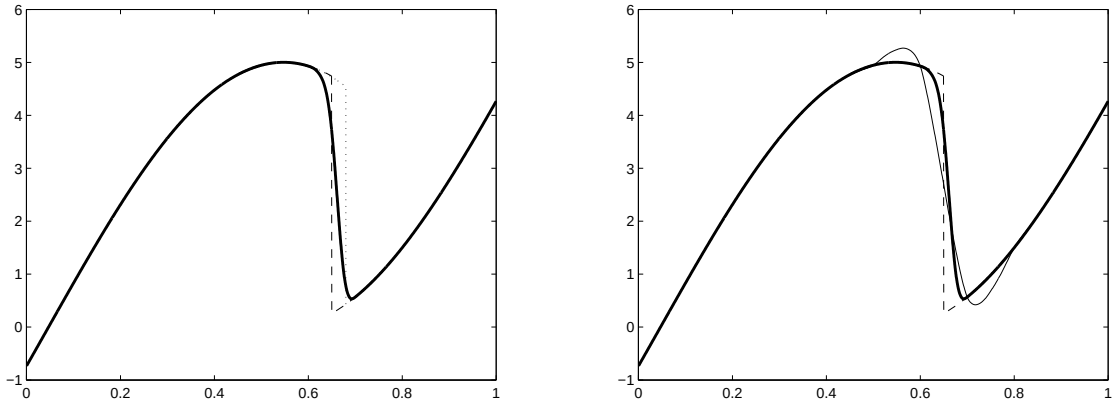

Figure 2.12: Comparison between PDL and ZDLB (left) and comparison between TIL and ZDLB (right): dashed line is the original function (both); dotted line is reconstructed by PDL (left); thin line is recovered by TIL (right); thick line is reconstructed by ZDLB (both).

l_2-error	h=0.2	h=0.1	h=0.05	h=0.025
PDL	9.4e-03	6.7e-03	4.8e-03	3.4e-03
TIL	1.32e-02	4e-03	4.1e-03	2.1e-03
ZDLB	1.34e-02	3.5e-03	2.5e-03	1.9e-03

Table 2.1: l_2-errors generated by PDL, TIL and ZDLB for different values of the sampling parameter h.

From Figure 2.12 TIL generates Gibbs oscillations around the point x_0; PDL, since

h is very small, does not generates oscillations but leads to a large L_2 error due to the mismatch between the segmentation point and the discontinuity. Using ZDLB not only erases the oscillations but also reduces the L^2 error.

2.5 Conclusion

In this section the general framework of linear subdivision has been introduced. Different tools for the convergence analysis have been reviewed and used to analyze various schemes. Zone dependent implementation have been introduced and tested. Emphasis has been given to the behavior of the different schemes in presence of strongly varying data (Gibbs phenomenon).

Chapter 3

Kriging-based subdivision scheme

3.1 Introduction

This chapter provides an overview on a new type of subdivision scheme originally introduced in [1] and based on Kriging theory which is widely used in the environmental community for the analysis of spatial data [9]. For sake of clarity, we first decouple in Section 3.2 the description of the Kriging theory from the subdivision framework and provide the main characteristics of Kriging prediction. Then, we introduce and fully study in Section 3.3 Kriging-based subdivision scheme. Finally, Section 3.4 is devoted to several numerical examples in order to evaluate its efficiency, compared to classical approaches of Lagrange type, for the reconstruction of non-regular data.

3.2 Overview on Kriging

Kriging interpolation belongs to the class of reconstruction methods. Considering N observations of a function, $f \in \mathcal{Y}$, $\{f_i\}_{i=0,\dots,N-1}$ on the grid $\{x_i\}_{i=0,..,N-1}$ of a bounded domain $\mathcal{D}$, the objective is to predict f at a location $x^\star$. $\mathcal{Y} = \{f(x), x \in \mathcal{D}\}$ is called regionalized variable and f_i is defined as a regionalized value ([10]).

3.2.1 Reconstruction method

There are two main classes of reconstruction methods. Their difference lies in the way to interpret the observations. In the first class, called deterministic, it is assumed that the observed data come from the discretization of the regionalized variable on the grid

$\{x_i\}_{i=0,...,N-1}$, the quantity $f(x)$ is seen as a deterministic unknown function. One of the main limitation of deterministic methods is that they do not provide a prediction error associated with each predicted value. On the contrary, the second class of reconstruction methods called stochastic allows one to quantify an a priori error (through an estimation variance) thanks to the underlying probabilistic framework. In this case, the available observations are considered as realizations of a subset of random variables $\{\mathcal{F}(x_i), i = 0, ..., N-1\}$ coming from a random process $\{\mathcal{F}(x), x \in \mathcal{D}\}$ that reads

$$\mathcal{F}(x) = m(x) + \delta(x), x \in \mathcal{D}, \tag{3.1}$$

where $m(x)$ is the deterministic mean structure of $\mathcal{F}(x)$ and $\{\delta(x), x \in \mathcal{D}\}$ is a zero-mean spatially correlated random process. This model allows one to represent a large variety of phenomenon. However, it is necessary to identify both a deterministic and a stochastic term.
A classical example of stochastic approach is Kriging interpolation ([10]). This approach was named by Matheron ([11]) after a south African mining engineer (D.G. Krige) who developed empirical methods for ore prospecting. From a mathematical point of view, Kriging can be seen as a minimum-mean-squared-error method. Its construction is fully specified in the next section.

3.2.2 Construction of the Kriging prediction

Modelling assumption

The characterization of the stochastic term requires to exhibit the multiple distribution function associated with the n-tuple for any $n \in \mathbb{N}$,

$$F_{\delta(x_0),...,\delta(x_n)}(d_1, \ldots, d_n) = P\left(\delta(x_0) \leq d_1, \ldots, \delta(x_n) \leq d_n\right).$$

However, in practice, due to few available observations, it is not possible to infer the previous quantities. Therefore, simplification is needed and achieved by assuming stationarity which is recalled in the next definition ([12]):

Definition 3.2.1 *The random function $\delta(x)$ is said to be strictly stationary if for any set of n points ($n \in \mathbb{N}$) and for any h, $F_{\delta(x_0),...,\delta(x_n)}(d_1, \ldots, d_n) = F_{\delta(x_0+h),...,\delta(x_n+h)}(d_1, \ldots, d_n)$.*

Strict stationarity still requires the identification of the multiple distribution function for any set of points $\{x_0, \ldots, x_n\}$. This assumption can be relaxed by considering only pairs of points $\{x_i, x_j\}$ and by characterizing only the first two moments instead of the full distribution. It leads to the notion of second-order stationarity or more generally to the notion of intrinsic stationarity of order two. More precisely, denoting by E, resp. var, the mathematical expectation, resp. variance, of a random variable [1], we have:

Definition 3.2.2 *The random function $\delta(x)$ is said to be intrinsically stationary of order two if*

$$\begin{cases} E[\delta(x+h) - \delta(x)] = 0, \\ var[\delta(x+h) - \delta(x)] = 2\gamma(h). \end{cases}$$

γ is called the semi-variogram associated with δ. It is a key quantity for the characterization of the stochastic term. Using Expression (3.1), it can be expressed as:

$$\gamma(h) = \frac{1}{2} E\left[(\mathcal{F}(x+h) - \mathcal{F}(x))^2\right] - \frac{1}{2}\left(m(x+h) - m(x)\right)^2. \tag{3.2}$$

which involves the random function associated with the observations. It is assumed for the remaining of this work that the deterministic term is constant. In this case, one speaks about ordinary Kriging and the construction of the prediction is performed in two steps: the semi-variogram is first estimated from the observations, then it is integrated to get the ordinary Kriging estimator as a linear combination of $\{\mathcal{F}_i\}_{i=0,\ldots,N-1}$. Replacing $\mathcal{F}(x_i)$ by f_i, this estimator leads to an approximation of $f(x^\star)$.

Spatial structure identification: semi-variogram

The semi-variogram is approximated, from the available data, by a least square fit of the discrete experimental semi-variogram,

$$\gamma_{exp}(h) = \frac{1}{2Card(N(h))} \sum_{(m,n)\in N(h)} (f_m - f_n)^2, \tag{3.3}$$

with $N(h) = \{(m,n) \in \{0, ..., N-1\},\ ||x_m - x_n||_2 = h\}$ with $||.||_2$ the Euclidean norm and for every h such that $Card(N(h))$, the cardinality of $N(h)$, is sufficiently large. In

[1] Let X be a real random variable of density f_X. Its mathematical expectation is defined as the integral over the realizations x of X weighted by the density function i.e. $E(X) = \int_{I\!R} x f_X(x) dx$. Moreover, its variance is given by $var(X) = E(X^2) - (E(X))^2$.

practice, the number of pairs (x_m, x_n) satisfying $||x_m - x_n||_2 = h$ is usually not sufficient to accurately estimate the semi-variogram. Therefore, the condition $||x_m - x_n||_2 = h$ in $N(h)$ is replaced by $h - \epsilon \leq ||x_m - x_n||_2 \leq h + \epsilon$ where ϵ is problem and user-dependent. The candidates for the experimental semi-variogram fitting have to be chosen among a family of valid semi-variogram models (Figure 3.1), denoted $\mathcal{G}$ (see [10] or [12]).

For the rest of the work, we focus on the two following families of semi-variograms (that differ according to the behavior of $\gamma(h)$ when h tends to zero) that encompass most of the classical models used in practice.

Definition 3.2.3 *We introduce $\mathcal{G}^\star_{OD}$ (resp. $\mathcal{G}^\star_{ED}$), the subsets of valid semi-variograms satisfying:*

$$\mathcal{G}^\star_{ED} = \{\gamma \in \mathcal{G},\ \gamma(h) =_{h\to 0} \sum_{n=0}^{+\infty} b_n h^{n+1} \text{ with } b_0 \neq 0\}, \tag{3.4}$$

$$\mathcal{G}^\star_{OD} = \{\gamma \in \mathcal{G},\ \gamma(h) =_{h\to 0} \sum_{n=0}^{+\infty} b_n h^{2n+2} \text{ with } \forall n \in I\!N,\ b_n \neq 0\}. \tag{3.5}$$

Note that the linear, spherical and exponential semi-variograms belong to $\mathcal{G}^\star_{ED}$ while the Gaussian, rational quadratic and hole-effect ones belong to $\mathcal{G}^\star_{OD}$ (see Figure 3.1). Each semi-variogram corresponds to different spatial structure of the data. Since it has a zero first derivative at the origin, the Gaussian model translates a stronger dependency between data at small scales than the exponential one. Therefore, it can be used to represent very regular data. There exists a more general formulation for theoretical semi-variograms involving an extra-parameter called nugget effect. It corresponds to a discontinuous semi-variogram at the origin and is therefore suitable to model data with strong variations at very small scales. In practice, it is difficult to specify the semi-variogram behavior near the origin since the available set of data is usually not substantial enough to exhibit very small scales dependency. Moreover, the strategy that will be introduced in the next section aims at considering only (locally) strongly dependent data for the prediction. Therefore, for the rest of the paper, the semi-variogram is assumed to be continuous at the origin, i.e., $\lim_{h\to 0^+} \gamma(h) = \gamma(0) = 0$.

Figure 3.2 displays the different steps of the semi-variogram identification.

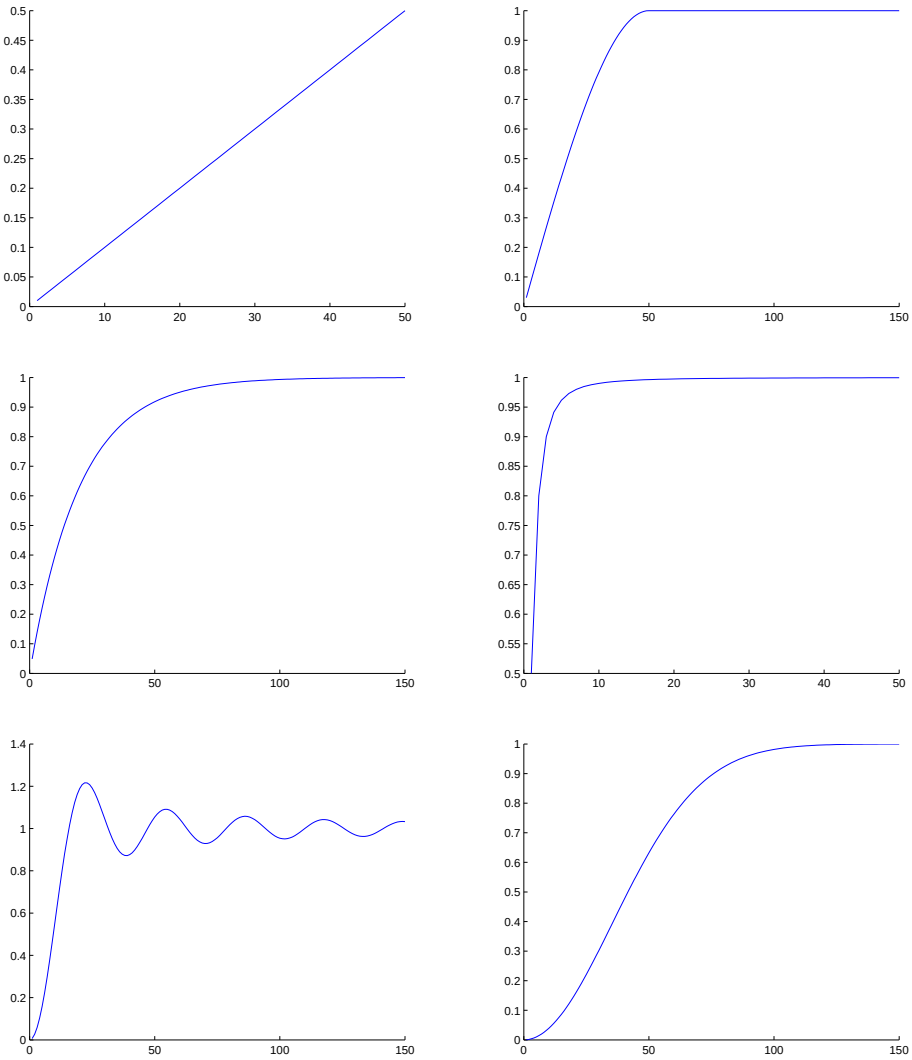

Figure 3.1: Examples of valid semi-variograms. From top, left to bottom, right, linear ($\gamma(h) = \frac{h}{100}$), spherical ($\gamma(h) = \frac{3}{2}\frac{h}{50} - \frac{1}{2}\frac{h^3}{50^3}$ for $h \leq 50$ and 1, elsewhere), exponential ($\gamma(h) = 1 - e^{-\frac{1}{20}h}$), rational-quadratic ($\gamma(h) = \frac{h^2}{1+h^2}$), hole-effect ($\gamma(h) = 1 - 5\frac{sin(0.2\ h)}{h}$) and Gaussian ($\gamma(h) = 1 - e^{-\frac{1}{50^2}h^2}$) semi-variograms.

Ordinary Kriging estimator

The ordinary Kriging estimator of the random process $\mathcal{F}$ at a new location $x^\star$ is denoted $\mathcal{P}(\mathcal{F}, x^\star)$. It is the linear, unbiased predictor[2] minimizing the estimation variance

[2] $\mathcal{P}(\mathcal{F}, x)$ is an unbiased estimator if and only if $E\left(\mathcal{P}(\mathcal{F}, x) - \mathcal{F}(x)\right) = 0$ where E is the mathematical expectation.

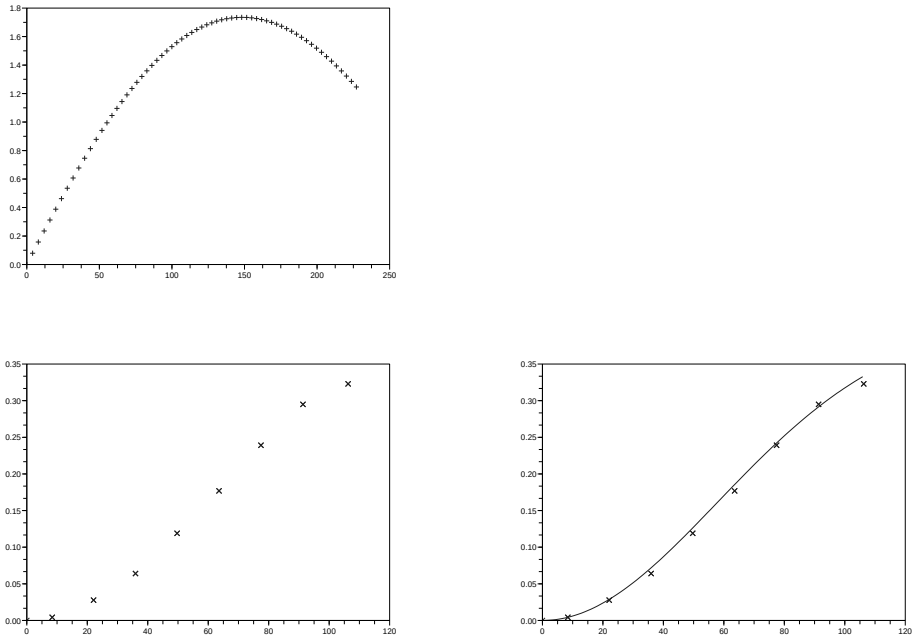

Figure 3.2: The different steps of the semi-variogram identification. From top to bottom right, data, experimental semi-variogram, identified semi-variogram model obtained by a least square fit.

$\sigma_K^2(x^\star) = var(\mathcal{F}(x^\star) - \mathcal{P}(\mathcal{F}, x^\star))$. It is written as

$$\mathcal{P}(\mathcal{F}, x^\star) = \sum_{i=0}^{N-1} \lambda_i \mathcal{F}(x_i), \tag{3.6}$$

where $\{\lambda_i\}_{i=0,\ldots,N-1}$ are called the Kriging weights. In the case of continuous semi-variograms, expanding the estimation variance as a function of γ and taking into account the unbiased condition, the Kriging weights are solutions of the classical optimization constrained problem ([12]):

$$\begin{cases} min_{\{\lambda_i\}_{i=0,\ldots,N-1}} \mathcal{J}\left(x^\star; \lambda_0, \ldots, \lambda_{N-1}\right), \\ \sum_{i=0}^{N-1} \lambda_i = 1, \end{cases} \tag{3.7}$$

where $\mathcal{J}\left(x^\star; \lambda_0, \ldots, \lambda_{N-1}\right) = -\frac{1}{2} \sum_{i=0}^{N-1} \sum_{n=0}^{N-1} \lambda_i \lambda_n \gamma(||x_i - x_n||_2) + \sum_{i=0}^{N-1} \lambda_i \gamma(||x_i - x^\star||_2)$. Denoting by the upper-script T the transpose operator and introducing $u =$

$(\lambda_0, \ldots, \lambda_{N-1})^T$, Problem (3.7) leads to the following linear system:

$$\begin{bmatrix} R & \mathbb{1} \\ \mathbb{1}^T & 0 \end{bmatrix} \begin{bmatrix} u \\ \mu \end{bmatrix} = \begin{bmatrix} b \\ 1 \end{bmatrix}, \tag{3.8}$$

where $R = \begin{bmatrix} 0 & \gamma(||x_0 - x_1||_2) & ... & \gamma(||x_0 - x_{N-1}||_2) \\ \gamma(||x_1 - x_0||_2) & 0 & ... & \gamma(||x_1 - x_{N-1}||_2) \\ ... & ... & ... & \\ \gamma(||x_{N-1} - x_0||_2) & \gamma(||x_{N-1} - x_1||_2) & ... & 0 \end{bmatrix}$,

$b = (\gamma(||x_0 - x^\star||_2), \ldots, \gamma(||x_{N-1} - x^\star||_2))^T$ and $\mathbb{1} = (1, \ldots, 1)^T$. Moreover, μ is the Lagrange multiplier enforcing the unbiasedness of the estimator. Solving Problem (3.8) leads to the Kriging estimator

$$\mathcal{P}(\mathcal{F}, x^\star) = u^T \left(\mathcal{F}(x_0), \ldots, \mathcal{F}(x_{N-1})\right), \text{ with } u^T = \left(b + \mathbb{1}\frac{1 - \mathbb{1}^T R^{-1} b}{\mathbb{1}^T R^{-1} \mathbb{1}}\right)^T R^{-1} \tag{3.9}$$

and to the estimation variance

$$\sigma_K^2(x^\star) = b^T R^{-1} b - \frac{\left(\mathbb{1}^T R^{-1} b - 1\right)^2}{\mathbb{1}^T R^{-1} \mathbb{1}}. \tag{3.10}$$

This last quantity is important in industrial applications since it allows one to quantify the a priori prediction error associated with each predicted point. It depends only on the type of identified semi-variogram and on the distance between points involved in the Kriging system.

With these notations, the minimization problem (3.7) can be reformulated as:

$$\begin{cases} min_{u \in I\!R^N} \left(-\frac{1}{2} < Ru, u >_2 + < b, u >_2\right), \\ < u, \mathbb{1} >_2 = 1, \end{cases} \tag{3.11}$$

where $< , >_2$ is the Euclidean scalar product. The matrix R is symmetric Toeplitz with positive coefficients and a null main diagonal. By definition ([12]), it satisfies $< Rx, x >_2 < 0, \forall x \in I\!R^N$ such that $x \neq 0$ and $\sum_{i=1}^N x_i = 0$. Since any vector u satisfying $< u, \mathbb{1} >_2 = 1$ can be decomposed as $u = x + \mathbb{1}$ with $< x, \mathbb{1} >_2 = \sum_{i=1}^N x_i = 0$,

$$-\frac{1}{2} < Ru, u >_2 + < b, u >_2 = -\frac{1}{2} < Rx, x >_2 + < b, x >_2 - \frac{1}{2}\alpha + < b, \mathbb{1} >_2,$$

where $\alpha = \sum_{i=1}^{N}\sum_{n=1}^{N} R_{i,n}$. Therefore, minimizing $-\frac{1}{2} < Ru, u >_2 + < b, u >_2$ under the constraint $< u, \mathbb{1} >_2 = 1$ is equivalent to minimize $-\frac{1}{2} < Rx, x >_2 + < b, x >_2$. Since R is negative definite on the set $\{x \in \mathbb{R}^N, \sum_{i=1}^{N} x_i = 0\}$ the minimum exists and is unique and therefore the matrix R is invertible.

By construction, the Kriging estimator is interpolating at the observations points i.e. when replacing $\mathcal{F}(x_i)$ by $f(x_i)$ in (3.9), $\mathcal{P}(\mathcal{F}, x_i) = f(x_i)$. In many applications, data are uncertain due to measurement errors or lack of information in the physical analysis for example. The constraint of interpolation can then be relaxed by introducing an error variance in the Kriging modelling.

3.2.3 Kriging with error variance

Kriging with error variance is a well-known approach in the Geo-statistics community to take into account uncertainty on observed data ([13]). More precisely, instead of $\mathcal{F}(x_i)$, the data are written $\mathcal{F}(x_i) + \epsilon(x_i)$ where the errors satisfy the three following properties:

- $E[\epsilon(x_i)] = 0$ for all i,
- $cov\ (\epsilon(x_i), \epsilon(x_n)) = 0$ for all $i \neq n$
- $cov\,(\epsilon(x_i), \mathcal{F}(x)) = 0$ for all i and all $x \in \mathcal{D}$

where cov denotes the covariance[3].
The Kriging estimator (3.6) becomes in this case:

$$\mathcal{P}(\mathcal{F}, x^\star) = \sum_{i=0}^{N-1} \lambda_i (\mathcal{F}(x_i) + \epsilon(x_i)). \tag{3.12}$$

It is also obtained by minimizing the estimation variance under unbiasedness constraint. Let us first notice that, according to the properties satisfied by the errors, the estimation variance can be written:

$$\begin{aligned} \sigma_K^2(x^\star) &= var(\mathcal{F}(x^\star) - \mathcal{P}(\mathcal{F}, x^\star)), \\ &= var(\mathcal{F}(x^\star) - \sum_{i=0}^{N-1} \lambda_i(\mathcal{F}(x_i))) + \sum_{i=0}^{N-1} \lambda_i^2 \sigma_i^2, \end{aligned} \tag{3.13}$$

[3]If X_1 and X_2 are two random variables, $cov(X_1, X_2) = E[(X_1 - E(X_1))\,(X_2 - E(X_2))]$.

where $\sigma_i^2 = var(\epsilon(x_i))$. It then comes that the Kriging weights are solutions in this case of a matricial problem of type (3.8) replacing R by $R - C$ where

$$C = \begin{bmatrix} c_1 & 0 & ... & 0 \\ 0 & c_2 & 0 & 0 \\ ... & ... & ... & \\ 0 & 0 & ... & c_N \end{bmatrix} \tag{3.14}$$

with $\forall i,\ c_i \geq 0$. The vector

$$\mathcal{C} = (c_1, ..., c_N) \tag{3.15}$$

is the vector of error variance. The corresponding prediction is no more interpolating at the observation locations where the error variance vector is non zero (Figure 3.3).

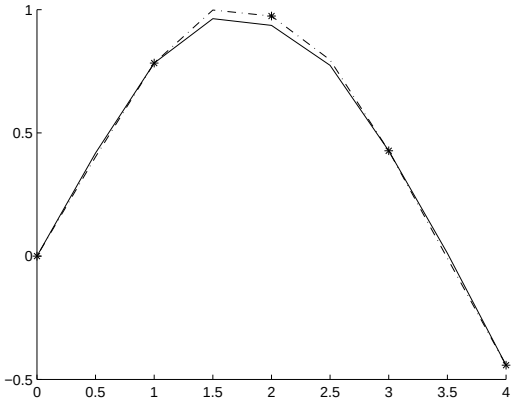

Figure 3.3: Prediction with and without error variance: $'*'$ are 5 observations, the dashed line stands for the prediction without error variance, the solid line is obtained after Kriging with error variance ($\mathcal{C} = (0, 0, 2, 0, 0)$).

In presence of error variance, the optimization problem (3.11) becomes:

$$\begin{cases} min_{u \in I\!R^N} \left(-\frac{1}{2} < Ru, u >_2 + \frac{1}{2} < Cu, u >_2 + < b, u >_2 \right), \\ < u, \mathbb{1} >_2 = 1. \end{cases} \tag{3.16}$$

and the vector $\mathcal{C}$ can be interpreted as a penalization of the L^2 norm of u, i.e as a penalization of the oscillations of the coefficients of u, keeping in mind that $< u, \mathbb{1} >_2 = 1$. With the same arguments as previously, the minimum of (3.16) exists and is unique.

3.3 Kriging-based interpolatory Subdivision Schemes

Ordinary Kriging theory (Section 3.2.2) is here plugged into the subdivision framework to derive a new type of interpolatory subdivision schemes introduced and fully analyzed in [1]. The question of integrating an error variance in the modelling will be addressed in the next chapters since this work has been performed during the Phd. The main results provided in this section are taken from [1].

3.3.1 Construction of the scheme

When replacing $x^\star$ by $(2k+1)2^{-j}$, N by $r+l$ and x_i by $(k+i-l)2^{-(j-1)}$, Expression (3.6) can be interpreted as a two-scale relation defining a non-stationary and non-homogeneous subdivision scheme. More precisely, assuming that the semi-variogram has been identified from the initial data f^0, the Kriging-based subdivision scheme is then defined as follows:

$$\begin{cases} f^j_{2k} = f^{j-1}_k, \\ f^j_{2k+1} = \sum_{m=-l_{j,2k+1}+1}^{r_{j,2k+1}} \lambda^{l_{j,2k+1},r_{j,2k+1}}_{j,m} f^{j-1}_{k+m}, \end{cases} \tag{3.17}$$

The family $\{\lambda^{l_{j,2k+1},r_{j,2k+1}}_{j,m}\}_m$ stands for the Kriging weights solution of Problem (3.8) where $x^\star$, N and $\{x_i\}_{i=0,\dots,N-1}$ are replaced by the corresponding quantities in the multi-scale framework (as mentioned at the beginning of this section) and the couple (l,r) is replaced by $(l_{j,2k+1}, r_{j,2k+1})$.

The mask associated with this subdivision scheme is written for even values as:

$$a^{j,2k} : \begin{cases} a^{j,2k}_0 = 1, \\ a^{j,2k}_m = 0, \ m \neq 0, \end{cases}$$

and for odd values as:

$$a^{j,2k-1} : \begin{cases} a^{j,2k+1}_{-2m-1} = \lambda^{l_{j,2k+1},r_{j,2k+1}}_{j-1,m}, \text{ for } m = -l_{j,2k+1}, \dots, r_{j,2k+1}-1, \\ a^{j,2k+1}_m = 0 \text{ otherwise.} \end{cases}$$

This kind of subdivision scheme has two main advantages. Since it is based on Kriging theory, its mask integrates the spatial structure of the data identified from the observations through the semi-variogram. Therefore, it avoids extra assumptions related to the

behavior of the data that could reduce the reliability of the results. Moreover, it keeps the flexibility of classical subdivision schemes allowing for example a position-dependent or zone-dependent strategy (Sections 2.3.4 and 2.3.5) that appears to be efficient for the reconstruction of non-regular phenomena.

3.3.2 Convergence analysis

Asymptotical subdivision scheme

As mentioned previously, Kriging-based schemes are non-stationary. The convergence analysis is therefore performed by exploiting Theorem 2.2.3 i.e. by studying the limit process and its connection to convergent stationary scheme. The next two propositions are devoted to the limit of the Kriging weights when $j \to +\infty$ for semi-variograms of types $\mathcal{G}^\star_{OD}$ and $\mathcal{G}^\star_{ED}$ (that encompass most of the classical semi-variograms used in practice). The proofs are not provided since they can be found in [1].

Proposition 3.3.1 *The Kriging weights associated with a $\mathcal{G}^\star_{OD}$-type semi-variogram satisfy:*

$$\begin{aligned}
(\lambda^{r,r}_{j,-r+1},\cdots,\lambda^{r,r}_{j,r}) &\to_{j\to+\infty} (L^{r,r}_{-r+1}(\frac{1}{2}),\cdots,L^{r,r}_{r}(\frac{1}{2})),\\
(\lambda^{r-1,r+1}_{j,-r+2},\cdots,\lambda^{r-1,r+1}_{j,r+1}) = (\lambda^{r+1,r-1}_{j,r-2},\cdots,\lambda^{r+1,r-1}_{j,-r-1}) &\to_{j\to+\infty} (L^{r-1,r+1}_{-r+2}(\frac{1}{2}),\cdots,L^{r-1,r+1}_{r+1}(\frac{1}{2})),\\
&\cdots\\
(\lambda^{1,2r-1}_{j,0},\cdots,\lambda^{1,2r-1}_{j,2r-1}) = (\lambda^{2r-1,1}_{j,0},\cdots,\lambda^{2r-1,1}_{j,-2r+1}) &\to_{j\to+\infty} (L^{1,2r-1}_{0}(\frac{1}{2}),\cdots,L^{1,2r-1}_{2r-1}(\frac{1}{2})),\\
(\lambda^{0,2r}_{j,1},\cdots,\lambda^{0,2r}_{j,2r}) = (\lambda^{2r,0}_{j,-1},\cdots,\lambda^{2r,0}_{j,-2r}) &\to_{j\to+\infty} (L^{0,2r}_{1}(\frac{1}{2}),\cdots,L^{0,2r}_{2r}(\frac{1}{2})).
\end{aligned}$$

Proposition 3.3.2 *The Kriging weights associated with a $\mathcal{G}^\star_{ED}$-type semi-variograms satisfy:*

$$\begin{aligned}
(\lambda^{r,r}_{j,-r+1},\cdots,\lambda^{r,r}_{j,r}) &\to_{j\to+\infty} \frac{1}{2}\delta_r+\frac{1}{2}\delta_{r+1},\\
(\lambda^{r-1,r+1}_{j,-r+2},\cdots,\lambda^{r-1,r+1}_{j,r+1}) = (\lambda^{r+1,r-1}_{j,r-2},\cdots,\lambda^{r+1,r-1}_{j,-r-1}) &\to_{j\to+\infty} \frac{1}{2}\delta_{r-1}+\frac{1}{2}\delta_r,\\
&\cdots\\
(\lambda^{1,2r-1}_{j,0},\cdots,\lambda^{1,2r-1}_{j,2r-1}) = (\lambda^{2r-1,1}_{j,0},\cdots,\lambda^{2r-1,1}_{j,-2r+1}) &\to_{j\to+\infty} \frac{1}{2}\delta_1+\frac{1}{2}\delta_2,\\
(\lambda^{0,2r}_{j,1},\cdots,\lambda^{0,2r}_{j,2r}) = (\lambda^{2r,0}_{j,-1},\cdots,\lambda^{2r,0}_{j,-2r}) &\to_{j\to+\infty} \delta_1.
\end{aligned}$$

where δ_{k_1} is the $2r$-vector defined by $\delta_{k_1,m}=1$ for $m=k_1$ and 0 otherwise.

Convergence of the asymptotical subdivision scheme

The analysis is restricted to Kriging-based schemes following translation-invariant and position-dependent (Figure 2.8) strategies as described in Chapter 2. According to Proposition 3.3.1, the asymptotical scheme associated with $\mathcal{G}^{\star}_{OD}$ semi-variograms coincides with the $2r$-point stencil Lagrange interpolatory scheme whose convergence has been proved in [8]. Therefore, we focus in the sequel on $\mathcal{G}^{\star}_{ED}$ semi-variograms. Following the matrix formalism and exploiting Proposition 3.3.2, a set of refinement and edge matrices can be constructed as follows.

Proposition 3.3.3 *The two refinement matrices associated with the translation-invariant asymptotical schemes are* $A_0 = \begin{bmatrix} 1 & 0 \\ \frac{1}{2} & \frac{1}{2} \end{bmatrix}$ *and* $A_1 = \begin{bmatrix} \frac{1}{2} & \frac{1}{2} \\ 0 & 1 \end{bmatrix}$ *with* $Sp(A_0) = Sp(A_1) = \{1, \frac{1}{2}\}$.

Moreover, the four edge matrices near the segmentation point y_0 *read:*

- *if* $y_0 \in [x^j_{2k_{j-1}-2}, x^j_{2k_{j-1}-1}[$, $A_2^- = \begin{bmatrix} \frac{1}{2} & \frac{1}{2} \\ 0 & 1 \end{bmatrix}$ *and* $A_2^+ = \begin{bmatrix} 1 & 0 \\ 1 & 0 \end{bmatrix}$ *with* $Sp(A_2^-) = \{\frac{1}{2}, 1\}$ *and* $Sp(A_2^+) = \{0, 1\}$.
- *if* $y_0 \in [x^j_{2k_{j-1}-1}, x^j_{2k_{j-1}}]$, $A_2^- = \begin{bmatrix} 0 & 1 \\ 0 & 1 \end{bmatrix}$ *and* $A_2^+ = \begin{bmatrix} 1 & 0 \\ \frac{1}{2} & \frac{1}{2} \end{bmatrix}$ *with* $Sp(A_2^-) = \{0, 1\}$ *and* $Sp(A_2^+) = \{\frac{1}{2}, 1\}$.

Since the eigenvalues except of the eigenvalue 1 are of modulus strictly less than 1, Theorem 2.2.2 ensures the uniform convergence of the asymptotical scheme and the next proposition finally holds.

Proposition 3.3.4 *The translation-invariant and position-dependent Kriging-based subdivision schemes of parameter (D,r,r) associated with a* $\mathcal{G}^{\star}_{OD}$*-type and* $\mathcal{G}^{\star}_{ED}$*-type semi-variogram are uniformly convergent.*

3.4 Numerical tests

3.4.1 Limit functions

This section provides the limit functions associated with Kriging-based interpolatory subdivision scheme with translation-invariant and position-dependent stencils. We are interested in the limiting process starting from an initial sequence $f^0 = \{\delta_{k,0}\}$ and the final level is $J_{max} = 6$. We assume that the data exhibit one of the following two structures:

$$\begin{cases} 1 - e^{-ah} : \mathcal{G}^{\star}_{ED}\text{-type semi-variogram} \\ 1 - e^{-(ah)^2} : \mathcal{G}^{\star}_{OD}\text{-type semi-variogram} \end{cases}$$

with $a \in I\!R$. Figure 3.4 displays the limit functions associated with translation-invariant Kriging-based interpolatory subdivision scheme with respect to a.

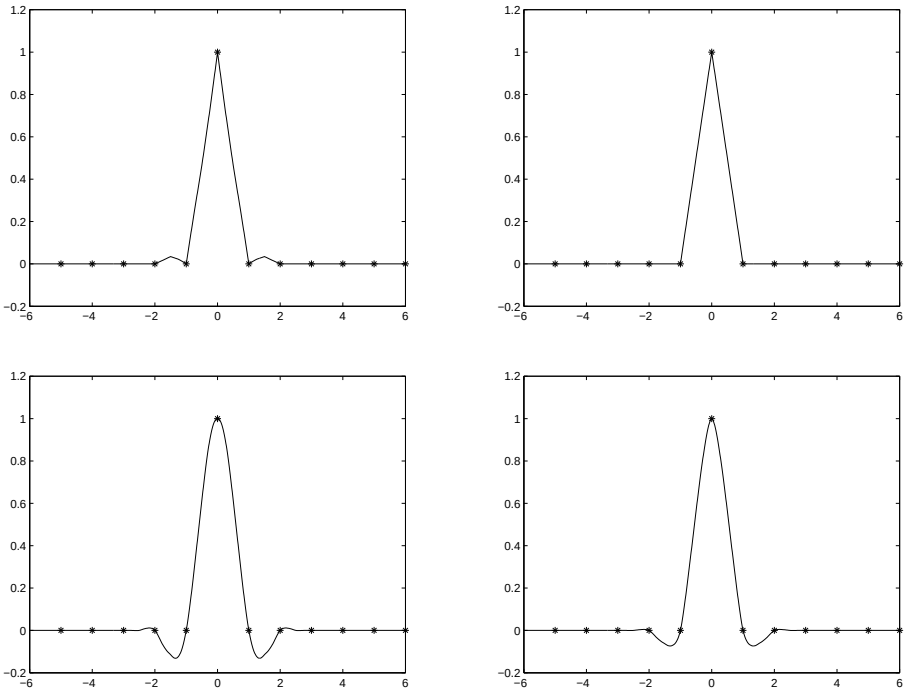

Figure 3.4: Limit functions of translation-invariant Kriging schemes starting from the initial sequence $(\delta_{n,0})_n$. Top left: exponential model with $a = 1$, top right: exponential model with $a = 0.004$, bottom left: Gaussian model with $a = 1$, bottom right: Gaussian model with $a = 0.04$.

On Figure 3.5, we plot the limit functions associated with position-dependent Kriging-based interpolatory subdivision scheme, assuming the position of discontinuity at $x_0 = -2$.

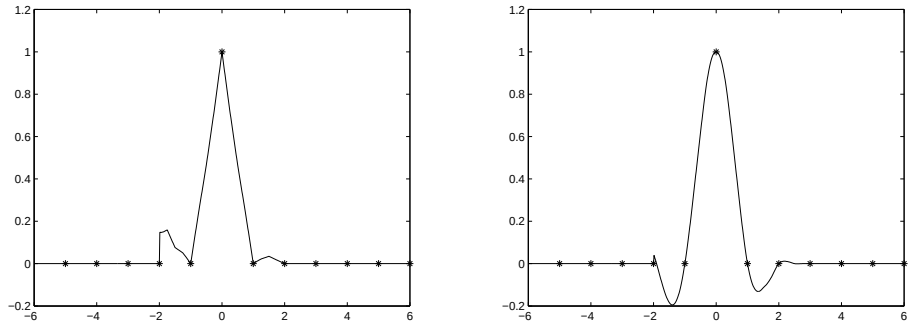

Figure 3.5: Limit functions of position-dependent Kriging schemes starting from the initial sequence $(\delta_{n,0})_n$ with the discontinuity position assumed at $x_0 = -2$. Left: exponential model with $a = 1$, right: Gaussian model with $a = 1$.

3.4.2 Prediction of 1D data

This numerical test is taken from [1].
Kriging and Lagrange interpolatory subdivision schemes are here compared on 1d discontinuous data. The test function (thick solid line on Figure 3.6) is defined on the interval $[0, 1000]$ by:

$$f(x) = \left(-2 \times \frac{sin(\frac{30}{1000}x)}{2 + \frac{x}{1000}} + 2\right) \chi_{[255,475]} - \left(2 \times \frac{sin(\frac{8}{1000}x)}{1 + \frac{x}{1000}}\right) \chi_{[0,1000]\setminus[255,475]}$$

For the sake of simplicity, in the case of a Kriging strategy, we have chosen to decouple the problem of the semi-variogram identification and the subdivision scheme-based prediction. For this simplified univariate example, the semi-variogram in each zone is therefore estimated by considering a sufficiently fine discretization of the test function. Moreover, since our goal is to focus on prediction, we assume that the segmentation points $\{255, 475\}$ are known at each scale j and we apply a position-dependent Kriging and Lagrange interpolatory predictions between $J_0 = 4$ and $J_{max} = 9$.

It turns out that the position-dependent Kriging-based strategy improves the prediction. As for the data in the vicinity of the segmentation points, a strong undershoot

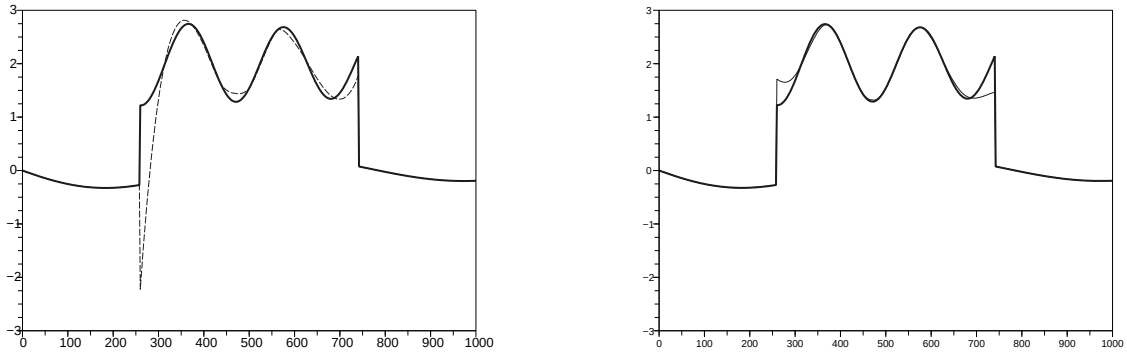

Figure 3.6: Predicted data ($J_0 = 4$, $J_{max} = 9$). Left, position-dependent Lagrange (dashed line) interpolation, right, Kriging (solid line) interpolation. The thick solid line corresponds to the exact surface.

appears at $x = 250$ in the Lagrange case whereas it is reduced with the Kriging-based prediction. Moreover, the improvement of the prediction is not restricted to the area around the segmentation points. Indeed, thanks to the construction of a semi-variogram in each zone, the structure of the data is faithfully identified leading to a better prediction around $x = 470$ for example.

3.5 Conclusion

A new type of subdivision scheme has been recalled. Its originality lies in the construction of the mask which is based on Kriging theory. This framework allows one to take into account the spatial structure of the data thanks to the identification of a semi-variogram and therefore avoids artificial assumptions related to the behavior of the studied phenomenon. After a full description of the Kriging-based scheme, a convergence analysis has been performed by exploiting the connection between Kriging and Lagrange weights. It came out that this new type of scheme is uniformly convergent for most of the semi-variogram models encountered in practice. Finally, the numerical tests devoted to the reconstruction of non-regular data have pointed out a significant improvement compared to classical Lagrange scheme due to the possibility to integrate the local spatial structure in the prediction operator. However, this scheme remains interpolatory. Therefore, the

quality of the position-dependent reconstruction is strongly reduced in case of inaccurate discontinuity detection and the presence of noise does not allow one to recover the original data. In order to circumvent these limitations, the next chapter introduces a new approach still based on Kriging theory but combining interpolatory and non-interpolatory predictions thanks to the introduction of an error variance.

Chapter 4

Kriging-based subdivision scheme with error variance

4.1 Introduction

This chapter is devoted to a generalization of Kriging-based subdivision schemes that combines interpolatory and non-interpolatory strategies. Its construction exploits the possibility to introduce in the Kriging framework an error variance (Chapter 3) to relax the constraint of interpolatory predictions at the observation points.
Section 4.2 provides a general description of this new type of scheme. Then, a connection with classical subdivision schemes is established in Section 4.3 by focussing on the analysis of the asymptotical behavior of the Kriging weights with respect to the number of non-zero error variances for a 4-point stencil. In order to improve the accuracy of the reconstruction of non-regular data, an example of Kriging-based scheme with error variance is given in Section 4.4. It is based on three main ingredients: a segmentation of the data leading to a splitting in different zones containing regular or non-regular data, the construction of a local predictor integrating the information coming from the segmentation and defining zone-dependent subdivision schemes, and the adaption of the schemes close to the segmentation points. Its convergence is analyzed as well. Finally in Section 4.5, several numerical experiments and comparisons with other classical subdivision schemes are performed.

4.2 Construction of Kriging-based subdivision schemes with error variance

Similarly to Section 3.3, the Kriging estimator including error variance can be interpreted as a two-scale relation involved in a subdivision scheme.
Assuming that the semi-variogram has been identified from the initial data f^0 and generalizing (3.17), the Kriging-based subdivision scheme with error variance is defined by:

$$\left\{\begin{array}{rcl} f^j_{2k} & = & \sum_{m=-l_{j,2k}+1}^{r_{j,2k}} \tilde{\lambda}^{l_{j,2k},r_{j,2k},\mathcal{C}_{j,2k}}_{j,m} f^{j-1}_{k+m} \ , \\ f^j_{2k+1} & = & \sum_{m=-l_{j,2k+1}+1}^{r_{j,2k+1}} \lambda^{l_{j,2k+1},r_{j,2k+1},\mathcal{C}_{j,2k+1}}_{j,m} f^{j-1}_{k+m} \ , \end{array}\right. \tag{4.1}$$

The family $\{\tilde{\lambda}^{l_{j,2k},r_{j,2k},\mathcal{C}_{j,2k}}_{j,m}\}_m$ (resp. $\{\lambda^{l_{j,2k+1},r_{j,2k+1},\mathcal{C}_{j,2k+1}}_{j,m}\}_m$) stands for the Kriging weights solution of the Kriging problem with error variance where $\mathcal{C}$ is replaced by $\mathcal{C}_{j,2k}$ (resp. $\mathcal{C}_{j,2k+1}$).
(4.1) is a generalization of the Kriging-based subdivision schemes described in the previous chapter. More precisely, if $\mathcal{C}_{j,2k}$ and $\mathcal{C}_{j,2k+1}$ are the null vectors, (4.1) is reduced to Algorithm 3.17. Therefore, besides the advantages mentioned in Section 3.3, the proposed Kriging-based scheme allows one to locally relax the interpolation constraint at the observation points by introducing an artificial vector of error variance (we refer to Section 4.4 for an example of such a choice). The next sections are devoted to the convergence analysis of this new scheme assuming $l_{j,2k} = l_{j,2k+1} = l_{j,k}$ and $r_{j,2k} = r_{j,2k+1} = r_{j,k}$ in the case of a 4-point centered stencil, i.e. $\forall (k,j) \in \mathbb{Z}^2$, $l_{j,k} = r_{j,k} = 2$. It is based on the asymptotical connection between Kriging and Lagrange weights which is fully established in the sequel.

4.3 Connection between Kriging and Lagrange weights

4.3.1 Main results

The two following propositions provide the limit when j goes to infinity of the Kriging weights including error variance. For the sake of clarity, we postpone the corresponding proofs to Sections 4.3.2 and 4.3.3.
Obviously, this analysis depends on the number and on the position of non-zero coefficients in the error variance vector. For the sake of simplicity and without loss of generality,

we focus on four cases corresponding to the following vectors: $(c_1, 0, 0, 0)$, $(c_1, c_2, 0, 0)$, $(c_1, c_2, c_3, 0)$ and (c_1, c_2, c_3, c_4) with $c_i > 0$.

Proposition 4.3.1
For any $(c_1, c_2, c_3, c_4) \in (\mathbb{R}^+)^4$, the limits when $j \to +\infty$ of the Kriging weights associated with a $\mathcal{G}^\star_{OD}$-type semi-variogram satisfy:

- *One non-zero error variance:*
  - $\left(\tilde{\lambda}^{2,2,\mathcal{C}}_{j,-1}, \tilde{\lambda}^{2,2,\mathcal{C}}_{j,0}, \tilde{\lambda}^{2,2,\mathcal{C}}_{j,1}, \tilde{\lambda}^{2,2,\mathcal{C}}_{j,2}\right) = (0, 1, 0, 0)$,
  - $\left(\lambda^{2,2,\mathcal{C}}_{j,-1}, \lambda^{2,2,\mathcal{C}}_{j,0}, \lambda^{2,2,\mathcal{C}}_{j,1}, \lambda^{2,2,\mathcal{C}}_{j,2}\right) \to_{j\to+\infty} \left(0, L^{1,2}_0(\frac{1}{2}), L^{1,2}_1(\frac{1}{2}), L^{1,2}_2(\frac{1}{2})\right)$.
- *Two non-zero penalization coefficients:*
  - $\left(\tilde{\lambda}^{2,2,\mathcal{C}}_{j,-1}, \tilde{\lambda}^{2,2,\mathcal{C}}_{j,0}, \tilde{\lambda}^{2,2,\mathcal{C}}_{j,1}, \tilde{\lambda}^{2,2,\mathcal{C}}_{j,2}\right) \to_{j\to+\infty} \left(0, 0, L^{0,2}_1(-1), L^{0,2}_2(-1)\right)$,
  - $\left(\lambda^{2,2,\mathcal{C}}_{j,-1}, \lambda^{2,2,\mathcal{C}}_{j,0}, \lambda^{2,2,\mathcal{C}}_{j,1}, \lambda^{2,2,\mathcal{C}}_{j,2}\right) \to_{j\to+\infty} \left(0, 0, L^{0,2}_1(-\frac{1}{2}), L^{0,2}_2(-\frac{1}{2})\right)$.
- *Three non-zero penalization coefficients:*
  - $\left(\tilde{\lambda}^{2,2,\mathcal{C}}_{j,-1}, \tilde{\lambda}^{2,2,\mathcal{C}}_{j,0}, \tilde{\lambda}^{2,2,\mathcal{C}}_{j,1}, \tilde{\lambda}^{2,2,\mathcal{C}}_{j,2}\right) \to_{j\to+\infty} (0, 0, 0, 1)$,
  - $\left(\lambda^{2,2,\mathcal{C}}_{j,-1}, \lambda^{2,2,\mathcal{C}}_{j,0}, \lambda^{2,2,\mathcal{C}}_{j,1}, \lambda^{2,2,\mathcal{C}}_{j,2}\right) \to_{j\to+\infty} (0, 0, 0, 1)$.
- *Four non-zero penalization coefficients:*
  - $\left(\tilde{\lambda}^{2,2,\mathcal{C}}_{j,-1}, \tilde{\lambda}^{2,2,\mathcal{C}}_{j,0}, \tilde{\lambda}^{2,2,\mathcal{C}}_{j,1}, \tilde{\lambda}^{2,2,\mathcal{C}}_{j,2}\right) \to_{j\to+\infty} (\frac{\Pi^4_{i=1,i\neq m} c_i}{\sum_{n=1}^4 \Pi^4_{i=1,i\neq n} c_i})_{1\leq m\leq 4}$,
  - $\left(\lambda^{2,2,\mathcal{C}}_{j,-1}, \lambda^{2,2,\mathcal{C}}_{j,0}, \lambda^{2,2,\mathcal{C}}_{j,1}, \lambda^{2,2,\mathcal{C}}_{j,2}\right) \to_{j\to+\infty} \to_{j\to+\infty} (\frac{\Pi^4_{i=1,i\neq m} c_i}{\sum_{n=1}^4 \Pi^4_{i=1,i\neq n} c_i})_{1\leq m\leq 4}$.

Proposition 4.3.2
For any $(c_1, c_2, c_3, c_4) \in (\mathbb{R}^+)^4$, the limits when $j \to +\infty$ of the Kriging weights associated with a $\mathcal{G}^\star_{ED}$-type semi-variogram satisfy:

- *One non-zero error variance:*
  - $\left(\tilde{\lambda}^{2,2,\mathcal{C}}_{j,-1}, \tilde{\lambda}^{2,2,\mathcal{C}}_{j,0}, \tilde{\lambda}^{2,2,\mathcal{C}}_{j,1}, \tilde{\lambda}^{2,2,\mathcal{C}}_{j,2}\right) = (0, 1, 0, 0)$,
  - $\left(\lambda^{2,2,\mathcal{C}}_{j,-1}, \lambda^{2,2,\mathcal{C}}_{j,0}, \lambda^{2,2,\mathcal{C}}_{j,1}, \lambda^{2,2,\mathcal{C}}_{j,2}\right) \to_{j\to+\infty} \left(0, \frac{1}{2}, \frac{1}{2}, 0\right)$.
- *Two non-zero penalization coefficients:*

  - $\left(\tilde{\lambda}^{2,2,\mathcal{C}}_{j,-1}, \tilde{\lambda}^{2,2,\mathcal{C}}_{j,0}, \tilde{\lambda}^{2,2,\mathcal{C}}_{j,1}, \tilde{\lambda}^{2,2,\mathcal{C}}_{j,2}\right) \to_{j\to+\infty} (0,0,1,0)$,
  - $\left(\lambda^{2,2,\mathcal{C}}_{j,-1}, \lambda^{2,2,\mathcal{C}}_{j,0}, \lambda^{2,2,\mathcal{C}}_{j,1}, \lambda^{2,2,\mathcal{C}}_{j,2}\right) \to_{j\to+\infty} (0,0,1,0)$.

- *Three non-zero penalization coefficients:*
  - $\left(\tilde{\lambda}^{2,2,\mathcal{C}}_{j,-1}, \tilde{\lambda}^{2,2,\mathcal{C}}_{j,0}, \tilde{\lambda}^{2,2,\mathcal{C}}_{j,1}, \tilde{\lambda}^{2,2,\mathcal{C}}_{j,2}\right) \to_{j\to+\infty} (0,0,0,1)$,
  - $\left(\lambda^{2,2,\mathcal{C}}_{j,-1}, \lambda^{2,2,\mathcal{C}}_{j,0}, \lambda^{2,2,\mathcal{C}}_{j,1}, \lambda^{2,2,\mathcal{C}}_{j,2}\right) \to_{j\to+\infty} (0,0,0,1)$.

- *Four non-zero penalization coefficients:*
  - $\left(\tilde{\lambda}^{2,2,\mathcal{C}}_{j,-1}, \tilde{\lambda}^{2,2,\mathcal{C}}_{j,0}, \tilde{\lambda}^{2,2,\mathcal{C}}_{j,1}, \tilde{\lambda}^{2,2,\mathcal{C}}_{j,2}\right) \to_{j\to+\infty} (\frac{\Pi^4_{i=1,i\neq m} c_i}{\sum_{n=1}^4 \Pi^4_{i=1,i\neq n} c_i})_{1\leq m\leq 4}$,
  - $\left(\lambda^{2,2,\mathcal{C}}_{j,-1}, \lambda^{2,2,\mathcal{C}}_{j,0}, \lambda^{2,2,\mathcal{C}}_{j,1}, \lambda^{2,2,\mathcal{C}}_{j,2}\right) \to_{j\to+\infty} \to_{j\to+\infty} (\frac{\Pi^4_{i=1,i\neq m} c_i}{\sum_{n=1}^4 \Pi^4_{i=1,i\neq n} c_i})_{1\leq m\leq 4}$.

4.3.2 Proofs of Proposition 4.3.1

We start by the following useful notations:

Definition 4.3.1
Denoting for any $(b_0, b_1) \in (\mathbb{R}^\star)^2$, $P_4(x) = b_0x^2 + b_1x^4$, *we introduce*

$$A_0 = \begin{bmatrix} 0 & P_{4,j}(1) & P_{4,j}(2) & P_{4,j}(3) & 1 \\ P_{4,j}(1) & 0 & P_{4,j}(1) & P_{4,j}(2) & 1 \\ P_{4,j}(2) & P_{4,j}(1) & 0 & P_{4,j}(1) & 1 \\ P_{4,j}(3) & P_{4,j}(2) & P_{4,j}(1) & 0 & 1 \\ 1 & 1 & 1 & 1 & 0 \end{bmatrix} \tag{4.2}$$

where $P_{4,j}(x) = P_4(2^{-j}x)$.
Moreover, when considering error variance vectors, we define for any $k \in \{1,\dots,4\}$,

$$A_k = \begin{bmatrix} -c_1 & P_{4,j}(1) & P_{4,j}(2) & P_{4,j}(3) & 1 \\ P_{4,j}(1) & -c_2 & P_{4,j}(1) & P_{4,j}(2) & 1 \\ P_{4,j}(2) & P_{4,j}(1) & \dots & P_{4,j}(1) & 1 \\ P_{4,j}(3) & P_{4,j}(2) & P_{4,j}(1) & -c_k & 1 \\ 1 & 1 & 1 & 1 & 0 \end{bmatrix}. \tag{4.3}$$

Finally, for any $k \in \{0,\dots,4\}$, *we note the general term* $[A_k^{-1}]_{in}$ *of* A_k^{-1} *as* $[A_k^{-1}]_{in} = A^{(k)}_{i-1,n-1}, 1 \leq i,n \leq 5$.

In the next propositions, we focus on the existence of the solution of $A_k U^{(k)} = f$ ($k \in \{0, \dots, 4\}$) where $f = (P_{4,j}(1), P_{4,j}(0), P_{4,j}(1), P_{4,j}(2), 1)^T$ or $f = (P_{4,j}(\frac{3}{2}), P_{4,j}(\frac{1}{2}), P_{4,j}(\frac{1}{2}), P_{4,j}(\frac{3}{2}), 1)^T$.

Proposition 4.3.3
For any $j \in \mathbb{Z}$, there exists a unique solution of $A_0 U^{(0)} = f$ satisfying:

- *If $f = (P_{4,j}(1), P_{4,j}(0), P_{4,j}(1), P_{4,j}(2), 1)^T$,*

$$U^{(0)} = (0, 1, 0, 0, 0)^T . \tag{4.4}$$

- *If $f = (P_{4,j}(\frac{3}{2}), P_{4,j}(\frac{1}{2}), P_{4,j}(\frac{1}{2}), P_{4,j}(\frac{3}{2}), 1)^T$,*

$$U^{(0)} = \left(L_{-2}^{2,2}(-\frac{1}{2}), L_{-1}^{2,2}(-\frac{1}{2}), L_{0}^{2,2}(-\frac{1}{2}), L_{1}^{2,2}(-\frac{1}{2}), \mu_L \right)^T . \tag{4.5}$$

where $\mu_L = P_{4,j}(\frac{3}{2}) - \left(\frac{9}{16} P_{4,j}(1) + \frac{9}{16} P_{4,j}(2) - \frac{1}{16} P_{4,j}(3)\right)$.

Moreover, the coefficients of A_0^{-1} can be expressed as: $\forall 0 \leq i \leq 3$,

$$\begin{cases} A_{i0}^{(0)} = \frac{2^{4j}}{b_1} \left(\frac{\alpha_{1,i}}{24} + \frac{\alpha_{2,i}}{6} + \frac{11}{24} \alpha_{3,i} \right) - \frac{\alpha_{3,i}}{48} \frac{b_0}{b_1^2} 2^{6j}, \\ A_{i1}^{(0)} = \frac{2^{4j}}{b_1} (-\frac{\alpha_{1,i}}{8} - \frac{5}{12} \alpha_{2,i} - \frac{3}{4} \alpha_{3,i}) + \frac{\alpha_{3,i} b_0 2^{6j}}{16 b_1^2}, \\ A_{i2}^{(0)} = \frac{2^{4j}}{b_1} (\frac{\alpha_{1,i}}{8} + \frac{1}{3} \alpha_{2,i} + \frac{3}{8} \alpha_{3,i}) - \frac{\alpha_{3,i} b_0 2^{6j}}{16 b_1^2}, \\ A_{i3}^{(0)} = \frac{2^{4j}}{b_1} (-\frac{\alpha_{1,i}}{24} - \frac{1}{12} \alpha_{2,i} - \frac{1}{12} \alpha_{3,i}) + \frac{\alpha_{3,i} b_0 2^{6j}}{48 b_1^2}, \end{cases} \tag{4.6}$$

with

$$\begin{bmatrix} \alpha_{0,0} & \alpha_{0,1} & \alpha_{0,2} & \alpha_{0,3} \\ \alpha_{1,0} & \alpha_{1,1} & \alpha_{1,2} & \alpha_{1,3} \\ \alpha_{2,0} & \alpha_{2,1} & \alpha_{2,2} & \alpha_{2,3} \\ \alpha_{3,0} & \alpha_{3,1} & \alpha_{3,2} & \alpha_{3,3} \end{bmatrix} = \begin{bmatrix} 1 & 0 & 0 & 0 \\ -\frac{11}{6} & 3 & -\frac{3}{2} & \frac{1}{3} \\ 1 & -\frac{5}{2} & 2 & -\frac{1}{2} \\ -\frac{1}{6} & \frac{1}{2} & -\frac{1}{2} & \frac{1}{6} \end{bmatrix}.$$

and

$$\begin{cases} A_{40}^{(0)} = 1 - 2^{-2j} b_0 (A_{10}^{(0)} + 4A_{20}^{(0)} + 9A_{30}^{(0)}) - 2^{-4j} b_1 (A_{10}^{(0)} + 16A_{20}^{(0)} + 81A_{30}^{(0)}), \\ A_{4i}^{(0)} = -2^{-2j} b_0 (A_{1i}^{(0)} + 4A_{2i}^{(0)} + 9A_{3i}^{(0)}) - 2^{-4j} b_1 (A_{1i}^{(0)} + 16A_{2i}^{(0)} + 81A_{3i}^{(0)}), \ i \in \{1, \dots, 4\}. \end{cases} \tag{4.7}$$

Proof:

The details of the proof related to the solution of $A_0U^{(0)} = f$ are not given in the sequel. This result can be obtained by performing the same calculation as in the proof of Proposition 4.6 (Step 3) in [1]. It is based on two steps: we first verify that the Lagrange weights are solution of $A_0U = f$ with $\mu = 0$ and $\mu = P_{4,j}(\frac{3}{2}) - \big(\frac{9}{16}P_{4,j}(1) + \frac{9}{16}P_{4,j}(2) - \frac{1}{16}P_{4,j}(3)\big)$; then, the uniqueness of the solution is ensured by studying the kernel of A_0 leading to a linear system involving a Vandermonde matrix.

Therefore, we focus in the remaining of this proof on the derivation of the first equation of Systems (4.6) and (4.7). The remaining of the system can be obtained following the same track.

The first column of A_0^{-1} is the solution of

$$A_0U = (1, 0, 0, 0, 0)^T \tag{4.8}$$

Introducing the polynomial $K(x) = A_{00}^{(0)}P_{4,j}(x) + A_{10}^{(0)}P_{4,j}(x-1) + A_{20}^{(0)}P_{4,j}(x-2) + A_{30}^{(0)}P_{4,j}(x-3) + A_{40}^{(0)} - L_0^{0,3}(x)$, (4.8) leads to $\forall i \in \{0, \ldots, 3\},\ K(i) = 0$ i.e. K has 4 roots. Since $A_{00}^{(0)} + A_{10}^{(0)} + A_{20}^{(0)} + A_{30}^{(0)} = 0$ (last equation of (4.8)), K is a polynomial of degree 3, therefore, $\forall x \in I\!R,\ K(x) = 0$. It implies that the coefficients associated with each power of x are equal to 0, i.e.

$$\begin{cases} \text{for } x^3 : -4b_1 2^{-4j} \sum_{i=0}^{3} iA_{i0}^{(0)} + \frac{1}{6} = 0, \\ \text{for } x^2 : 6b_1 2^{-4j} \sum_{i=0}^{3} i^2 A_{i0}^{(0)} - 1 = 0, \\ \text{for } x : -4b_1 2^{-4j} \sum_{i=0}^{3} i^3 A_{i0}^{(0)} + \frac{11}{6} - \frac{2^{2j}b_0}{12b_1} = 0, \\ \text{for } 1 : 2^{-2j}b_0(A_{10}^{(0)} + 4A_{20}^{(0)} + 9A_{30}^{(0)}) + 2^{-4j}b_1(A_{10}^{(0)} + 16A_{20}^{(0)} + 81A_{30}^{(0)}) + A_{40}^{(0)} - 1 = 0, \end{cases}$$

leading to

$$\begin{bmatrix} 1 & 1 & 1 & 1 \\ 0 & 1 & 2 & 3 \\ 0 & 1 & 4 & 9 \\ 0 & 1 & 8 & 27 \end{bmatrix} \begin{bmatrix} A_{00}^{(0)} \\ A_{10}^{(0)} \\ A_{20}^{(0)} \\ A_{30}^{(0)} \end{bmatrix} = \begin{bmatrix} 0 \\ \frac{1}{24b_1}2^{4j} \\ \frac{1}{6b_1}2^{4j} \\ \frac{11}{24b_1}2^{4j} - \frac{b_0}{48b_1^2}2^{6j} \end{bmatrix}, \tag{4.9}$$

and $A_{40}^{(0)} = 1 - 2^{-2j} b_0 (A_{10}^{(0)} + 4A_{20}^{(0)} + 9A_{30}^{(0)}) - 2^{-4j} b_1 (A_{10}^{(0)} + 16A_{20}^{(0)} + 81A_{30}^{(0)})$.

Denoting by M the left hand side matrix in Equation (4.9), our goal is to calculate M^{-1}. By definition, since M is a Vandermonde matrix, its transpose M^T connects the basis $(1, x, x^2, x^3)$ to the basis $(L_0^{0,4}(x), L_1^{0,4}(x), L_2^{0,4}(x), L_3^{0,4}(x))$. Therefore, writing $\forall i \in \{0, \dots, 3\},\ L_i^{0,4}(x) = \alpha_{3,i} x^3 + \alpha_{2,i} x^2 + \alpha_{1,i} x + \alpha_{0,i}$, we have

$$M^T \begin{bmatrix} \alpha_{0,i} \\ \alpha_{1,i} \\ \alpha_{2,i} \\ \alpha_{3,i} \end{bmatrix} = \Delta_i,$$

where Δ_i is the vector such that $\forall n \in \{1, \dots, 4\}$, $(\Delta_i)_n = \delta_{n,i}$. It then turns out that $(\alpha_{0,i}\ \alpha_{1,i}\ \alpha_{2,i}\ \alpha_{3,i})^T$ is the i^{th} column of $(M^T)^{-1}$. Therefore, after a short calculus,

$$M^{-1} = \begin{bmatrix} \alpha_{0,0} & \alpha_{0,1} & \alpha_{0,2} & \alpha_{0,3} \\ \alpha_{1,0} & \alpha_{1,1} & \alpha_{1,2} & \alpha_{1,3} \\ \alpha_{2,0} & \alpha_{2,1} & \alpha_{2,2} & \alpha_{2,3} \\ \alpha_{3,0} & \alpha_{3,1} & \alpha_{3,2} & \alpha_{3,3} \end{bmatrix} = \begin{bmatrix} 1 & 0 & 0 & 0 \\ -\frac{11}{6} & 3 & -\frac{3}{2} & \frac{1}{3} \\ 1 & -\frac{5}{2} & 2 & -\frac{1}{2} \\ -\frac{1}{6} & \frac{1}{2} & -\frac{1}{2} & \frac{1}{6} \end{bmatrix}.$$

Coming back to (4.9), it finally provides the first equation of System (4.6). That concludes the proof.

■

Proposition 4.3.4
For any $j \in \mathbb{Z}$, if $c_1 \in D_j$ where $D_j = \{c_1 > 0 / c_1 \neq \frac{1}{A_{00}^{(0)}}$ with $A_{00}^{(0)} \neq 0\}$, there exists a unique solution of $A_1 U^{(1)} = f$ that satisfies:

- *If $f = (P_{4,j}(1), P_{4,j}(0), P_{4,j}(1), P_{4,j}(2), 1)^T$,*

$$U^{(1)} = (0, 1, 0, 0, 0)^T. \tag{4.10}$$

- *If* $f = (P_{4,j}(\frac{3}{2}), P_{4,j}(\frac{1}{2}), P_{4,j}(\frac{1}{2}), P_{4,j}(\frac{3}{2}), 1)^T$,

$$U^{(1)} = \begin{bmatrix} \frac{1}{(1-c_1 A_{00}^{(0)})} U_0^{(0)} \\ U_1^{(0)} + \frac{c_1 A_{10}^{(0)}}{(1-c_1 A_{00}^{(0)})} U_0^{(0)} \\ U_2^{(0)} + \frac{c_1 A_{20}^{(0)}}{(1-c_1 A_{00}^{(0)})} U_0^{(0)} \\ U_3^{(0)} + \frac{c_1 A_{30}^{(0)}}{(1-c_1 A_{00}^{(0)})} U_0^{(0)} \\ U_4^{(0)} + \frac{c_1 A_{40}^{(0)}}{(1-c_1 A_{00}^{(0)})} U_0^{(0)} \end{bmatrix}. \tag{4.11}$$

where $\{A_{i0}^{(0)}\}_{i=0,\dots,4}$ *is given by Systems (4.6) and (4.7).*

Proof:

- Existence and uniqueness of the solution:

Splitting A_1 into $A_0 + \tilde{A}_1$ and writing, since A_0^{-1} exists, $A_1 = A_0(I + A_0^{-1}\tilde{A}_1)$, the invertibility of A_1 is ensured as soon as $B_0 = (I + A_0^{-1}\tilde{A}_1)$ is invertible. B_0 can be expressed as:

$$B_0 = \begin{bmatrix} 1 - c_1 A_{00}^{(0)} & 0 & 0 & 0 & 0 \\ -c_1 A_{10}^{(0)} & 1 & 0 & 0 & 0 \\ -c_1 A_{20}^{(0)} & 0 & 1 & 0 & 0 \\ -c_1 A_{30}^{(0)} & 0 & 0 & 1 & 0 \\ -c_1 A_{40}^{(0)} & 0 & 0 & 0 & 1 \end{bmatrix}, \tag{4.12}$$

and it is straightforward that $\det(B_0) = 1 - c_1 A_{00}^{(0)}$. When $A_{00}^{(0)} \neq 0$, it then implies that for any $j \in \mathbb{Z}$, B_0 is invertible (and therefore the solution of $A_1 U^{(1)} = f$ exists and is unique) if $c_1 \neq \frac{1}{A_{00}^{(0)}}$.

- Expression of the solution:

Introducing B_0, it comes:

$$U^{(1)} = B_0^{-1} A_0^{-1} f.$$

Noticing that

$$B_0^{-1} = \begin{bmatrix} \frac{1}{1-c_1 A_{00}^{(0)}} & 0 & 0 & 0 & 0 \\ \frac{c_1 A_{10}^{(0)}}{1-c_1 A_{00}^{(0)}} & 1 & 0 & 0 & 0 \\ \frac{c_1 A_{20}^{(0)}}{1-c_1 A_{00}^{(0)}} & 0 & 1 & 0 & 0 \\ \frac{c_1 A_{30}^{(0)}}{1-c_1 A_{00}^{(0)}} & 0 & 0 & 1 & 0 \\ \frac{c_1 A_{40}^{(0)}}{1-c_1 A_{00}^{(0)}} & 0 & 0 & 0 & 1 \end{bmatrix}, \tag{4.13}$$

and exploiting Proposition 4.3.3, one can get (4.10) and (4.11). ∎

Proposition 4.3.5
For any $j \in \mathbb{Z}$ and any $c_1 \in D_j$, let us denote $D_{j,c_1} = \{c_2 > 0 / c_2 \neq \frac{1}{A_{11}^{(0)} + \frac{c_1 \left(A_{01}^{(0)}\right)^2}{1-c_1 A_{00}^{(0)}}}\}$ with $\{A_{in}^{(0)}\}_{(i,n)\in\{0,\dots,3\}^2}$ given by System (4.6). if $c_2 \in D_{j,c_1}$, there exists a unique solution of $A_2 U^{(2)} = f$ that satisfies for any f:

$$U^{(2)} = \begin{bmatrix} U_0^{(1)} + \frac{c_2 A_{01}^{(1)}}{1-c_2 A_{11}^{(1)}} U_1^{(1)} \\ \frac{1}{1-c_2 A_{11}^{(1)}} U_1^{(1)} \\ U_2^{(1)} + \frac{c_2 A_{21}^{(1)}}{1-c_2 A_{11}^{(1)}} U_1^{(1)} \\ U_3^{(1)} + \frac{c_2 A_{31}^{(1)}}{1-c_2 A_{11}^{(1)}} U_1^{(1)} \\ U_4^{(1)} + \frac{c_2 A_{41}^{(1)}}{1-c_2 A_{11}^{(1)}} U_1^{(1)} \end{bmatrix}, \tag{4.14}$$

where $\{U_i^{(1)}\}_{i=0,\dots,4}$ is provided by (4.10) or (4.11). Moreover, $\{A_{in}^{(1)}\}_{(i,n)\in\{0,\dots,4\}^2}$ satisfies:

$$\begin{cases} A_{0n}^{(1)} = \frac{A_{0n}^{(0)}}{1-c_1 A_{00}^{(0)}} \quad \textit{for } n \in \{0,\dots,4\} \\ A_{in}^{(1)} = A_{in}^{(0)} + \frac{c_1 A_{i0}^{(0)} A_{0n}^{(0)}}{1-c_1 A_{00}^{(0)}} \quad \textit{for } i \in \{1,\dots,4\} \textit{ and } n \in \{0,\dots,4\} \end{cases} \tag{4.15}$$

Proof:

The proof is similar to the previous one taking into account that A_1 is invertible (Proposition 4.3.4). More precisely, splitting A_2 as $A_2 = A_1 + \tilde{A}_2$, the invertibility of A_2 is connected to the invertibility of $B_1 = (I + A_1^{-1}\tilde{A}_2)$. According to the previous proof, $A_1^{-1} = B_0^{-1}A_0^{-1}$ with B_0 given by (4.12). It is then straightforward that $\{A_{in}^{(1)}\}_{(i,n)\in\{0,\dots,4\}^2}$ satisfies (4.15). Since B_1 can be written:

$$B_1 = \begin{bmatrix} 1 & -c_2 A_{01}^{(1)} & 0 & 0 & 0 \\ 0 & 1 - c_2 A_{11}^{(1)} & 0 & 0 & 0 \\ 0 & -c_2 A_{21}^{(1)} & 1 & 0 & 0 \\ 0 & -c_2 A_{31}^{(1)} & 0 & 1 & 0 \\ 0 & -c_2 A_{41}^{(1)} & 0 & 0 & 1 \end{bmatrix}, \tag{4.16}$$

one can deduce that $\det(B_1) = 1 - c_2 A_{11}^{(1)}$. It then comes out that for any $j \in \mathbb{Z}$ and any $c_1 \in \mathbb{R}^+ \backslash D_j$, B_1 is invertible (and therefore the weights associated with the penalized Lagrange scheme exist) if $c_2 \neq \frac{1}{A_{11}^{(0)} + \frac{c_1 \left(A_{01}^{(0)}\right)^2}{1-c_1 A_{00}^{(0)}}}$.

Similarly to the proof of Proposition 4.3.4, since $U^{(2)} = B_1^{-1}A_1^{-1}f$, and

$$B_1^{-1} = \begin{bmatrix} 1 & \frac{c_2 A_{01}^{(1)}}{1-c_2 A_{11}^{(1)}} & 0 & 0 & 0 \\ 0 & \frac{1}{1-c_2 A_{11}^{(1)}} & 0 & 0 & 0 \\ 0 & \frac{c_2 A_{21}^{(1)}}{1-c_2 A_{11}^{(1)}} & 1 & 0 & 0 \\ 0 & \frac{c_2 A_{31}^{(1)}}{1-c_2 A_{11}^{(1)}} & 0 & 1 & 0 \\ 0 & \frac{c_2 A_{41}^{(1)}}{1-c_2 A_{11}^{(1)}} & 0 & 0 & 1 \end{bmatrix}, \tag{4.17}$$

(4.10), (4.11) and (4.16) leads to (4.14). ∎

Proposition 4.3.6

For any $j \in \mathbb{Z}$ and any $(c_1, c_2) \in D_j \times D_{j,c_1}$, let us denote $D_{j,c_1,c_2} = \{c_3 > 0 / c_3 \neq \frac{1}{A_{22}^{(1)} + \frac{c_2 \left(A_{12}^{(1)}\right)^2}{1 - c_2 A_{11}^{(1)}}}\}$ with $\{A_{in}^{(1)}\}_{(i,n)\in\{0,\dots,3\}^2}$ provided by System (4.15). If $c_3 \in D_{j,c_1,c_2}$, there exists a unique solution of $A_3 U^{(3)} = f$ that satisfies for any f:

$$U^{(3)} = \begin{bmatrix} U_0^{(2)} + \frac{c_3 A_{02}^{(2)}}{1 - c_3 A_{22}^{(2)}} U_2^{(2)} \\ U_1^{(2)} + \frac{c_3 A_{12}^{(2)}}{1 - c_3 A_{22}^{(2)}} U_2^{(2)} \\ \frac{1}{1 - c_3 A_{22}^{(2)}} U_2^{(2)} \\ U_3^{(2)} + \frac{c_3 A_{32}^{(2)}}{1 - c_3 A_{22}^{(2)}} U_2^{(2)} \\ U_4^{(2)} + \frac{c_3 A_{42}^{(2)}}{1 - c_3 A_{22}^{(2)}} U_2^{(2)} \end{bmatrix}, \tag{4.18}$$

where $\{U_i^{(2)}\}_{i=0,\dots,4}$ is given by (4.14). Moreover, $\{A_{in}^{(2)}\}_{(i,n)\in\{0,\dots,4\}^2}$ satisfies:

$$\begin{cases} A_{1n}^{(2)} = \frac{A_{1n}^{(1)}}{1 - c_2 A_{11}^{(1)}}, \quad \text{for } n \in \{0, \dots, 4\}, \\ A_{in}^{(2)} = A_{in}^{(1)} + \frac{c_2 A_{i1}^{(1)} A_{1n}^{(1)}}{1 - c_2 A_{11}^{(1)}}, \quad \text{for } i \in \{0, 2, 3, 4\} \text{ and } n \in \{0, \dots, 4\}. \end{cases} \tag{4.19}$$

Proof:

The proof is similar to the two previous ones. Expression (4.19) comes from $A_2^{-1} = B_1^{-1} A_1^{-1}$ with B_1 given by (4.16). Moreover, writing $A_3 = A_2 + \tilde{A}_3$, we want to show that $\det(B_2) \neq 0$ with $B_2 = (I + A_2^{-1}\tilde{A}_3)$. This can be achieved following the same track replacing (4.16) by

$$B_2 = \begin{bmatrix} 1 & 0 & -c_3 A_{02}^{(2)} & 0 & 0 \\ 0 & 1 & -c_3 A_{12}^{(2)} & 0 & 0 \\ 0 & 0 & 1 - c_3 A_{22}^{(2)} & 0 & 0 \\ 0 & 0 & -c_3 A_{32}^{(2)} & 1 & 0 \\ 0 & 0 & -c_3 A_{42}^{(2)} & 0 & 1 \end{bmatrix}.$$

Since $\det(B_2) = 1 - c_3 A_{22}^{(2)}$, the invertibility is ensured as soon as $c_3 \neq \frac{1}{A_{22}^{(1)} + \frac{c_2 \left(A_{12}^{(1)}\right)^2}{1 - c_2 A_{11}^{(1)}}}$.

Then, keeping in mind that $U^{(3)} = B_2^{-1} A_2^{-1} f$ and

$$B_2^{-1} = \begin{bmatrix} 1 & 0 & \frac{c_3 A_{02}^{(2)}}{1 - c_3 A_{22}^{(2)}} & 0 & 0 \\ 0 & 1 & \frac{c_3 A_{12}^{(2)}}{1 - c_3 A_{22}^{(2)}} & 0 & 0 \\ 0 & 0 & \frac{1}{1 - c_3 A_{22}^{(2)}} & 0 & 0 \\ 0 & 0 & \frac{c_3 A_{32}^{(2)}}{1 - c_3 A_{22}^{(2)}} & 1 & 0 \\ 0 & 0 & \frac{c_3 A_{42}^{(2)}}{1 - c_3 A_{22}^{(2)}} & 0 & 1 \end{bmatrix}, \tag{4.20}$$

Expression (4.18) is straightforward.

■

We also get this last proposition:

Proposition 4.3.7

For any $j \in \mathbb{Z}$ and any $(c_1, c_2, c_3) \in D_j \times D_{j,c_1} \times D_{j,c_1,c_2}$, let us denote $D_{j,c_1,c_2,c_3} = \{c_4 > 0 / c_4 \neq \frac{1}{A_{33}^{(2)} + \frac{c_2 \left(A_{23}^{(2)}\right)^2}{1 - c_2 A_{22}^{(2)}}}\}$ with $\{A_{in}^{(2)}\}_{(i,n) \in \{0,\dots,3\}^2}$ provided by System (4.19). If $c_4 \in D_{j,c_1,c_2,c_3}$, there exists a unique solution of $A_4 U^{(4)} = f$ that satisfies for any f:

$$U^{(4)} = \begin{bmatrix} U_0^{(3)} + \frac{c_4 A_{03}^{(3)}}{1 - c_4 A_{33}^{(3)}} U_3^{(3)} \\ U_1^{(3)} + \frac{c_4 A_{13}^{(3)}}{1 - c_4 A_{33}^{(3)}} U_3^{(3)} \\ U_2^{(3)} + \frac{c_4 A_{23}^{(3)}}{1 - c_4 A_{33}^{(3)}} U_3^{(3)} \\ \frac{1}{1 - c_4 A_{33}^{(3)}} U_3^{(3)} \\ U_4^{(3)} + \frac{c_4 A_{43}^{(3)}}{1 - c_4 A_{33}^{(3)}} U_3^{(3)} \end{bmatrix}. \tag{4.21}$$

where $\{U_i^{(3)}\}_{i=0,\dots,4}$ is given by (4.18). Moreover, $\{A_{in}^{(3)}\}_{(i,n) \in \{0,\dots,4\}^2}$ satisfies:

$$\begin{cases} A^{(3)}_{2n} = \frac{A^{(2)}_{2n}}{1-c_3 A^{(2)}_{22}}, \quad \textit{for } n \in \{0,\dots,4\} \\ A^{(3)}_{in} = A^{(2)}_{in} + \frac{c_3 A^{(2)}_{i2} A^{(2)}_{2n}}{1-c_3 A^{(2)}_{22}}, \quad \textit{for } i \in \{0,1,3,4\} \textit{ and } n \in \{0,\dots,4\} \end{cases} \tag{4.22}$$

According to the previous propositions, one can derive the asymptotical behavior of the solution of $A_k U^{(k)} = f$ ($k \in \{0,\dots,4\}$).

Proposition 4.3.8
For a zero error variance vector, the solution satisfies:

$$\lim_{j\to+\infty} U^{(0)} = \left(L^{2,2}_{-2}(-\frac{1}{2}), L^{2,2}_{-1}(-\frac{1}{2}), L^{2,2}_{0}(-\frac{1}{2}), L^{2,2}_{1}(-\frac{1}{2}), 0 \right)^T.$$

When considering non-zero error variance vectors, it turns out that for any $(c_1,c_2,c_3,c_4)) \in (I\!R^+)^4$, there exists $J > 0$ such that for all $j \geq J$, the solution of $A_k U^{(k)} = f$ ($k \in \{1,\dots,4\}$) exists. Moreover, we have

- *One non-zero error variance:*
  - *If $f = (P_{4,j}(1), P_{4,j}(0), P_{4,j}(1), P_{4,j}(2), 1)^T$: $U^{(1)} = (0,1,0,0,0)^T$,*
  - *If $f = (P_{4,j}(\frac{3}{2}), P_{4,j}(\frac{1}{2}), P_{4,j}(\frac{1}{2}), P_{4,j}(\frac{3}{2}), 1)^T$:*
    $\lim_{j\to+\infty} U^{(1)} = \left(0, L^{1,2}_{-1}(-\frac{1}{2}), L^{1,2}_{0}(-\frac{1}{2}), L^{1,2}_{1}(-\frac{1}{2}), 0\right)^T$.
  - *For large enough j, $||A^{(1)}||_\infty \leq K 2^{4j}$ with K independent of j.*
- *Two non-zero error variances:*
  - *If $f = (P_{4,j}(1), P_{4,j}(0), P_{4,j}(1), P_{4,j}(2), 1)^T$: $\lim_{j\to+\infty} U^{(2)} \left(0, 0, L^{0,2}_{0}(-1), L^{0,2}_{1}(-1), 0\right)^T$,*
  - *If $f = (P_{4,j}(\frac{3}{2}), P_{4,j}(\frac{1}{2}), P_{4,j}(\frac{1}{2}), P_{4,j}(\frac{3}{2}), 1)^T$: $\lim_{j\to+\infty} U^{(2)} = \left(0, 0, L^{0,2}_{0}(-\frac{1}{2}), L^{0,2}_{1}(-\frac{1}{2}), 0\right)^T$.*
  - *For large enough j, $||A^{(2)}||_\infty \leq K 2^{4j}$ with K independent of j.*
- *Three non-zero error variances:*
  - *For any f, $\lim_{j\to+\infty} U^{(3)} = (0,0,0,1,0)^T$,*
  - *For large enough j, $||A^{(3)}||_\infty \leq K 2^{4j}$ with K independent of j.*
- *Four non-zero error variances: for any f,*
  $\lim_{j\to+\infty} U^{(4)} = \left(\frac{\Pi^4_{i=1,i\neq1} c_i}{\sum_{n=1}^4 \Pi^4_{i=1,i\neq n} c_i}, \frac{\Pi^4_{i=1,i\neq2} c_i}{\sum_{n=1}^4 \Pi^4_{i=1,i\neq n} c_i}, \frac{\Pi^4_{i=1,i\neq3} c_i}{\sum_{n=1}^4 \Pi^4_{i=1,i\neq n} c_i}, \frac{\Pi^4_{i=1,i\neq4} c_i}{\sum_{n=1}^4 \Pi^4_{i=1,i\neq n} c_i}, c_1 \frac{\Pi^4_{i=1,i\neq1} c_i}{\sum_{n=1}^4 \Pi^4_{i=1,i\neq n} c_i} \right)^T$

Proof:

In the case of a zero error variance vector, the limit is straightforward from (4.5).

The proof for both existence and behavior of the solutions when introducing one, two and three non-zero error variances is based on the asymptotical expansion of $\{A_{in}^{(k)}\}_{(k,i,n)\in\{1,2\}\times\{0,\dots,4\}^2}$ that can be obtained by combining (4.6)-(4.7) with (4.15) and (4.19). For four non-zero error variances, we avoid a too technical proof by exploiting that the limit of A_4 is invertible.

- One non-zero error variance:

It is straightforward that for any $c_1 \in I\!R^+$, $\det(B_0) \sim_{j\to+\infty} -2^{6j}c_1\frac{b_0}{288b1^2}$. Therefore, for large enough j, B_0 is invertible and the solution of $A_1U^{(1)} = f$ exists.

Moreover, according to (4.6) and (4.7), we get:

$$\begin{cases} A_{10}^{(0)} &= -\frac{1}{16b_1}2^{4j} - \frac{b_0}{96b_1^2}2^{6j}, \\ A_{20}^{(0)} &= \frac{1}{24b_1}2^{4j} + \frac{b_0}{96b_1^2}2^{6j}, \\ A_{30}^{(0)} &= \frac{1}{144b_1}2^{4j} - \frac{b_0}{288b_1^2}2^{6j}, \\ A_{40}^{(0)} &= -\frac{1}{6} - \frac{b_0}{24b_1}2^{2j}, \\ A_{41}^{(0)} &= \frac{2}{3} + \frac{b_0}{24b_1}2^{2j} \end{cases} \tag{4.23}$$

and $\forall i \in \{0,\dots,4\}$, $|A_{4i}^{(0)}| \leq K2^{4j}$ where K does not depend on j. Plugging (4.23) in (4.11) leads to $\lim_{j\to+\infty} U^{(1)} = \left(0, \frac{3}{8}, \frac{3}{4}, -\frac{1}{8}, 0\right)$, which is the expected expression when $f = (P_{4,j}(\frac{3}{2}), P_{4,j}(\frac{1}{2}), P_{4,j}(\frac{1}{2}), P_{4,j}(\frac{3}{2}), 1)^T$.

Moreover, from (4.15), after a technical calculus, we obtain

$$\begin{cases} A^{(1)}_{01} \sim_{j\to+\infty} \frac{3}{c_1}, \\ A^{(1)}_{02} \sim_{j\to+\infty} -\frac{3}{c_1}, \\ A^{(1)}_{03} \sim_{j\to+\infty} \frac{1}{c_1}, \\ A^{(1)}_{11} \sim_{j\to+\infty} \frac{1}{24b_1}2^{4j}, \\ A^{(1)}_{12} \sim_{j\to+\infty} -\frac{1}{12b_1}2^{4j}, \\ A^{(1)}_{13} \sim_{j\to+\infty} \frac{1}{24b_1}2^{4j}, \\ A^{(1)}_{22} \sim_{j\to+\infty} \frac{1}{6b_1}2^{4j}, \\ A^{(1)}_{23} \sim_{j\to+\infty} -\frac{1}{12b_1}2^{4j}, \\ A^{(1)}_{33} \sim_{j\to+\infty} \frac{1}{24b_1}2^{4j}, \\ A^{(1)}_{41} \sim_{j\to+\infty} -\frac{b_0}{12b_1}2^{2j}, \\ A^{(1)}_{42} \sim_{j\to+\infty} \frac{b_0}{6b_1}2^{2j} \end{cases} \tag{4.24}$$

and for large j, $\forall i \in \{0,\dots,4\}$, $|A^{(1)}_{4i}| \leq K2^{4j}$ where K does not depend on j. Therefore, since $A^{(1)}$ is symmetrical, $||A^{(1)}||_\infty \leq K2^{4j}$.

- Two and three non-zero error variances:

To check the invisibility it requires to study for large j $det(B_1) = 1 - c_2A^{(1)}_{11}$, $det(B_2) = 1 - c_3A^{(2)}_{22}$ and the solutions given by (4.14) and (4.18).
Note that according to (4.24), it is straightforward that for any $c_2 \in I\!R^+$, $\det(B_1) \sim_{j\to+\infty} \frac{1}{24b_1}2^{4j}$. Therefore, for large enough j, B_1 is invertible and the solution of $A_2U^{(2)} = f$ exists. Concerning $det(B_2)$, Expression (4.19) leads to $A^{(2)}_{22} \sim_{j\to+\infty} -\frac{1}{2b_0}2^{2j}$ ensuring also in this case also that the solution of $A_3U^{(3)} = f$ exists.

Moreover, from (4.24) and (4.19),

$$\begin{cases} A^{(2)}_{02} \sim_{j\to+\infty} \frac{3}{c_1}, \\ A^{(2)}_{12} \sim_{j\to+\infty} \frac{2}{c_2}, \\ A^{(2)}_{22} \sim_{j\to+\infty} -\frac{1}{2b_0}2^{2j}, \\ A^{(2)}_{23} \sim_{j\to+\infty} \frac{1}{2b_0}2^{2j}, \\ A^{(2)}_{42} \sim_{j\to+\infty} \frac{1}{2}. \end{cases} \tag{4.25}$$

(4.24) and (4.25) allows one to conclude that

$$lim_{j\to+\infty}U^{(2)} = \begin{cases} (0,0,2,-1,0)^T \text{ if } f = (P_{4,j}(1), P_{4,j}(0), P_{4,j}(1), P_{4,j}(2), 1)^T, \\ \left(0,0,\frac{3}{2},-\frac{1}{2},0\right)^T \text{ if } f = (P_{4,j}(\frac{3}{2}), P_{4,j}(\frac{1}{2}), P_{4,j}(\frac{1}{2}), P_{4,j}(\frac{3}{2}), 1)^T, \end{cases}$$

and $lim_{j\to+\infty}U^{(3)} = (0,0,0,1,0)^T$ for any f, which are the expected results related to the asymptotical behavior of the solutions.

Finally, since $A^{(2)} = B_1^{-1}A^{(1)}$ and $A^{(3)} = B_2^{-1}A^{(2)}$ with B_1^{-1} and B_2^{-1} given by (4.17) and (4.20), it is straightforward using (4.15) and (4.24) (resp. (4.19) and (4.25)) that $||B_1^{-1}||_\infty \leq K$ (resp. $||B_2^{-1}||_\infty \leq K$) where K does not depend on j. Finally, it leads to $||A^{(2)}||_\infty \leq K||A^{(1)}||_\infty$ and $||A^{(3)}||_\infty \leq K||A^{(2)}||_\infty$. That concludes the proof

- Four non-zero error variances:

Let us first notice that $\lim_{j\to+\infty} A_4 = G$ and $\lim_{j\to+\infty} f = g$ with

$$G = \begin{bmatrix} -c_1 & 0 & 0 & 0 & 1 \\ 0 & -c_2 & 0 & 0 & 1 \\ 0 & 0 & -c_3 & 0 & 1 \\ 0 & 0 & 0 & -c_4 & 1 \\ 1 & 1 & 1 & 1 & 0 \end{bmatrix} \text{ and } g = (0,0,0,0,1)'.$$

Since G is invertible and $||G^{-1}||_\infty \leq K$ (K independent of j), one gets for large j, $||A^{(4)}||_\infty \leq K$. Moreover, it comes $\lim_{j\to+\infty} U^{(4)} = G^{-1}g$ ensuring that the solution exists and one can easily verify that the unique solution of $GU = g$ is

$$U = \left(\frac{\Pi_{i=1,i\neq1}^4 c_i}{\sum_{n=1}^4 \Pi_{i=1,i\neq n}^4 c_i}, \frac{\Pi_{i=1,i\neq2}^4 c_i}{\sum_{n=1}^4 \Pi_{i=1,i\neq n}^4 c_i}, \frac{\Pi_{i=1,i\neq3}^4 c_i}{\sum_{n=1}^4 \Pi_{i=1,i\neq n}^4 c_i}, \frac{\Pi_{i=1,i\neq4}^4 c_i}{\sum_{n=1}^4 \Pi_{i=1,i\neq n}^4 c_i}, c_1\frac{\Pi_{i=1,i\neq1}^4 c_i}{\sum_{n=1}^4 \Pi_{i=1,i\neq n}^4 c_i} \right)^T.$$

That concludes the proof.

■

The previous result is now used to get Proposition 4.3.1. More precisely,

Proposition 4.3.9

The Kriging weights associated with the 4-point stencil for a $\mathcal{G}^{\star}_{OD}$ semi-variogram satisfy,

$$\lim_{j\to+\infty}\left(\tilde{\lambda}^{2,2,\mathcal{C}}_{j,m}\right)_{m\in\{-1,\dots,2\}} = \lim_{j\to+\infty} A^{(k)} f, \text{ with } f=(P_{4,j}(1),P_{4,j}(0),P_{4,j}(1),P_{4,j}(2),1)^T, \tag{4.26}$$

$$\lim_{j\to+\infty}\left(\lambda^{2,2,\mathcal{C}}_{j,m}\right)_{m\in\{-1,\dots,2\}} = \lim_{j\to+\infty} A^{(k)} f, \text{ with } f=(P_{4,j}(\frac{3}{2}),P_{4,j}(\frac{1}{2}),P_{4,j}(\frac{1}{2}),P_{4,j}(\frac{3}{2}),1)^T. \tag{4.27}$$

Proof:

Let us first note that in the case of a four non-zero error variance vector, the asymptotical Kriging system is exactly the asymptotical system studied in Proposition 4.3.8. Therefore, we focus in this proof on one, two and three non-zero error variances and only provide the different steps to get $\lim_{j\to+\infty}\left(\tilde{\lambda}^{2,2,\mathcal{C}}_{j,m}\right)_{m\in\{-2,\dots,1\}}$ since (4.27) can be obtained similarly.

Let us write $\gamma(h)=P_4(h)+O(h^6)$,. The Kriging system including a vector of non-zero error variance becomes:

$$(A_k+A_\epsilon)\,\mathcal{U}_{j+1} = f+f_\epsilon,\ k\in\{1,2,3\} \tag{4.28}$$

where $||A_\epsilon||_2 \le K2^{-6j}$ and $||f_\epsilon||_2 \le K2^{-6j}$ and K independent of j.
Since A_k is invertible, the solution of (4.28) can then be formally written as:

$$\begin{aligned}\mathcal{U}_{j+1} &= (A_k+A_\epsilon)^{-1}(f+f_\epsilon),\\ &= \left(I_5+A_k^{-1}A_\epsilon\right)^{-1}A_k^{-1}f\\ &+ \left(I_5+A_k^{-1}A_\epsilon\right)^{-1}A_k^{-1}f_\epsilon,\end{aligned} \tag{4.29}$$

where I_5 is the 5×5 identity matrix.

According to Proposition 4.3.8, it is straightforward that for large enough j,

$$||A_k^{-1}A_\epsilon||_\infty \leq K2^{-2j}, \tag{4.30}$$

where K does not depend on j. Therefore, $\left(I_5 + A_k^{-1}A_\epsilon\right)^{-1} = \sum_{i=0}^{\infty}(-1)^i \left(A_k^{-1}A_\epsilon\right)^i$.

Expression (4.29) becomes:

$$\mathcal{U}_{j+1} = A_k^{-1}f + \left(\sum_{i=1}^{\infty}(-1)^i \left(A_k^{-1}A_\epsilon\right)^i A_k^{-1}f + \sum_{i=0}^{\infty}(-1)^i \left(A_k^{-1}A_\epsilon\right)^i A_k^{-1}f_\epsilon\right). \tag{4.31}$$

Since for large enough j, $||A_k^{-1}f||_\infty \leq K$ (Proposition 4.3.8), Inequality (4.30) leads to

$$\begin{aligned} ||\sum_{i=1}^{\infty}(-1)^i \left(A_k^{-1}A_\epsilon\right)^i A_k^{-1}f||_\infty &\leq K\sum_{i=1}^{\infty}2^{-2ij}, \\ ||\sum_{i=0}^{\infty}(-1)^i \left(A_k^{-1}A_\epsilon\right)^i A_k^{-1}f_\epsilon||_\infty &\leq K2^{-2j}\sum_{i=0}^{\infty}2^{-2ij}, \end{aligned}$$

which becomes for sufficiently large j,

$$\begin{aligned} ||\sum_{i=1}^{\infty}(-1)^i \left(A_k^{-1}A_\epsilon\right)^i A_k^{-1}f||_\infty &\leq K2^{-2j}, \\ ||\sum_{i=0}^{\infty}(-1)^i \left(A_k^{-1}A_\epsilon\right)^i A_k^{-1}f_\epsilon||_\infty &\leq K2^{-2j}. \end{aligned}$$

Coming back to (4.31), we get $\lim_{j\to+\infty}\mathcal{U}_{j+1} = \lim_{j\to+\infty}\left(A_k^{-1}f\right)$. That concludes the proof.

■

4.3.3 Proofs of Proposition 4.3.2

The proof is similar to the previous one. Therefore, the details of the different steps are not provided in the sequel but only the main results leading to Proposition 4.3.2.

Definition 4.3.2
Denoting for any $b_0 \in \mathbb{R}^\star$, $P_1(x) = b_0 x$, we introduce

$$A_0 = \begin{bmatrix} 0 & P_{1,j}(1) & P_{1,j}(2) & P_{1,j}(3) & 1 \\ P_{1,j}(1) & 0 & P_{1,j}(1) & P_{1,j}(2) & 1 \\ P_{1,j}(2) & P_{1,j}(1) & 0 & P_{1,j}(1) & 1 \\ P_{1,j}(3) & P_{1,j}(2) & P_{1,j}(1) & 0 & 1 \\ 1 & 1 & 1 & 1 & 0 \end{bmatrix} \tag{4.32}$$

where $P_{1,j}(x) = P_1(2^{-j}x)$.
Moreover, when considering error variance vectors, we define for any $k \in \{1, \ldots, 4\}$,

$$A_k = \begin{bmatrix} -c_1 & P_{1,j}(1) & P_{1,j}(2) & P_{1,j}(3) & 1 \\ P_{1,j}(1) & -c_2 & P_{1,j}(1) & P_{1,j}(2) & 1 \\ P_{1,j}(2) & P_{1,j}(1) & \ldots & P_{1,j}(1) & 1 \\ P_{1,j}(3) & P_{1,j}(2) & P_{1,j}(1) & -c_k & 1 \\ 1 & 1 & 1 & 1 & 0 \end{bmatrix}. \tag{4.33}$$

In the next proposition, we focus on the existence of the solution of $A_0 U^{(0)} = f$ where $f = (P_{1,j}(1), P_{1,j}(0), P_{1,j}(1), P_{1,j}(2), 1)^T$ or $f = (P_{1,j}(\frac{3}{2}), P_{1,j}(\frac{1}{2}), P_{1,j}(\frac{1}{2}), P_{1,j}(\frac{3}{2}), 1)^T$.

Proposition 4.3.10
For any $j \in \mathbb{Z}$, there exists a unique solution of $A_0 U^{(0)} = f$ satisfying:

- *If $f = (P_{1,j}(1), P_{1,j}(0), P_{1,j}(1), P_{1,j}(2), 1)^T$,*

$$U^{(0)} = (0, 1, 0, 0, 0)^T. \tag{4.34}$$

- *If $f = (P_{1,j}(\frac{3}{2}), P_{1,j}(\frac{1}{2}), P_{1,j}(\frac{1}{2}), P_{1,j}(\frac{3}{2}), 1)^T$,*

$$U^{(0)} = \left(0, \frac{1}{2}, \frac{1}{2}, 0, 0\right)^T. \tag{4.35}$$

Moreover,

$$A_0^{-1} = \begin{bmatrix} -\frac{2^j}{2b_0} & \frac{2^j}{2b_0} & 0 & 0 & \frac{1}{2} \\ \frac{2^j}{2b_0} & -\frac{2^j}{b_0} & \frac{2^j}{2b_0} & 0 & 0 \\ 0 & \frac{2^j}{2b_0} & -\frac{2^j}{2b_0} & \frac{2^j}{2b_0} & 0 \\ 0 & 0 & \frac{2^j}{2b_0} & -\frac{2^j}{b_0} & \frac{1}{2} \\ \frac{1}{2} & 0 & 0 & \frac{1}{2} & -3b_0 2^{-(j+1)} \end{bmatrix}. \tag{4.36}$$

Proof:

Expressions (4.34) to (4.36) can be obtained by direct calculus using (4.32).

■

Propositions 4.3.4 to 4.3.7 still hold when A_k is defined by (4.33) and similarly to the previous section, one can derive the following asymptotical behavior.

Proposition 4.3.11
For any $(c_1, c_2, c_3, c_4)) \in (\mathbb{R}^+)^4$, there exists $J > 0$ such that for all $j \geq J$, the solution of $A_k U^{(k)} = f$ ($k \in \{1, \ldots, 4\}$) exists. Moreover, we have

- *One non-zero error variance:*
  - *If $f = (P_{1,j}(1), P_{1,j}(0), P_{1,j}(1), P_{1,j}(2), 1)^T$: $U^{(1)} = (0, 1, 0, 0, 0)^T$,*
  - *If $f = (P_{1,j}(\frac{3}{2}), P_{1,j}(\frac{1}{2}), P_{1,j}(\frac{1}{2}), P_{1,j}(\frac{3}{2}), 1)^T$: $\lim_{j\to+\infty} U^{(1)} = \left(0, \frac{1}{2}, \frac{1}{2}, 0, 0\right)^T$.*
  - *For large enough j, $||A^{(1)}||_\infty \leq K 2^j$ with K independent of j.*
- *Two non-zero error variances:*
  - *for any f, $\lim_{j\to+\infty} U^{(2)}\, (0, 0, 1, 0, 0)^T$,*
  - *For large enough j, $||A^{(2)}||_\infty \leq K 2^j$ with K independent of j.*
- *Three non-zero error variances:*
  - *For any f, $\lim_{j\to+\infty} U^{(3)} = (0, 0, 0, 1, 0)^T$,*
  - *For large enough j, $||A^{(3)}||_\infty \leq K 2^j$ with K independent of j.*

- *Four non-zero error variances: for any f,*
  $\lim_{j\to+\infty} U^{(4)} = \left(\frac{\Pi^4_{i=1,i\neq 1} c_i}{\sum_{n=1}^4 \Pi^4_{i=1,i\neq n} c_i}, \frac{\Pi^4_{i=1,i\neq 2} c_i}{\sum_{n=1}^4 \Pi^4_{i=1,i\neq n} c_i}, \frac{\Pi^4_{i=1,i\neq 3} c_i}{\sum_{n=1}^4 \Pi^4_{i=1,i\neq n} c_i}, \frac{\Pi^4_{i=1,i\neq 4} c_i}{\sum_{n=1}^4 \Pi^4_{i=1,i\neq n} c_i}, c_1 \frac{\Pi^4_{i=1,i\neq 1} c_i}{\sum_{n=1}^4 \Pi^4_{i=1,i\neq n} c_i} \right)^T$

Proof:

We mimic the proof of Proposition 4.3.8 and compute the asymptotical behavior of the matrix coefficients. A direct calculus leads to:

$$\begin{cases} A^{(1)}_{00} \sim_{j\to+\infty} \frac{1}{c_1}, \\ A^{(1)}_{01} \sim_{j\to+\infty} -\frac{1}{c_1}, \\ A^{(1)}_{02} = 0, \\ A^{(1)}_{03} = 0, \\ A^{(1)}_{11} \sim_{j\to+\infty} -\frac{2^j}{2b_0}, \\ A^{(1)}_{12} \sim_{j\to+\infty} \frac{2^j}{2b_0}, \\ A^{(1)}_{13} = 0, \\ A^{(1)}_{22} \sim_{j\to+\infty} -\frac{2^j}{b_0}, \\ A^{(1)}_{23} \sim_{j\to+\infty} \frac{2^j}{2b_0}, \\ A^{(1)}_{33} \sim_{j\to+\infty} -\frac{2^j}{2b_0}, \\ A^{(1)}_{40} \sim_{j\to+\infty} -\frac{b_0}{c_1} 2^{-j} \\ A^{(1)}_{41} \sim_{j\to+\infty} \frac{1}{2}, \\ A^{(1)}_{42} = 0, \\ A^{(1)}_{43} \sim_{j\to+\infty} \frac{1}{2}, \\ A^{(1)}_{44} \sim_{j\to+\infty} -b_0 2^{-j}, \end{cases} \tag{4.37}$$

$$\begin{cases} A^{(2)}_{02} \sim_{j\to+\infty} -\frac{1}{c_1}, \\ A^{(2)}_{12} \sim_{j\to+\infty} -\frac{1}{c_2}, \\ A^{(2)}_{22} \sim_{j\to+\infty} -\frac{2^j}{2b_0}, \\ A^{(2)}_{23} \sim_{j\to+\infty} \frac{2^j}{2b_0}, \\ A^{(2)}_{42} \sim_{j\to+\infty} \frac{1}{2}, \end{cases} \tag{4.38}$$

which allows one to conclude in the case of one, two and three error variances. For four non-zero error variances, the proof is exactly the same as in Proposition 4.3.8.

■

Finally, we have:

Proposition 4.3.12

The Kriging weights associated with the 4-point stencil for a $\mathcal{G}^{\star}_{ED}$ semi-variogram satisfy,

$$\begin{aligned}
\lim_{j\to+\infty}\left(\tilde{\lambda}^{2,2,\mathcal{C}}_{j,m}\right)_{m\in\{-1,\dots,2\}} &= \lim_{j\to+\infty} A^{(k)}f, \ \textit{with } f=(P_{1,j}(1),P_{1,j}(0),P_{1,j}(1),P_{1,j}(2),1)^T,\\
\lim_{j\to+\infty}\left(\lambda^{2,2,\mathcal{C}}_{j,m}\right)_{m\in\{-1,\dots,2\}} &= \lim_{j\to+\infty} A^{(k)}f, \ \textit{with } f=(P_{1,j}(\frac{3}{2}),P_{1,j}(\frac{1}{2}),P_{1,j}(\frac{1}{2}),P_{1,j}(\frac{3}{2}),1)^T.
\end{aligned}$$

Proof:

The proof follows the same track as in Proposition 4.3.9 writing $\gamma(h)=P_1(h)+O(h^2)$. The Kriging system can then be written as (4.28) where $||A_\epsilon||_2 \leq K2^{-2j}$ and $||f_\epsilon||_2 \leq K2^{-2j}$ with K independent of j.

Starting from (4.29) and keeping in mind that for large j, according to Proposition 4.3.11,

$$||A_k^{-1}A_\epsilon||_\infty \leq K2^{-j}, \tag{4.39}$$

where K does not depend on j and $||A_k^{-1}f||_\infty \leq K$, it comes

$$\begin{aligned}
||\sum_{i=1}^{\infty}(-1)^i\left(A_k^{-1}A_\epsilon\right)^i A_k^{-1}f||_\infty &\leq K2^{-j},\\
||\sum_{i=0}^{\infty}(-1)^i\left(A_k^{-1}A_\epsilon\right)^i A_k^{-1}f_\epsilon||_\infty &\leq K2^{-j}.
\end{aligned}$$

Coming back to (4.31), we get $\lim_{j\to+\infty}\mathcal{U}_{j+1}=\lim_{j\to+\infty}\left(A_k^{-1}f\right)$. That concludes the proof.

■

4.4 Zone-dependent Kriging-based subdivision scheme

This section is devoted to the definition and the convergence analysis of a subdivision scheme aimed to be adapted to the reconstruction of non-regular data. It combines the

interpolatory and non-interpolatory approaches previously introduced and is based on an a priori segmentation of the data in different zones (Figure 4.1 top left) characterized by different regularity in the same philosophy as in Section 2.3.5. According to this regularity and therefore to the zone, error variance vectors are affected to the Kriging system, leading to a zone dependent subdivision scheme.

4.4.1 Construction of the zone-dependent scheme

Once the segmentation of the data has been performed, the prediction is defined as follows:

- Local predictors (in the interior of the zones):

  Local Kriging-based subdivision predictors are constructed independently in each zone. The semi-variogram of the zone is first identified according to Expression (3.3). Then an error variance function $C(x)$ is defined on the real line. This function provides for each point $x_k^j = k2^{-j}$ the corresponding error variance $C(x_k^j)$. In this work, $C = \chi_{]y_0,y_1[}$ (Figure 4.1, top, right).

  In the interior of each zone, a four point centered scheme is applied (i.e $l_{j,k} = r_{j,k} = 2$). For regular zones a subdivision scheme of type (3.17) i.e a Kriging scheme with $c = 0$ is used whereas for $]y_0, y_1[$ the scheme corresponds to (4.1) with $c_i = 1, 1 \leq i \leq 4$.

- Adaption at the edges of the zones:

  These schemes can not be applied close to the edges of the zone and a specific adaption is required. For the sake of clarity, we describe this adaption around the segmentation point y_0 written for any j as $y_0 = k_0^j 2^{-(j-1)}$. The adaption close to y_1 is performed similarly.

  Regular zone: the adaption is performed following the position dependent strategy proposed in [8] and recalled on Figure 2.8. As shown on Figure 4.1 (bottom, left), the stencil associated to the prediction at position $(2k_0^j - 1)2^{-j}$ is shifted to the left.

  Non-regular zone: the interior scheme can not be used to predict the first two points of the zone at positions $(2k_0^j + 1)2^{-j}$ and $(2k_0^j + 2)2^{-j}$ (Figure 4.1, bottom, right). We propose to estimate the first one by a 4-point Kriging extrapolation from the regular zone and the second one as an average between the extrapolation from the regular zone and the value at the previous level.

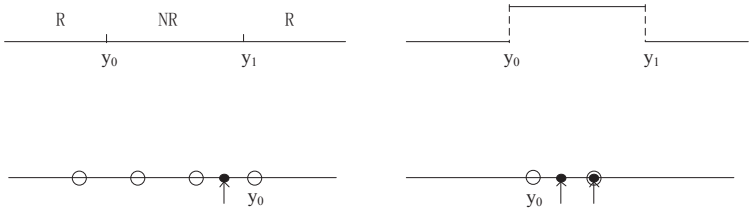

Figure 4.1: From left to right and top to bottom: segmentation of the line (R:Regular; NR: Non-Regular); $C(x)$; adaption in the regular zone near the segmentation point y_0; adaption in the non-regular zone near the segmentation point y_0.

4.4.2 Convergence analysis of the zone-dependent scheme

Based on Theorem 2.2.3, the convergence analysis of our scheme can be reached provided the corresponding stationary asymptotical subdivision scheme is convergent. Therefore, the following sections are first devoted to the evaluation of the (zone-dependent) asymptotical subdivision scheme. Then, its convergence is proved, leading, thanks to Theorem 2.2.3 to the convergence of our zone-dependent Kriging based subdivision scheme.

Limit of the Kriging weights

For the regular zone $]-\infty, y_0]$: the following proposition is borrowed from [4]:

Proposition 4.4.1 *The Kriging weights satisfy:*

- *Prediction in the interior zone:*
  - *for $\mathcal{G}^{\star}_{OD}$-type semi-variogram:*

$$\begin{aligned} \left(\lambda_{-1}^{2,2,\mathbf{0}}, \lambda_{0}^{2,2,\mathbf{0}}, \lambda_{1}^{2,2,\mathbf{0}}, \lambda_{2}^{2,2,\mathbf{0}}\right) &= (0,1,0,0)\,, \\ \lim_{j\to+\infty} \left(\lambda_{-1}^{2,2,\mathbf{0}}, \lambda_{0}^{2,2,\mathbf{0}}, \lambda_{1}^{2,2,\mathbf{0}}, \lambda_{2}^{2,2,\mathbf{0}}\right) &= \left(-\frac{1}{16}, \frac{9}{16}, \frac{9}{16}, -\frac{1}{16}\right). \end{aligned}$$

  - *for $\mathcal{G}^{\star}_{ED}$-type semi-variogram:*

$$\begin{aligned} \left(\tilde{\lambda}_{-1}^{2,2,\mathbf{0}}, \tilde{\lambda}_{0}^{2,2,\mathbf{0}}, \tilde{\lambda}_{1}^{2,2,\mathbf{0}}, \tilde{\lambda}_{2}^{2,2,\mathbf{0}}\right) &= (0,1,0,0)\,, \\ \lim_{j\to+\infty} \left(\lambda_{-1}^{2,2,\mathbf{0}}, \lambda_{0}^{2,2,\mathbf{0}}, \lambda_{1}^{2,2,\mathbf{0}}, \lambda_{2}^{2,2,\mathbf{0}}\right) &= \left(0, \frac{1}{2}, \frac{1}{2}, 0\right). \end{aligned}$$

- *Prediction near the edge at* $x^j_{2k_0^j-1} = (2k_0^j - 1)2^{-j}$*:*
  - *for* $\mathcal{G}^\star_{OD}$*-type semi-variogram:*

$$\lim_{j\to+\infty} \left(\lambda^{3,1,\mathbf{0}}_{-2}, \lambda^{3,1,\mathbf{0}}_{-1}, \lambda^{3,1,\mathbf{0}}_{0}, \lambda^{3,1,\mathbf{0}}_{1}\right) = \left(\frac{1}{16}, -\frac{5}{16}, \frac{15}{16}, \frac{5}{16}\right).$$

  - *for* $\mathcal{G}^\star_{ED}$*-type semi-variogram:*

$$\lim_{j\to+\infty} \left(\lambda^{3,1,\mathbf{0}}_{-2}, \lambda^{3,1,\mathbf{0}}_{-1}, \lambda^{3,1,\mathbf{0}}_{0}, \lambda^{3,1,\mathbf{0}}_{1}\right) = \left(0, 0, \frac{1}{2}, \frac{1}{2}\right)$$

As for the non-regular zone $]y_0, y_1[$, we have:

Proposition 4.4.2 *The Kriging weights satisfy:*

- *Prediction in the interior of the zone: for both* $\mathcal{G}^\star_{OD}$ *and* $\mathcal{G}^\star_{ED}$*-type semi-variograms:*

$$\begin{aligned}
\lim_{j\to+\infty} \left(\tilde\lambda^{2,2,\mathcal{C}}_{-1}, \tilde\lambda^{2,2,\mathcal{C}}_{0}, \tilde\lambda^{2,2,\mathcal{C}}_{1}, \tilde\lambda^{2,2,\mathcal{C}}_{2}\right) &= \left(\frac{1}{4}, \frac{1}{4}, \frac{1}{4}, \frac{1}{4}\right), \\
\lim_{j\to+\infty} \left(\lambda^{2,2,\mathcal{C}}_{-1}, \lambda^{2,2,\mathcal{C}}_{0}, \lambda^{2,2,\mathcal{C}}_{1}, \lambda^{2,2,\mathcal{C}}_{2}\right) &= \left(\frac{1}{4}, \frac{1}{4}, \frac{1}{4}, \frac{1}{4}\right).
\end{aligned}$$

- *Prediction near the edge:*
  - *for* $\mathcal{G}^\star_{OD}$*-type semi-variogram:*

$$\begin{aligned}
\textit{When } x^j_{2k_0^j+1} = (2k_0^j+1)2^{-j},\ \lim_{j\to+\infty} \left(\lambda^{4,0,\mathbf{0}}_{-3}, \lambda^{4,0,\mathbf{0}}_{-2}, \lambda^{4,0,\mathbf{0}}_{-1}, \lambda^{4,0,\mathbf{0}}_{0}\right) &= \left(-\frac{5}{16}, \frac{21}{16}, -\frac{35}{16}, \frac{35}{16}\right) \\
\textit{When } x^j_{2k_0^j+2} = (2k_0^j+2)2^{-j},\ \lim_{j\to+\infty} \left(\tilde\lambda^{4,0,\mathbf{0}}_{-3}, \tilde\lambda^{4,0,\mathbf{0}}_{-2}, \tilde\lambda^{4,0,\mathbf{0}}_{-1}, \tilde\lambda^{4,0,\mathbf{0}}_{0}\right) &= (-1, 4, -6, 4).
\end{aligned}$$

  - *for* $\mathcal{G}^\star_{ED}$*-type semi-variogram:*

$$\begin{aligned}
\textit{When } x^j_{2k_0^j+1} = (2k_0^j+1)2^{-j},\ \lim_{j\to+\infty} \left(\lambda^{4,0,\mathbf{0}}_{-3}, \lambda^{4,0,\mathbf{0}}_{-2}, \lambda^{4,0,\mathbf{0}}_{-1}, \lambda^{4,0,\mathbf{0}}_{0}\right) &= (0, 0, 0, 1), \\
\textit{When } x^j_{2k_0^j+2} = (2k_0^j+2)2^{-j},\ \lim_{j\to+\infty} \left(\tilde\lambda^{4,0,\mathbf{0}}_{-3}, \tilde\lambda^{4,0,\mathbf{0}}_{-2}, \tilde\lambda^{4,0,\mathbf{0}}_{-1}, \tilde\lambda^{4,0,\mathbf{0}}_{0}\right) &= (0, 0, 0, 1).
\end{aligned}$$

Proof:

The computation of the asymptotical weights when predicting near the edge is just an extension of the result provided by Proposition 4.4.1 of [4]. As for the prediction in the interior zone, the limits are straightforward according to Propositions 4.3.1 and 4.3.2.

■

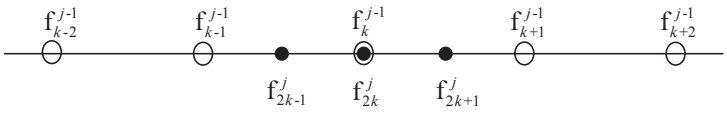

Figure 4.2: Prediction in the non-regular zone: available values at level $j-1$ (o) and predicted values at the next level ($\bullet$).

Convergence of the asymptotical scheme

The convergence of the asymptotical scheme in the regular zone has already been proved in [8]. Therefore, this section is devoted to the convergence analysis in the non-regular zone.

- Convergence in the interior of the zone:

  Since the scheme is uniform, it is enough to focus on the differences $d_1^{j,k} = f_{2k}^j - f_{2k-1}^j$ and $d_2^{j,k} = f_{2k+1}^j - f_{2k}^j$ (Figure 4.2). According to Proposition 4.4.2, $f_{2k+1}^j = f_{2k}^j = \frac{1}{4}(f_{k-1}^{j-1} + f_k^{j-1} + f_{k+1}^{j-1} + f_{k+2}^{j-1})$ and $f_{2k-1}^j = \frac{1}{4}(f_{k-2}^{j-1} + f_{k-1}^{j-1} + f_k^{j-1} + f_{k+1}^{j-1})$. Then,

  $$\begin{cases} d_1^{j,k} &= \frac{1}{4}[(f_{k+2}^{j-1} - f_{k+1}^{j-1}) + (f_{k+1}^{j-1} - f_k^{j-1}) + (f_k^{j-1} - f_{k-1}^{j-1}) + (f_{k-1}^{j-1} - f_{k-2}^{j-1})] \ , \\ d_2^{j,k} &= 0. \end{cases}$$

  Since $\forall j,k, d_2^{j,k} = 0$,

  - if k is even ($k = 2m$), $f_{k+1}^{j-1} - f_k^{j-1} = f_{2m+1}^{j-1} - f_{2m}^{j-1} = d_2^{j-1,m} = 0$, $f_{k-1}^{j-1} - f_{k-2}^{j-1} = f_{2m-1}^{j-1} - f_{2m-2}^{j-1} = d_2^{j-1,m-1} = 0$. Therefore,

    $$d_1^{j,k} = \frac{1}{4}[(f_{k+2}^{j-1} - f_{k+1}^{j-1}) + (f_k^{j-1} - f_{k-1}^{j-1})] \ ,$$

  - if k is odd ($k = 2m+1$), $f_{k+2}^{j-1} - f_{k+1}^{j-1} = f_{2m+3}^{j-1} - f_{2m+2}^{j-1} = d_2^{j-1,m+1} = 0$, $f_k^{j-1} - f_{k-1}^{j-1} = f_{2m+1}^{j-1} - f_{2m}^{j-1} = d_2^{j-1,m} = 0$. Therefore,

    $$d_1^{j,k} = \frac{1}{4}[(f_{k+1}^{j-1} - f_k^{j-1}) + (f_{k-1}^{j-1} - f_{k-2}^{j-1})] \ .$$

  Since $|\frac{1}{4}| + |\frac{1}{4}| < 1$, $d_1^{j,k} \to_{j \to +\infty} 0$.

- Convergence near the edge:

  We focus on the differences $d_1^{j,k_0^j} = f_{2k_0^j+1}^j - f_{2k_0^j}^j$ and $d_2^{j,k_0^j} = f_{2k_0^j+2}^j - f_{2k_0^j+1}^j$ (Figure 4.3). Let us first consider a $\mathcal{G}_{OD}^\star$-type semi-variogram. According to Proposition

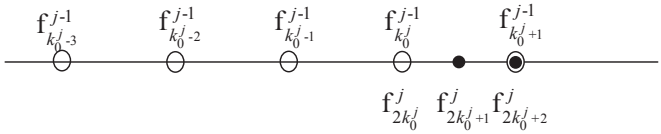

Figure 4.3: Prediction near the edge in the non-regular zone: available values at level $j-1$ (o) and predicted values at the next level (•).

4.4.2, $f^j_{2k_0^j+1} = \frac{35}{16}f^{j-1}_{k_0^j} - \frac{35}{16}f^{j-1}_{k_0^j-1} + \frac{21}{16}f^{j-1}_{k_0^j-2} - \frac{5}{16}f^{j-1}_{k_0^j-3}$ and $f^j_{2k_0^j+2} = \frac{1}{2}[(4f^{j-1}_{k_0^j} - 6f^{j-1}_{k_0^j-1} + 4f^{j-1}_{k_0^j-2} - f^{j-1}_{k_0^j-3}) + f^{j-1}_{k_0^j+1}]$. Therefore

$$\begin{cases} d_1^{j,k_0^j} &= f^j_{2k_0^j+1} - f^j_{2k_0^j} = \frac{19}{16}(f^{j-1}_{k_0^j} - f^{j-1}_{k_0^j-1}) - (f^{j-1}_{k_0^j-1} - f^{j-1}_{k_0^j-2}) + \frac{5}{16}(f^{j-1}_{k_0^j-2} - f^{j-1}_{k_0^j-3}) \ , \\ d_2^{j,k_0^j} &= f^j_{2k_0^j+2} - f^j_{2k_0^j+1} \\ &= \frac{1}{2}(f^{j-1}_{k_0^j+1} - f^{j-1}_{k_0^j}) + \frac{5}{16}(f^{j-1}_{k_0^j} - f^{j-1}_{k_0^j-1}) - \frac{1}{2}(f^{j-1}_{k_0^j-1} - f^{j-1}_{k_0^j-2}) + \frac{3}{16}(f^{j-1}_{k_0^j-2} - f^{j-1}_{k_0^j-3}) \ . \end{cases}$$

Since the terms $(f^{j-1}_{k_0^j} - f^{j-1}_{k_0^j-1})$, $(f^{j-1}_{k_0^j-1} - f^{j-1}_{k_0^j-2})$ and $(f^{j-1}_{k_0^j-2} - f^{j-1}_{k_0^j-3})$ are differences between data of the regular zone, their limit is zero since the Kriging subdivision scheme is convergent in this zone [4]. Therefore $d_1^{j,k_0^j} \to_{j\to+\infty} 0$. Moreover, since $f^{j-1}_{k_0^j+1} - f^{j-1}_{k_0^j} = f^{j-1}_{2k_0^{j-1}+1} - f^{j-1}_{2k_0^{j-1}} = d_1^{j-1,k_0^{j-1}}$ we also get that $d_2^{j,k_0^j} \to_{j\to+\infty} 0$.
If we consider now a $\mathcal{G}^\star_{ED}$-type semi-variogram, according to Proposition 4.4.2, $f^j_{2k_0^j+1} = f^{j-1}_{k_0^j}$ and $f^j_{2k_0^j+2} = \frac{1}{2}(f^{j-1}_{k_0^j} + f^{j-1}_{k_0^j+1})$. Therefore we have:

$$\begin{cases} d_1^{j,k_0^j} &= f^j_{2k_0^j+1} - f^j_{2k_0^j} = 0 \ , \\ d_2^{j,k_0^j} &= f^j_{2k_0^j+2} - f^j_{2k_0^j+1} = \frac{1}{2}(f^{j-1}_{k_0^j+1} - f^{j-1}_{k_0^j}) \ . \end{cases}$$

Noticing that $f^{j-1}_{k_0^j+1} - f^{j-1}_{k_0^j} = f^{j-1}_{2k_0^{j-1}+1} - f^{j-1}_{2k_0^{j-1}} = d_1^{j-1,k_0^{j-1}} = 0$, we also get that $d_2^{j,k_0^j} = 0$.

From Section 2.2, the asymptotical subdivision scheme is then convergent. Applying Theorem 2.2.3 leads to the convergence of our zone-dependent Kriging-based scheme.

4.5 Numerical results

This section is devoted to several applications of the zone-dependent Kriging-based scheme. The two first numerical experiments are performed to evaluate the deficiency of the scheme

compared to classical ones. They concern the reconstruction of discontinuous data and curve generation starting from locally noisy data. The third one is an attempt towards the use of our scheme for the approximation of computer codes in presence of uncertainties.

4.5.1 Discontinuous data

There exists many subdivision schemes that are suitable to reconstruct non-regular data. Among them, the position-dependent Lagrange scheme introduced in [8] and recalled in Chapter 2 has provided promising results when its construction integrates precisely the information related to the discontinuity position. However as shown in [8], the quality of this scheme strongly deteriorates as soon as the segmentation of the line does not coincide with the discontinuity points. In this section we investigate how the zone-dependent Kriging-based scheme can circumvent this limitation. More precisely, we analyze the influence of the zone segmentation on the limit function, starting from a fixed initial data set exhibiting a single discontinuity point. We consider the following test function:

$$f = \begin{cases} 5 * sin(\pi * (x - 0.1) + \frac{1}{6} & \text{if } x \in [0, 0.65] \\ 5 - 5 * sin(\pi * (x - 0.1) + \frac{1}{6} & \text{if } x \in]0.65, 1] \end{cases}$$

with one discontinuity at $x_0 = 0.65$. The initial sequence is $f^{J_0} = (f(k2^{-J_0}), 0 \leq k \leq 2^{J_0}$.

In the following tests, it is assumed that the segmentation procedure has provided an inaccurate estimation leading to the segmentation point $y_0 = 0.68$ and we compare the reconstruction for the three following schemes:

- Zone-dependent Kriging-based subdivision scheme(ZDK): the segmentation in different zones takes into account that a bad detection can occur. Therefore, 3 zones are defined: 2 regular ($[0, 0.6]$ and $[0.7, 1]$) and one non-regular ($]0.6, 0.7[$). That corresponds to $y_0 = 0.6$, $y_1 = 0.7$ with $y_0 < x_0 < y_1$. The construction of Kriging-based scheme requires to identify the spatial structure of the data through the computation of the semi-variogram. For the rest of the section, this spatial structure is assumed to be the same in each zone and is estimated once and for all. The identified semi-variogram is of Gaussian type and is provided by Figure 4.4, right.

- Position-dependent Lagrange-based subdivision scheme(PDL) assuming that the segmentation position is located at $y_0 = 0.68$, reminding that $y_0 \neq x_0$.

Table 4.1: l_2-error for TIL, PDL, ZDK.

l_2-error	$J_0 = 4$	$J_0 = 5$	$J_0 = 6$	$J_0 = 7$
PDL	0.0401	0.0293	0.0094	0.0127
TIL	0.0227	0.0227	0.0114	0.0057
ZDK	0.0203	0.0143	0.0098	0.0059

- Translation-invariant Lagrange-based subdivision scheme(TIL) since this scheme is the archetype of the schemes not adapted to singularities.

Figure 4.5 displays the limit functions reached by the different schemes starting from $f^{J_0}, J_0 = 4$. Table 4.1 provides the l_2-error $||f_k^{Jmax} - f(2^{-Jmax}k)||_{l_2}$, $k \in [0, 2^{Jmax}]$ for $Jmax = 12$ and different values of J_0.

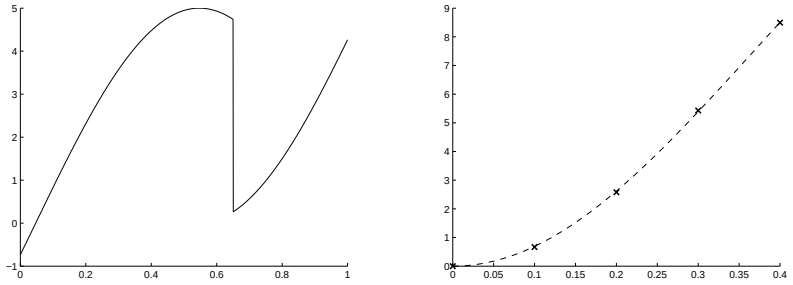

Figure 4.4: Test function (left) and its experimental semi-variogram(right): the cross signs are the experimental values of the semi-variogram and the dashed line is the fitted γ.

From Figure 4.5 it appears that the position-dependent Lagrange reconstruction (PDL) does not exhibit the oscillations generated by the translation-invariant one (TIL) thanks to its adaption to segmentation point. However it leads to a large l_2-error due to the mismatch between y_0 and x_0. On the contrary, the zone-dependent Kriging strategy (ZDK) is not penalized by the poor estimate of the discontinuity point (as soon as $y_0 < x_0 < y_1$). As a result, it keeps the interesting property of Gibbs phenomenon reduction of position-dependent approaches leading to an acceptable l^2 error while damping the strong dependence on the segmentation precision.

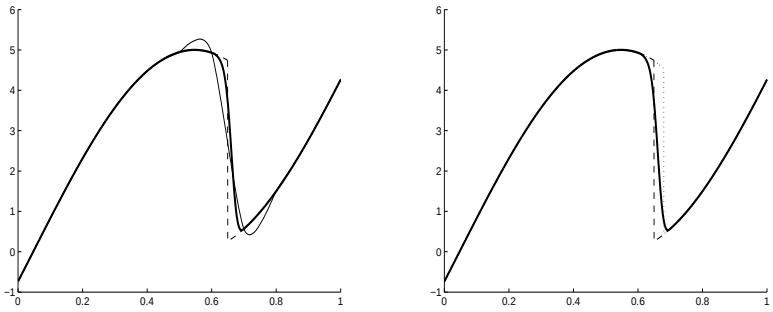

Figure 4.5: Limit functions starting from $f^{J_0}, J_0 = 4$: From left to right, comparison between the test function (dashed line), TIL (thin line) and ZDK (thick line), comparison between the test function (dashed line), PDL (dotted line) and ZDK (thick line).

4.5.2 Curve generation

Our zone-dependent Kriging-based subdivision scheme (ZDK) is here applied to curve generation. More precisely, we evaluate the capability of this approach in presence of noisy control points. Figure 4.6 displays an example of curve reconstruction, where some control points have been polluted by a white noise. It is assumed that a zone segmentation has been performed, including the noisy data in a single "non regular" zone $[y_0, y_1]$. As it is well known, translation invariant interpolatory subdivision schemes such as Lagrange-based ones are not tailored to adapt to noisy data and lead to undesirable oscillations (Figure 4.6 left). On the contrary, since the zone-dependent Kriging strategy allows to combine interpolatory (in the zone without noise) and non-interpolatory (in the noisy zone) schemes, the oscillations are reduced and the reconstructed curve is more convenient (Figure 4.6 right).

4.5.3 Application to real bivariate data

This test is a first attempt to illustrate the use of Kriging-based subdivision schemes for the approximation of complex computer codes involving uncertainties. The propagation of uncertainties through a computer code requires to perform a high number of simulations in order to explore the whole range of variation of code responses. This is not affordable in industrial applications due to a prohibitive computational cost. Therefore, the computer code is often replaced by an accurate approximation which is constructed from an initial (small) set of simulations called a design of experiments ([14]). In what follows, we

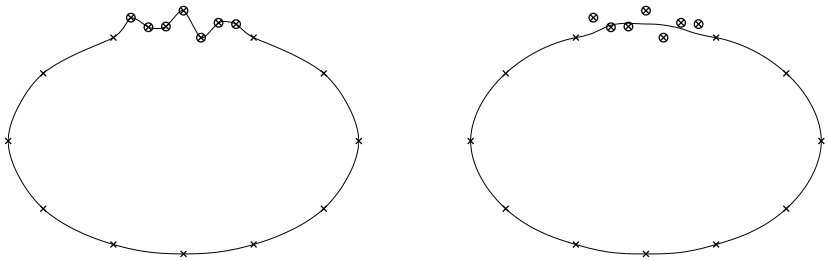

Figure 4.6: Curve generation from a set of control points (cross signs), in which several ones are polluted (circled cross signs): left, reconstruction by a Lagrange interpolatory scheme ; right, reconstruction by a zone-dependent Kriging-based subdivision.

investigate how zone-dependent Kriging subdivision can contribute to the reconstruction of non-regular code response.
More precisely, we focus in the sequel on a simplified case study coming from the analysis performed by IRSN on the mechanical cracking of materials. We consider a microstructure composed of a metal matrix with one rectangular inclusion as depicted on Figure 4.7.

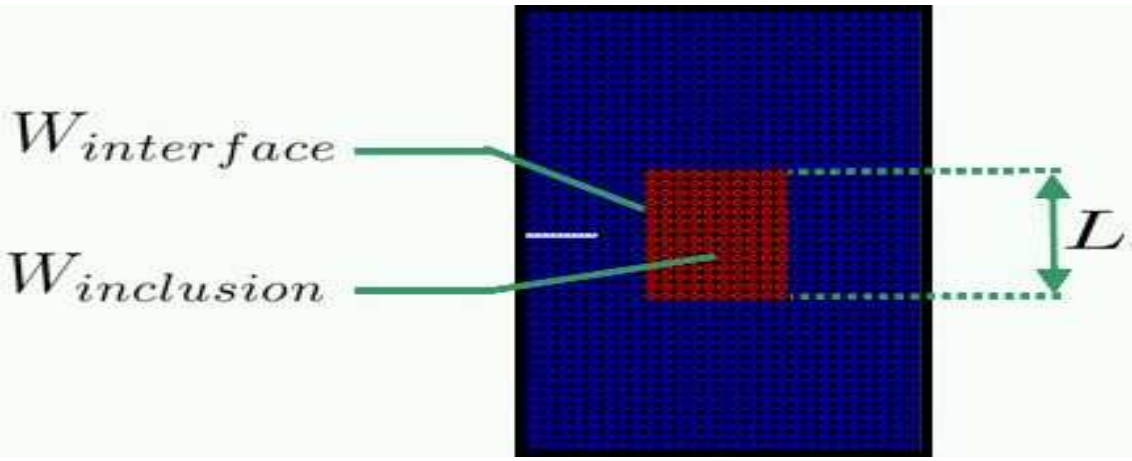

Figure 4.7: Metal matrix with a rectangular inclusion.

The code output is here the fracture energy denoted E_{fr}. The first uncertain input parameters is $Log(W)$ where W is the ratio between the interface energy ($W_{interface}$) and

Table 4.2: Uncertain parameters and range of variation.

$Log(W)$	$L_{inclusion}$
$[-7, 3]$	$[1.5\ 10^{-3}, 1.35\ 10^{-2}]$

the inclusion energy (W_{energy}) while the second one is the inclusion length ($L_{inclusion}$). Table 4.2 provides their range of variation.

Figure 4.8, left, displays the 91 available simulations. They were obtained by running the code on a dyadic design of experiments of $[-7, 3] \times [1.5\ 10^{-3}, 1.35\ 10^{-2}]$. It comes out that the data exhibits two smooth regions and a strong transition between them. Therefore, a local prediction including a zone-dependent strategy seems to be appropriate to handle this type of reconstruction.

Defining, for any $j \geq 0$, the 2d-grid $\{(x^j_{k_1}, y^j_{k_2})\}_{(k_1,k_2)\in\{0,\dots,2^j\}^2}$ where $x^j_{k_1} = -7 + 10 * k_1 * 2^{-j}$ and $y^j_{k_2} = 1.5\ 10^{-3} + 1.2\ 10^{-2} * k_2 * 2^{-j}$, a zone-dependent Kriging-based subdivision scheme is applied from $j = 0$ to $j = 5$. The prediction is constructed by tensor product ([15]) of 1d schemes (i.e. subdivision along the x-axis then along the y-axis). Figure 4.8, right, provides the reconstructed fracture energy by our scheme.

As expected, the segmentation in three zones and the introduction of an error variance vector in the Kriging-based subdivision scheme erase the Gibbs phenomenon in the reconstruction of the strong transition. In this way, it avoids unrealistic values that could occur due to oscillations.

4.6 Conclusion

A new Kriging-based subdivision scheme has been constructed. It is based on a data segmentation in different zones and combines interpolatory and non-interpolatory predictions thanks to the introduction of a zone-dependent error variance in the Kriging model. A full convergence analysis in the case of a 4-point stencil has been performed, establishing a connection between this non-stationary scheme and a convergent stationary one. The applications to the reconstruction of non-regular or noisy data have pointed out three main advantages of this type of approach:

- Adaption to data: it allows to integrate information related to discontinuities in the data which is necessary to avoid the so called Gibbs phenomenon.

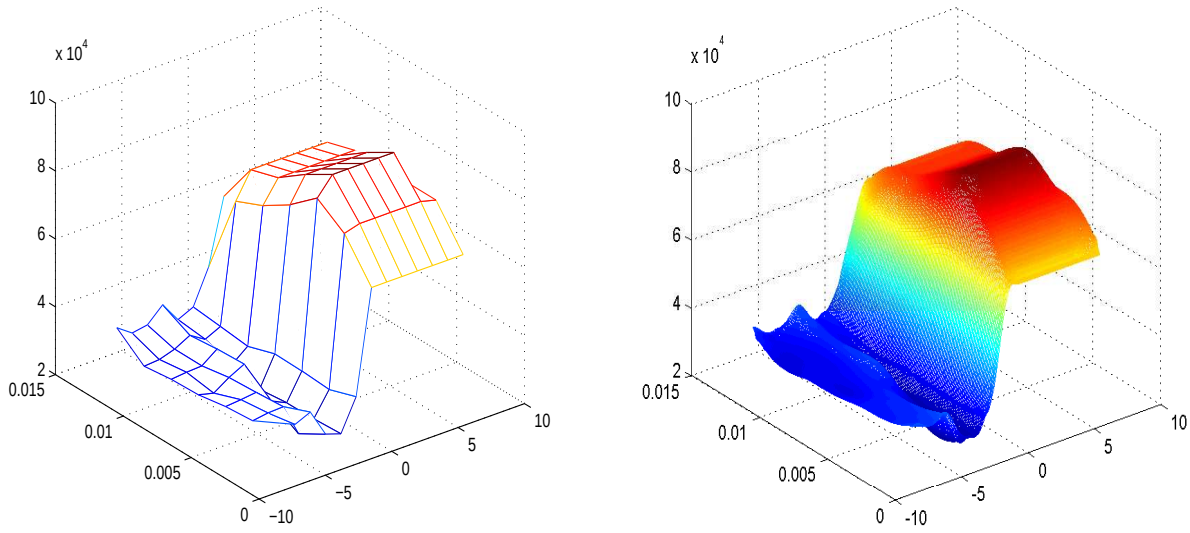

Figure 4.8: Reconstruction of the fracture energy by zone-dependent Kriging-based subdivision. Left, original data, right, reconstructed fracture energy.

- Robustness to errors in the discontinuity detection: the capabilities of the prediction are less sensitive to an inaccurate segmentation that is the main limitation of position-dependent schemes.
- Efficiency in the reconstruction of noisy data: combining interpolatory (in zones without noise) and non-interpolatory (in zones with noise) predictions, leads to regular reconstructed curves reducing the oscillations associated to fully interpolatory schemes.

Chapter 5

On four-point penalized Lagrange subdivision schemes

On one hand, the previous chapters have shown that Kriging theory is flexible enough to construct subdivision schemes combining interpolatory and non-interpolatory predictions thanks to the introduction of error variance. On the other hand, Lagrange subdivision schemes have been intensively used in practice for multi-scale analysis but their main drawback is that they are interpolatory which reduces their efficiency for the reconstruction of discontinuous or noisy data. Therefore, we propose in this chapter to modify the classical 4-point Lagrange prediction in order to relax the interpolation constraint by exploiting the asymptotical connection introduced in Chapters 3 and 4 between stochastic Kriging and deterministic Lagrange frameworks. This new type of subdivision schemes is called penalized Lagrange. Its construction is based on an extension of the use of error variance. This work has been submitted to Computer Aided Geometric Design Journal. Therefore, this chapter mainly includes the corresponding article. However, for a better understanding, several comments are first formulated to emphasize the key points related to the construction, the analysis and the application of this new scheme.

5.1 Overview on the different sections of the article

The article is composed of four main parts: After a brief recall of the basic notations on binary subdivision schemes, the first part (Section 5.5) is devoted to an original reformulation for the construction of the mask associated with the classical 4-point Lagrange

interpolatory subdivision scheme leading to penalized Lagrange scheme. In the second one (Section 5.6), we focus on the computation and the analysis of the corresponding mask. This new approach is coupled in the third part (Section 5.7) with a zone-dependent strategy in order to accurately reconstruct discontinuous or locally noisy data. The convergence of the corresponding zone-dependent scheme is studied as well. Finally, the last part (Section 5.8) provides several numerical tests in order to point out the efficiency of these schemes compared to standard approaches.

5.1.1 First part

The starting point is the reformulation of the Kriging problem with error variance as a constrained minimization one including a penalization term as described in Section 3.2.3 of Chapter 3. More precisely, it turns out that in a deterministic framework, the error variance vector can be seen as a penalization of the oscillations of the solutions of (5.7). Therefore, the weights of the 4-point Lagrange prediction are first written as the solution of a Kriging-like problem (Proposition 5.5.1). Note that these results have already been introduced in Proposition 4.3.3 (Expressions (4.4) and (4.5)) up to a change in the notations for the polynomial involved in the left hand side matrix of the Kriging-like problem.
Then, similarly to the Kriging case, the diagonal of R can be modified to relax the interpolating property. Following [1], the result provided by Proposition 5.5.1 can be generalized to any Lagrange schemes with a $2r$-point stencil ($r > 1$) replacing $P_j(x) = b_0 2^{-2j} x^2 + b_1 2^{-4j} x^4$ by $P_j(x) = \sum_{n=0}^{r-1} b_n \left(2^{-j}x\right)^{2n+2}$.

5.1.2 Second part

The computation and the analysis of the mask associated with the Lagrange penalized scheme are based on a direct calculus of the inverse of the left hand side matrix. They mimic the different steps followed in Section 4.3.2 of Chapter 4 replacing $\{U_i^{(k)}\}_{i\in\{0,\dots,4\}}$ by $\{a_i^{(k)}\}_{i\in\{0,\dots,4\}}$. In the numerical study, we focus on a penalization vector characterized by a single coefficient c. Besides the verification of the asymptotical behavior of the mask, two conclusions need to be emphasized for practical issues: the first one is that for large enough j, the mask exists for any c. The analyst can therefore choose the penalization vector according to her/his knowledge of the problem (related to the size of the jump for discontinuous data or to the noise variance for noisy ones). The second important

point to mention concerns the sign of the coefficients of the mask: it turns out that they become non-negative for large enough c which is an important property to reduce the Gibbs phenomenon.

5.1.3 Third part

A new zone-dependent penalized Lagrange scheme is defined following the same philosophy as for the Kriging-based one introduced in Section 4.4. It is performed in two steps:

- A segmentation of the data in different zones and the choice of a penalization function for each zone.
- the construction of a zone-dependent penalized Lagrange scheme taking into account the information of the first step.

However, the main difference with Chapter 4 stands in the zone-dependent strategy. More precisely, the stencil here is fixed (4-point centered stencil) and the penalization vector is position-dependent whereas for Kriging-based scheme, the stencil is adapted (i.e. position-dependent) at the edge of the zones in order to avoid crossing segmentation points and the penalization vector is fixed in each zone. As a consequence, the asymptotical (with respect to j) penalized Lagrange scheme which is used for the convergence analysis in this article combines predictions with stencils of different lengths.

5.1.4 Fourth part

The numerical applications point out that the penalized Lagrange scheme combined with a zone-dependent strategy leads to promising results in practice. A large enough c allows one to drastically reduce the Gibbs phenomenon associated with discontinuous data which was one of the main drawback of classical interpolatory Lagrange scheme. Moreover, the flexibility in the choice of the penalization improves the capability of this kind of scheme to handle the reconstruction of noisy data involved in signal processing and computer-aided design.

5.2 Abstract

This paper is devoted to the definition and analysis of new subdivision schemes called penalized Lagrange. Their construction is based on an original reformulation for the

construction of the coefficients of the mask associated with the classical 4-point Lagrange interpolatory subdivision scheme: these coefficients can be formally interpreted as the solution of a linear system similar to the one resulting from the constrained minimization problem in Kriging theory which is commonly used for Geo-statistical studies. In such a framework, the introduction in the matricial formulation of a so-called error variance can be viewed as a penalization of the oscillations of the coefficients. Following this idea, we propose to penalize the 4-point Lagrange system in order to transform the interpolatory schemes into approximating ones with specific properties suitable for locally noisy or strongly oscillating data. A full theoretical study is first performed to analyze this new type of subdivision scheme. Then, several numerical tests are provided to point out the efficiency of these schemes compared to standard approaches.

5.3 Introduction

Since Deslaurier and Dubuc ([16]), Lagrange interpolatory subdivision schemes have been intensively used. Originally, they are designed for generating curves starting from initial control polygons by repeated refinements. These schemes and their extensions are working horses for multi-scale approximation and are used in many applications of numerical analysis including numerical solutions of partial differential equations, data reconstruction or image and signal analysis. Their convergence is well understood (at least when they remain linear). Smooth curves can then be generated leading to efficient tools for approximation problems. Their major drawback lays in the existence of Gibbs oscillations for the limit curve when initial data exhibit strong gradients (see Figure 5.6 top left). These oscillations are connected to the oscillations of the coefficients involved in the Lagrange prediction. Subdivision schemes are characterized by set of coefficients called masks of the scheme. In a recent paper ([1]), the mask of the Lagrange interpolatory subdivision schemes appeared as the limit mask of a non-stationary subdivision scheme based on Kriging approach. Kriging ([10]) is a stochastic data modeling and reconstruction tool widely used in the framework of spatial data analysis. Its main advantages stand in the possibility to integrate in the prediction the spatial dependency of the available data and to quantify the precision of the prediction thanks to the model describing this dependency. When they are interpolatory, Kriging schemes are subject to Gibbs oscillations ([17]) in the vicinity of strong gradients. However, it can be corrected introducing a so called error variance vector ([18]). This vector can be interpreted as a penalization of the oscillation

of the subdivision mask coefficients that appear, in the Kriging approach, as solution of an optimization procedure.

The goal of this paper is to mimic the use of error variance in Kriging to generate new schemes derived from the Lagrange interpolatory framework. They will be called penalized Lagrange subdivision schemes. Our work is organized as follows: after a quick overview of binary subdivision schemes in Section 5.4, we establish in Section 5.5 the connection between the Lagrange and Kriging frameworks. It will lead to the construction of penalized Lagrange subdivision schemes. This new type of schemes is fully analyzed in Section 5.6 in the case of a 4-point centered prediction. Then, in Section 5.7, it is coupled with a zone-dependent strategy in order to accurately reconstruct discontinuous or locally noisy data. The convergence of the corresponding zone-dependent scheme is studied as well. Finally, Section 5.8 provides several numerical tests in order to point out the efficiency of these schemes compared to standard approaches.

5.4 Basic notations and results for binary subdivision schemes

5.4.1 Lagrange interpolatory subdivision scheme

A subdivision scheme S is here defined as a linear operator from $l^\infty(\mathbb{Z})$ to itself constructed from a mask $(a_k)_{k\in\mathbb{Z}}$ which is a sequence of real numbers null but a finite number of them as:

$$(f_k)_{k\in\mathbb{Z}} \in l^\infty(\mathbb{Z}) \mapsto ((Sf)_k)_{k\in\mathbb{Z}} \in l^\infty(\mathbb{Z}) \quad \text{with} \quad (Sf)_k = \sum_{l\in\mathbb{Z}} a_{k-2l} f_l.$$

The mask plays a key role in the subdivision process since it controls the refinement rule. There exists many works dealing with its construction. Among them, one can mention [19], [20] and [21], that are devoted to interpolatory Lagrange-based scheme. For interpolatory schemes, the coefficients of the mask are characterized by $a_0 = 1$, $a_{2\alpha} = 0$ for $\alpha \neq 0$. Moreover, in the case of Lagrange prediction,

$$a_{2\alpha+1} = L_\alpha^{l,r}(-\frac{1}{2}), -l \leq \alpha \leq r-1,$$

where $L_\alpha^{l,r}$ is the elementary Lagrange interpolatory polynomial defined by:

$$L_\alpha^{l,r}(x) = \Pi_{n=-l,n\neq\alpha}^{r-1} \frac{x-n}{\alpha-n}.$$

In this article, we will mainly consider the 4-point centered Lagrange interpolatory scheme corresponding to $l = r = 2$. It can be written with respect to the parity of k ($k = 2\alpha$ or $k = 2\alpha + 1$) as:

$$\begin{cases} (Sf)_{2\alpha} &= f_\alpha, \\ (Sf)_{2\alpha+1} &= -\frac{1}{16}f_{\alpha-1} + \frac{9}{16}f_\alpha + \frac{9}{16}f_{\alpha+1} - \frac{1}{16}f_{\alpha+2}. \end{cases}$$

Subdivision is iterated from an initial sequence $(f_k^0)_{k\in\mathbb{Z}}$ to generate $(f_k^j)_{k\in\mathbb{Z}}$ for $j \geq 1$ as

$$f^{j+1} = Sf^j, j \geq 0.$$

Parameter j is called the scale parameter and is linked to the dyadic grid $X_j = \{k2^{-j}, k \in \mathbb{Z}\}$. If the masks are scale invariant, the scheme is stationary whereas non-stationary when they depend on j.

5.4.2 Convergence of subdivision schemes

The uniform convergence of subdivision schemes is made precise in the following definition.

Definition 5.4.1
The subdivision scheme S is said to be l^∞-convergent if for any real sequence $(f_k^0)_{k\in\mathbb{Z}}$, there exists a continuous function f (called the limit function associated with f^0) such that: $\forall\epsilon, \exists J$ such that $\forall j \geq J$, $\| S^j f^0 - f\left(\frac{\cdot}{2^j}\right) \|_\infty \leq \epsilon$.

Following [19], the convergence of stationary linear subdivision schemes can be analyzed from the scheme S_1 associated with the difference $\delta f_k^j = f_{k+1}^j - f_k^j$ that exists as soon as the initial scheme S reproduces constants, i.e

$$\forall k \in \mathbb{Z}, f_k = 1 \Rightarrow \forall k \in \mathbb{Z}, Sf_k = 1.$$

More precisely, we have:

Theorem 5.4.1
Let S be a stationary subdivision scheme defined by a mask reproducing constants and S_1 the scheme associated with the differences. S is uniformly convergent if and only if S_1 converges uniformly to the zero function for all initial data f^0.

For non-stationary subdivision schemes, the convergence analysis is generally more involved. However, the convergence of the mask towards a fixed mask associated with a convergent stationary scheme can be used to reach the result. This will be fully specified in Section 5.7.

5.5 From error variance ordinary Kriging to penalized Lagrange prediction

The main steps related to the construction of a Kriging prediction are first recalled in the following section. For the sake of clarity, they are described independently of the subdivision framework.

5.5.1 Overview on ordinary Kriging prediction

Considering N observations of a function, $f \in F$, $\{f_i\}_{i=0,\dots,N-1}$ on the grid $\{x_i\}_{i=0,..,N-1}$, Kriging addresses the problem of the prediction of f at a new location $x^\star$. Ordinary Kriging ([10]) belongs to the class of stochastic prediction method. It is assumed that $\{f_i\}_{i\in\mathbb{Z}}$ are realizations of a subset of random variables $\{\mathcal{F}(x_i), i \in \mathbb{Z}\}$ coming from a random process $\mathcal{F}(x)$ that can be decomposed as $\mathcal{F}(x) = m + \delta(x)$, where m is the constant deterministic mean structure of $\mathcal{F}(x)$ and $\delta(x)$ is a spatially correlated random process. Under stationarity assumptions and constant deterministic mean structure, the spatial structure associated with $\delta(x)$ is identified to the spatial correlation of the data and is exhibited by computing the semi-variogram, $\gamma(h) = \frac{1}{2}E((\mathcal{F}(x+h)-\mathcal{F}(x))^2)$, where E denotes the mathematical expectation[1]. The ordinary Kriging estimator of the random process $\mathcal{F}$ at a new location $x^\star$ is denoted $\mathcal{P}(\mathcal{F}, x^\star)$. It is the linear, unbiased predictor[2] minimizing the estimation variance $\sigma_K^2 = var(\mathcal{F}(x^\star) - \mathcal{P}(\mathcal{F}, x^\star))$. It is written as

$$\mathcal{P}(\mathcal{F}, x^\star) = \sum_{i=0}^{N-1} \lambda_i \mathcal{F}(x_i), \tag{5.1}$$

where $\{\lambda_i\}_{i=0,\dots,N-1}$ are called the Kriging weights. In the case of continuous semi-variograms, expanding the estimation variance as a function of γ and taking into account

[1] Let X be a real random variable of density f_X. Its mathematical expectation is defined as the integral over the realizations x of X weighted by the density function i.e. $E(X) = \int_{\mathbb{R}} x f_X(x) dx$.

[2] $\mathcal{P}(\mathcal{F}, x)$ is an unbiased estimator if and only if $E\left(\mathcal{P}(\mathcal{F}, x) - \mathcal{F}(x)\right) = 0$ where E is the mathematical expectation.

the unbiased condition, the Kriging weights are solutions of the classical optimization under constraint problem ([12]):

$$\begin{cases} min_{\{\lambda_i\}_{i=0,\dots,N-1}} \mathcal{J}\left(x^\star;\lambda_0,\dots,\lambda_{N-1}\right), \\ \sum_{i=0}^{N-1}\lambda_i = 1, \end{cases} \tag{5.2}$$

where $\mathcal{J}\left(x^\star;\lambda_0,\dots,\lambda_{N-1}\right) = -\frac{1}{2}\sum_{i=0}^{N-1}\sum_{n=0}^{N-1}\lambda_i\lambda_n\gamma(||x_i-x_n||_2) + \sum_{i=0}^{N-1}\lambda_i\gamma(||x_i - x^\star||_2)$ with $||.||_2$ the Euclidean norm. Denoting by the upper-script T the transpose operator and introducing $u = (\lambda_0,\dots,\lambda_{N-1})^T$, Problem (5.2) leads to the following linear system:

$$\begin{bmatrix} R & \mathbb{1} \\ \mathbb{1}^T & 0 \end{bmatrix} \begin{bmatrix} u \\ \mu \end{bmatrix} = \begin{bmatrix} b \\ 1 \end{bmatrix}, \tag{5.3}$$

where $R = \begin{bmatrix} 0 & \gamma(||x_0-x_1||_2) & ... & \gamma(||x_0-x_{N-1}||_2) \\ \gamma(||x_1-x_0||_2) & 0 & ... & \gamma(||x_1-x_{N-1}||_2) \\ ... & ... & ... & \\ \gamma(||x_{N-1}-x_0||_2) & \gamma(||x_{N-1}-x_1||_2) & ... & 0 \end{bmatrix}$,

$b = (\gamma(||x_0-x^\star||_2),\dots,\gamma(||x_{N-1}-x^\star||_2))^T$ and $\mathbb{1} = (1,\dots,1)^T$. Here, μ is the Lagrange multiplier enforcing the unbiasedness of the estimator.
With these notations, the minimization problem (5.2) can be reformulated as:

$$\begin{cases} min_{u\in\mathbb{R}^N}\left(-\frac{1}{2} < Ru, u >_2 + < b, u >_2\right), \\ < u, \mathbb{1} >_2 = 1, \end{cases} \tag{5.4}$$

where $< , >_2$ is the Euclidean scalar product. The matrix R is symmetric Toeplitz with positive coefficients and a null main diagonal. By definition ([12]), it satisfies $< Rv, v >_2 < 0, \forall v \in \mathbb{R}^N$ such that $v \neq 0$ and $\sum_{i=1}^N v_i = 0$. Since any vector u satisfying $< u, \mathbb{1} >_2 = 1$ can be decomposed as $u = v + \mathbb{1}$ with $< v, \mathbb{1} >_2 = \sum_{i=1}^N v_i = 0$,

$$-\frac{1}{2} < Ru, u >_2 + < b, u >_2 = -\frac{1}{2} < Rv, v >_2 + < b, v >_2 -\frac{1}{2}\alpha + < b, \mathbb{1} >_2,$$

where $\alpha = \sum_{i=1}^N\sum_{n=1}^N R_{i,n}$. Therefore, minimizing $-\frac{1}{2} < Ru, u >_2 + < b, u >_2$ under the constraint $< u, \mathbb{1} >_2 = 1$ is equivalent to minimize $-\frac{1}{2} < Rv, v >_2 + < b, v >_2$. Since

R is negative definite on the set $\{v \in \mathbb{R}^N, \sum_{i=1}^N v_i = 0\}$ the minimum exists and is unique and therefore the matrix R is invertible; the Kriging weights are therefore well defined.

The previous Kriging estimator (5.1) is an exact interpolator. The constraint of exact interpolation can be released introducing non-zero coefficients on the diagonal of R i.e. replacing R by $R - C$ where:

$$C = \begin{bmatrix} c_1 & 0 & ... & 0 \\ 0 & c_2 & 0 & 0 \\ ... & ... & ... & \\ 0 & 0 & ... & c_N \end{bmatrix} \tag{5.5}$$

with $\forall i,\ c_i \geq 0$. The vector

$$\mathcal{C} = (c_1, ..., c_N) \tag{5.6}$$

is called the vector of error variance ([18]) since it allows to take into account measurement errors or uncertainties on the data. As a result, the corresponding prediction is no more interpolating at points where the error variance vector is non-zero. The optimization problem (5.4) becomes in this case:

$$\begin{cases} min_{u \in I\!R^N} \left(-\frac{1}{2} < Ru, u >_2 + \frac{1}{2} < Cu, u >_2 + < b, u >_2 \right), \\ < u, \mathbb{1} >_2 = 1. \end{cases} \tag{5.7}$$

and the vector $\mathcal{C}$ can be interpreted as a penalization of the l_2-norm of u, i.e as a penalization of the oscillations of the coefficients of u, keeping in mind that $< u, \mathbb{1} >_2 = 1$. With the same arguments as previously, the minimum of (5.7) exists and is unique.

This short review shows that the Kriging approach is flexible enough to include interpolatory and non-interpolatory predictions in the same framework. In the next section, this flexibility is adapted to the Lagrange framework. To reach our goal, a two-step procedure is involved. First (Section 5.5.2), the Lagrange prediction is formally reformulated as a Kriging-like prediction, constructing a linear system of type (5.3) which solution is the Lagrange weight vector. In the second step, (Section 5.6), a penalization vector $\mathcal{C}$ is introduced and the analysis of the corresponding new schemes is performed.

5.5.2 Combining interpolatory and non-interpolatory predictions within the Lagrange framework

The reformulation of the 4-point interpolatory Lagrange subdivision scheme inside the Kriging framework is summarized in the following

Proposition 5.5.1
For any $(b_0 \neq 0, b_1 \neq 0)$, let us introduce the polynomial $P_j(x) = b_0 2^{-2j} x^2 + b_1 2^{-4j} x^4$ and define the matrix

$$R = \begin{bmatrix} 0 & P_j(1) & P_j(2) & P_j(3) \\ P_j(1) & 0 & P_j(1) & P_j(2) \\ P_j(2) & P_j(1) & 0 & P_j(1) \\ P_j(3) & P_j(2) & P_j(1) & 0 \end{bmatrix}, \tag{5.8}$$

as well as the vectors
$b = \left(P_j(\frac{3}{2}), P_j(\frac{1}{2}), P_j(\frac{1}{2}), P_j(\frac{3}{2})\right)^T$ *(resp.* $b = (P_j(1), P_j(0), P_j(1), P_j(2))^T$*).*

The unique solutions of Equation (5.3) are $\left(-\frac{1}{16}, \frac{9}{16}, \frac{9}{16}, -\frac{1}{16}, \mu_L\right)$ *(resp.* $(0, 1, 0, 0, 0)$*) where* $\mu_L = P_j(\frac{3}{2}) - \left(\frac{9}{16}P_j(1) + \frac{9}{16}P_j(2) - \frac{1}{16}P_j(3)\right)$.

Proof:

The details of the proof are not given in the sequel. The result stated by this proposition can be obtained by performing the same calculation as in the proof of Proposition 4.6 (Step 3) in [1]. In this paper, the polynomial P_j that appeared was $2^{-2j}x^2 - \frac{1}{2}2^{-4j}x^4$ as the first terms of the Taylor expansion of the Gaussian variogram $\gamma(x) = 1 - e^{-2^{-2j}x^2}$. It is based on two steps: we first verify that the Lagrange weights are solution of Equation (5.3) with $\mu = \mu_L$ or $\mu = 0$; then, the uniqueness of the solution is ensured by studying the kernel of the left hand side matrix of (5.3) leading to a linear system involving a Vandermonde matrix. ∎

As in the previous section, one can now introduce a penalization vector $\mathcal{C}$ of type (5.6) to modify the diagonal of (5.8). We postpone to Section 5.6 the analysis of the invertibility of the new matrix $R - C$ and of the weights solution of the corresponding

system. However, after a short calculus, it is interesting to notice that the new prediction does not involve anymore the Lagrange weights and is no more interpolating. Therefore, this reformulation of the Lagrange problem and its connection to the linear equation of a Kriging-like estimation allows to introduce more flexibility in the prediction which is of prime importance for data reconstruction: instead of defining once and for all a prediction operator that will be used for the whole data, one can introduce local strategies (based on the choice of $\mathcal{C}$) with respect to their behavior to improve the accuracy of the result.

5.6 Analysis of the weights associated with the penalized Lagrange prediction

5.6.1 Existence and expression of the weights

The following propositions are devoted to the analysis of the linear system (5.3) written with $R - C$ where R is the matrix (5.8) and C the matrix (5.5). For induction argument, this global matrix is denoted A_0 when $C = \mathbf{0}$ ($\mathbf{0}$ stands for the null matrix) and is then used to provide the existence and the expression of the weights associated with the penalized Lagrange scheme ($C \neq \mathbf{0}$).

Proposition 5.6.1
Denoting the general term of the symmetric matrix A_0^{-1} by $[A_0^{-1}]_{in} = A^0_{(i-1)(n-1)}, 1 \leq i, n \leq 5$, then

$\forall 0 \leq i \leq 3,$

$$\begin{cases} A_{i0}^{(0)} = \frac{1}{b_1}\left(\frac{\alpha_{1,i}}{24} + \frac{\alpha_{2,i}}{6} + \frac{11}{24}\alpha_{3,i}\right) 2^{4j} - \frac{\alpha_{3,i}}{48}\frac{b_0}{b_1^2}2^{6j}, \\ A_{i1}^{(0)} = \frac{2^{4j}}{b_1}(-\frac{\alpha_{1,i}}{8} - \frac{5}{12}\alpha_{2,i} - \frac{3}{4}\alpha_{3,i}) + \frac{\alpha_{3,i}b_0 2^{6j}}{16b_1^2}, \\ A_{i2}^{(0)} = \frac{2^{4j}}{b_1}(\frac{\alpha_{1,i}}{8} + \frac{1}{3}\alpha_{2,i} + \frac{3}{8}\alpha_{3,i}) - \frac{\alpha_{3,i}b_0 2^{6j}}{16b_1^2}, \\ A_{i3}^{(0)} = \frac{2^{4j}}{b_1}(-\frac{\alpha_{1,i}}{24} - \frac{1}{12}\alpha_{2,i} - \frac{1}{12}\alpha_{3,i}) + \frac{\alpha_{3,i}b_0 2^{6j}}{48b_1^2}, \end{cases} \tag{5.9}$$

with

$$\begin{bmatrix} \alpha_{0,0} & \alpha_{0,1} & \alpha_{0,2} & \alpha_{0,3} \\ \alpha_{1,0} & \alpha_{1,1} & \alpha_{1,2} & \alpha_{1,3} \\ \alpha_{2,0} & \alpha_{2,1} & \alpha_{2,2} & \alpha_{2,3} \\ \alpha_{3,0} & \alpha_{3,1} & \alpha_{3,2} & \alpha_{3,3} \end{bmatrix} = \begin{bmatrix} 1 & 0 & 0 & 0 \\ -\frac{11}{6} & 3 & -\frac{3}{2} & \frac{1}{3} \\ 1 & -\frac{5}{2} & 2 & -\frac{1}{2} \\ -\frac{1}{6} & \frac{1}{2} & -\frac{1}{2} & \frac{1}{6} \end{bmatrix}.$$

Proof:

In this proof, we show how to derive the first equation of System (5.9). The remaining of the system can be obtained following the same track.

The first column of A_0^{-1} is the solution of

$$A_0 \times U = (1, 0, 0, 0, 0)^T \tag{5.10}$$

Introducing the polynomial $K(x) = A_{00}^{(0)} P_j(x) + A_{10}^{(0)} P_j(x-1) + A_{20}^{(0)} P_j(x-2) + A_{30}^{(0)} P_j(x-3) + A_{40}^{(0)} - L_0^{0,4}(x)$, (5.10) leads to $\forall i \in \{0, \ldots, 3\},\ K(i) = 0$. Therefore K has 4 roots. Since $A_{00}^{(0)} + A_{10}^{(0)} + A_{20}^{(0)} + A_{30}^{(0)} = 0$ (last equation of (5.10)), K is a polynomial of degree 3, and finally $\forall x \in I\!R,\ K(x) = 0$. It implies that the coefficients associated with each power of x are equal to 0, i.e.

$$\begin{cases} \text{for } x^3 : -4b_1 2^{-4j} \sum_{i=0}^{3} i A_{i0}^{(0)} + \frac{1}{6} = 0, \\ \text{for } x^2 : 6b_1 2^{-4j} \sum_{i=0}^{3} i^2 A_{i0}^{(0)} - 1 = 0, \\ \text{for } x : -4b_1 2^{-4j} \sum_{i=0}^{3} i^3 A_{i0}^{(0)} + \frac{11}{6} - \frac{2^{2j} b_0}{12 b_1} = 0, \\ \text{for } 1 : 2^{-2j} b_0 (A_{10}^{(0)} + 4A_{20}^{(0)} + 9A_{30}^{(0)}) + 2^{-4j} b_1 (A_{10}^{(0)} + 16A_{20}^{(0)} + 81A_{30}^{(0)}) + A_{40}^{(0)} - 1 = 0, \end{cases}$$

leading to

$$\begin{bmatrix} 1 & 1 & 1 & 1 \\ 0 & 1 & 2 & 3 \\ 0 & 1 & 4 & 9 \\ 0 & 1 & 8 & 27 \end{bmatrix} \begin{bmatrix} A_{00}^{(0)} \\ A_{10}^{(0)} \\ A_{20}^{(0)} \\ A_{30}^{(0)} \end{bmatrix} = \begin{bmatrix} 0 \\ \frac{1}{24 b_1} 2^{4j} \\ \frac{1}{6 b_1} 2^{4j} \\ \frac{11}{24 b_1} 2^{4j} - \frac{b_0}{48 b_1^2} 2^{6j} \end{bmatrix}, \tag{5.11}$$

and $A_{40}^{(0)} = 1 - 2^{-2j}(A_{10}^{(0)} + 4A_{20}^{(0)} + 9A_{30}^{(0)}) - 2^{-4j}(A_{10}^{(0)} + 16A_{20}^{(0)} + 81A_{30}^{(0)})$.
Denoting by M the left hand side matrix in Equation (5.11), our goal is to calculate

M^{-1}. By definition, since M is a Vandermonde matrix, its transpose M^T connects the basis $(1, x, x^2, x^3)$ to the basis $(L_0^{0,4}(x), L_1^{0,4}(x), L_2^{0,4}(x), L_3^{0,4}(x))$. Therefore, writing $\forall i \in \{0, \ldots, 3\},\ L_i^{0,4}(x) = \alpha_{3,i}x^3 + \alpha_{2,i}x^2 + \alpha_{1,i}x + \alpha_{0,i}$, we have

$$M^T \begin{bmatrix} \alpha_{0,i} \\ \alpha_{1,i} \\ \alpha_{2,i} \\ \alpha_{3,i} \end{bmatrix} = \Delta_i,$$

where Δ_i is the vector such that $\forall n \in \{1, \ldots, 4\}$, $(\Delta_i)_n = \delta_n^i$. It then comes out that $(\alpha_{0,i}\ \alpha_{1,i}\ \alpha_{2,i}\ \alpha_{3,i})^T$ is the i^{th} column of $(M^T)^{-1}$. Therefore, after a short calculus,

$$M^{-1} = \begin{bmatrix} \alpha_{0,0} & \alpha_{0,1} & \alpha_{0,2} & \alpha_{0,3} \\ \alpha_{1,0} & \alpha_{1,1} & \alpha_{1,2} & \alpha_{1,3} \\ \alpha_{2,0} & \alpha_{2,1} & \alpha_{2,2} & \alpha_{2,3} \\ \alpha_{3,0} & \alpha_{3,1} & \alpha_{3,2} & \alpha_{3,3} \end{bmatrix} = \begin{bmatrix} 1 & 0 & 0 & 0 \\ -\frac{11}{6} & 3 & -\frac{3}{2} & \frac{1}{3} \\ 1 & -\frac{5}{2} & 2 & -\frac{1}{2} \\ -\frac{1}{6} & \frac{1}{2} & -\frac{1}{2} & \frac{1}{6} \end{bmatrix}.$$

Coming back to (5.11), it finally provides the first equation of System (5.9). That concludes the proof.

■

The previous proposition is now used to study the existence of the weights associated with the penalized Lagrange system. An expression of the weights is derived as well for the prediction of f_k^j, $(k, j) \in \mathbb{Z}^2$ when $k = 2\alpha$ and $k = 2\alpha + 1$. Obviously, this analysis depends on the number and on the position of non-zero coefficients in the penalization vector. For the sake of simplicity and without loss of generality, we focus on four cases corresponding to the following penalization vectors: $(c_1, 0, 0, 0)$, $(c_1, c_2, 0, 0)$, $(c_1, c_2, c_3, 0)$ and (c_1, c_2, c_3, c_4) with $c_i > 0$. The four left hand side matrices involved in the penalized Lagrange system (5.3) are denoted:

$$A_m = \begin{bmatrix} -c_1 & P_j(1) & P_j(2) & P_j(3) & 1 \\ P_j(1) & \ldots & P_j(1) & P_j(2) & 1 \\ P_j(2) & P_j(1) & -c_m & P_j(1) & 1 \\ P_j(3) & P_j(2) & P_j(1) & 0 & 1 \\ 1 & 1 & 1 & 1 & 0 \end{bmatrix}, \quad m \in \{1, \ldots, 4\}, \tag{5.12}$$

and the corresponding solution is written $\Lambda^{(m)} = \left(a_0^{(m)}, a_1^{(m)}, a_2^{(m)}, a_3^{(m)}, \mu^{(m)}\right)^T$. As previously, we note the general term $[A_m^{-1}]_{in}$ of A_m^{-1} as $[A_m^{-1}]_{in} = A_{i-1,n-1}^{(m)}, 1 \leq i, n \leq 5$. In the following propositions, we focus on the existence and the computation of $\{a_i^{(m)}\}_{i=0,\ldots,3}$ associated with the system $A_m\Lambda^{(m)} = f$ where $f = (P_j(1), P_j(0), P_j(1), P_j(2), 1)^T$ and $f = (P_j(\frac{3}{2}), P_j(\frac{1}{2}), P_j(\frac{1}{2}), P_j(\frac{3}{2}), 1)^T$.

Proposition 5.6.2
For any $j \in \mathbb{Z}$, if $c_1 \in D_j$ where $D_j = \{c_1 > 0 / c_1 \neq \frac{1}{\frac{2^{4j}}{72b_1} + 2^{6j}\frac{b_0}{288b_1^2}}\}$ then the weights associated with the penalized Lagrange system including one non-zero penalization coefficient exist. They satisfy:

- *if $k = 2\alpha$:*

$$\begin{bmatrix} a_0^{(1)} \\ a_1^{(1)} \\ a_2^{(1)} \\ a_3^{(1)} \end{bmatrix} = \begin{bmatrix} 0 \\ 1 \\ 0 \\ 0 \end{bmatrix}. \tag{5.13}$$

- *if $k = 2\alpha + 1$:*

$$\begin{bmatrix} a_0^{(1)} \\ a_1^{(1)} \\ a_2^{(1)} \\ a_3^{(1)} \end{bmatrix} = \begin{bmatrix} -\frac{1}{16(1-c_1A_{00}^{(0)})} \\ \frac{9}{16} - \frac{c_1A_{10}^{(0)}}{16(1-c_1A_{00}^{(0)})} \\ \frac{9}{16} - \frac{c_1A_{20}^{(0)}}{16(1-c_1A_{00}^{(0)})} \\ -\frac{1}{16} - \frac{c_1A_{30}^{(0)}}{16(1-c_1A_{00}^{(0)})} \end{bmatrix}, \tag{5.14}$$

where $\{A_{i0}^{(0)}\}_{i=0,\ldots,3}$ is given by System (5.9).

Proof:

- Existence of the weights:

Splitting A_1 as $A_1 = A_0 + \tilde{A}_1$ and writing, since A_0^{-1} exists, $A_1 = A_0(I + A_0^{-1}\tilde{A}_1)$, the invertibility of A_1 is ensured as soon as $B_0 = (I + A_0^{-1}\tilde{A}_1)$ is invertible. B_0 can be expressed as:

$$B_0 = \begin{bmatrix} 1 - c_1 A_{00}^{(0)} & 0 & 0 & 0 & 0 \\ -c_1 A_{10}^{(0)} & 1 & 0 & 0 & 0 \\ -c_1 A_{20}^{(0)} & 0 & 1 & 0 & 0 \\ -c_1 A_{30}^{(0)} & 0 & 0 & 1 & 0 \\ -c_1 A_{40}^{(0)} & 0 & 0 & 0 & 1 \end{bmatrix}, \tag{5.15}$$

and it is straightforward that $\det(B_0) = 1 - c_1 A_{00}^{(0)}$. According to the first equation of System (5.9),

$$\det(B_0) = 1 - c_1 \left(\frac{2^{4j}}{72 b_1} + 2^{6j} \frac{b_0}{288 b 1^2} \right). \tag{5.16}$$

It then implies that for any $j \in \mathbb{Z}$, B_0 is invertible (and therefore the weights associated with the penalized Lagrange scheme exist) if $c_1 \neq \frac{1}{\frac{2^{4j}}{72 b_1} + 2^{6j} \frac{b_0}{288 b 1^2}}$.

- Expression of the weights:

Introducing B_0, it comes:

$$\Lambda^{(1)} = B_0^{-1} A_0^{-1} f.$$

Exploiting Proposition 5.5.1 and (5.15), the previous equation leads to (5.13) and (5.14). ∎

Proposition 5.6.3
For any $j \in \mathbb{Z}$ and any $c_1 \in D_j$, let us denote $D_{j,c_1} = \{c_2 > 0 / c_2 \neq \frac{1}{A_{11}^{(0)} + \frac{c_1 \left(A_{01}^{(0)}\right)^2}{1 - c_1 A_{00}^{(0)}}}\}$ with $\{A_{in}^{(0)}\}_{(i,n) \in \{0,\dots,3\}^2}$ given by System (5.9). if $c_2 \in D_{j,c_1}$, then the weights associated with

the penalized Lagrange system including two non-zero penalization coefficients exist. In this case, they satisfy:

$$\begin{bmatrix} a_0^{(2)} \\ a_1^{(2)} \\ a_2^{(2)} \\ a_3^{(2)} \end{bmatrix} = \begin{bmatrix} a_0^{(1)} + \frac{c_2 A_{01}^{(1)}}{1-c_2 A_{11}^{(1)}} a_1^{(1)} \\ \frac{1}{1-c_2 A_{11}^{(1)}} a_1^{(1)} \\ a_2^{(1)} + \frac{c_2 A_{21}^{(1)}}{1-c_2 A_{11}^{(1)}} a_1^{(1)} \\ a_3^{(1)} + \frac{c_2 A_{31}^{(1)}}{1-c_2 A_{11}^{(1)}} a_1^{(1)} \end{bmatrix}, \tag{5.17}$$

where $\{a_i^{(0)}\}_{i=0,\dots,3}$ *is provided by (5.13) or (5.14). Moreover,* $\{A_{in}^{(1)}\}_{(i,n)\in\{0,\dots,3\}^2}$ *satisfies:*

$$\begin{cases} A_{0n}^{(1)} = \frac{A_{0n}^{(0)}}{1-c_1 A_{00}^{(0)}} \quad \textit{for } n \in \{0,1,2,3\} \\ A_{in}^{(1)} = A_{in}^{(0)} + \frac{c_1 A_{i0}^{(0)} A_{0n}^{(0)}}{1-c_1 A_{00}^{(0)}} \quad \textit{for } i \in \{1,2,3\} \textit{ and } n \in \{0,1,2,3\} \end{cases} \tag{5.18}$$

Proof:

The proof is similar to the previous one taking into account that A_1 is invertible (Proposition 5.6.2). More precisely, splitting A_2 as $A_2 = A_1 + \tilde{A}_2$, the invertibility of A_2 is connected to the invertibility of $B_1 = (I + A_1^{-1}\tilde{A}_2)$. According to the previous proof, $A_1^{-1} = B_0^{-1}A_0^{-1}$ with B_0 given by (5.15). It is then straightforward that $\{A_{in}^{(1)}\}_{(i,n)\in\{0,\dots,3\}^2}$ satisfies (5.18). Since B_1 can be written:

$$B_1 = \begin{bmatrix} 1 & -c_2 A_{01}^{(1)} & 0 & 0 & 0 \\ 0 & 1-c_2 A_{11}^{(1)} & 0 & 0 & 0 \\ 0 & -c_2 A_{21}^{(1)} & 1 & 0 & 0 \\ 0 & -c_2 A_{31}^{(1)} & 0 & 1 & 0 \\ 0 & -c_2 A_{41}^{(1)} & 0 & 0 & 1 \end{bmatrix}, \tag{5.19}$$

one can deduce that $\det(B_1) = 1 - c_2 A_{11}^{(1)}$. It then comes out that for any $j \in \mathbb{Z}$ and any $c_1 \in \mathbb{R}^+ \backslash D_j$, B_1 is invertible (and therefore the weights associated with the penalized

Lagrange scheme exist) if $c_2 \neq \frac{1}{A_{11}^{(0)}+\frac{c_1\left(A_{01}^{(0)}\right)^2}{1-c_1A_{00}^{(0)}}}$.

Similarly to the proof of Proposition 5.6.2, since $\Lambda^{(2)} = B_1^{-1}A_1^{-1}f$, (5.13), (5.14) and (5.19) leads to (5.17).

■

Proposition 5.6.4

For any $j \in \mathbb{Z}$ and any $(c_1, c_2) \in D_j \times D_{j,c_1}$, let us denote $D_{j,c_1,c_2} = \{c_3 > 0 / c_3 \neq \frac{1}{A_{22}^{(1)}+\frac{c_2\left(A_{12}^{(1)}\right)^2}{1-c_2A_{11}^{(1)}}}\}$ with $\{A_{in}^{(1)}\}_{(i,n)\in\{0,\dots,3\}^2}$ provided by System (5.18). If $c_3 \in D_{j,c_1,c_2}$, then the weights associated with the penalized Lagrange system including three non-zero penalization coefficients exists. In this case, they satisfy:

$$\begin{bmatrix} a_0^{(3)} \\ a_1^{(3)} \\ a_2^{(3)} \\ a_3^{(3)} \end{bmatrix} = \begin{bmatrix} a_0^{(2)} + \frac{c_3A_{02}^{(2)}}{1-c_3A_{22}^{(2)}}a_2^{(2)} \\ a_1^{(2)} + \frac{c_3A_{12}^{(2)}}{1-c_3A_{22}^{(2)}}a_2^{(2)} \\ \frac{1}{1-c_3A_{22}^{(2)}}a_2^{(2)} \\ a_3^{(2)} + \frac{c_3A_{32}^{(2)}}{1-c_3A_{22}^{(2)}}a_2^{(2)} \end{bmatrix}, \tag{5.20}$$

where $\{a_i^{(2)}\}_{i=0,\dots,3}$ is given by (5.17). Moreover, $\{A_{in}^{(2)}\}_{(i,n)\in\{0,\dots,3\}^2}$ satisfies:

$$\begin{cases} A_{1n}^{(2)} = \frac{A_{1n}^{(1)}}{1-c_2A_{11}^{(1)}}, \quad \text{for } n \in \{0,1,2,3\}, \\ A_{in}^{(2)} = A_{in}^{(1)} + \frac{c_2A_{i1}^{(1)}A_{1n}^{(1)}}{1-c_2A_{11}^{(1)}}, \quad \text{for } i \in \{0,2,3\} \text{ and } n \in \{0,1,2,3\}. \end{cases} \tag{5.21}$$

Proof:

The proof is similar to the two previous ones. Writing $A_3 = A_2 + \tilde{A}_3$, we want to show that $\det(B_2) \neq 0$ with $B_2 = (I + A_2^{-1}\tilde{A}_3)$. This can be achieved following the same track replacing (5.19) by

$$B_2 = \begin{bmatrix} 1 & 0 & -c_3A_{02}^{(2)} & 0 & 0 \\ 0 & 1 & -c_3A_{12}^{(2)} & 0 & 0 \\ 0 & 0 & 1-c_3A_{22}^{(2)} & 0 & 0 \\ 0 & 0 & -c_3A_{32}^{(2)} & 1 & 0 \\ 0 & 0 & -c_3A_{42}^{(2)} & 0 & 1 \end{bmatrix}.$$

Since $\det(B_2) = 1 - c_3A_{22}^{(2)}$, the invertibility is ensured as soon as $c_3 \neq \frac{1}{A_{22}^{(1)} + \frac{c_2\left(A_{12}^{(1)}\right)^2}{1-c_2A_{11}^{(1)}}}$. Then, keeping in mind that the weights are the four first components of $\Lambda^{(3)} = B_2^{-1}A_2^{-1}f$, Expression (5.20) is straightforward.

■

We also get this last proposition:

Proposition 5.6.5

For any $j \in \mathbb{Z}$ and any $(c_1, c_2, c_3) \in D_j \times D_{j,c_1} \times D_{j,c_1,c_2}$, let us denote $D_{j,c_1,c_2,c_3} = \{c_4 > 0 / c_4 \neq \frac{1}{A_{33}^{(2)} + \frac{c_2\left(A_{23}^{(2)}\right)^2}{1-c_2A_{22}^{(2)}}}\}$ with $\{A_{in}^{(2)}\}_{(i,n)\in\{0,\dots,3\}^2}$ provided by System (5.21). If $c_4 \in D_{j,c_1,c_2,c_3}$, then the weights associated with the penalized Lagrange system including four non-zero penalization coefficients exist. In this case, they satisfy:

$$\begin{bmatrix} a_0^{(4)} \\ a_1^{(4)} \\ a_2^{(4)} \\ a_3^{(4)} \end{bmatrix} = \begin{bmatrix} a_0^{(3)} + \frac{c_4A_{03}^{(3)}}{1-c_4A_{33}^{(3)}}a_3^{(3)} \\ a_1^{(3)} + \frac{c_4A_{13}^{(3)}}{1-c_4A_{33}^{(3)}}a_3^{(3)} \\ a_2^{(3)} + \frac{c_4A_{23}^{(3)}}{1-c_4A_{33}^{(3)}}a_3^{(3)} \\ \frac{1}{1-c_4A_{33}^{(3)}}a_3^{(3)} \end{bmatrix}, \tag{5.22}$$

where $\{a_i^{(3)}\}_{i=0,\dots,3}$ is given by (5.20). Moreover, $\{A_{in}^{(3)}\}_{(i,n)\in\{0,\dots,3\}^2}$ satisfies:

$$\begin{cases} A_{2n}^{(3)} = \frac{A_{2n}^{(2)}}{1-c_3A_{22}^{(2)}}, \quad \textit{for } n \in \{0,1,2,3\} \\ A_{in}^{(3)} = A_{in}^{(2)} + \frac{c_3A_{i2}^{(2)}A_{2n}^{(2)}}{1-c_3A_{22}^{(2)}}, \quad \textit{for } i \in \{0,1,3\} \textit{ and } n \in \{0,1,2,3\} \end{cases}. \tag{5.23}$$

Remarque 5.6.1
Propositions 5.6.2 to 5.6.5 provide sufficient conditions for the existence of the weights in the four configurations of the penalization vector. Therefore, their union is a necessary and sufficient condition for the simultaneous existence of the weights in these cases. This situation is required in Section 5.7.

5.6.2 Asymptotical behavior of the weights

Propositions 5.6.2 to 5.6.5 allow to quantify the expression of the weights for any j and any $\{c_i\}_{i\in\{1,\dots,4\}}$. Therefore, in this section, they are exploited to derive their asymptotical behavior with respect to the scale and to the penalization constants. The first result will be useful for the convergence analysis of Section 5.7 while the second is important in practice to choose the values of the penalization vector.

Asymptotical behavior with respect to the scale

The following proposition holds:

Proposition 5.6.6
For any $(c_1, c_2, c_3, c_4)) \in (\mathbb{R}^+)^4$, there exists $j^* > 0$ such that for all $j \geq j^*$, the weights associated with the penalized Lagrange system exists. Moreover, when $j \to +\infty$ their limit are the following asymptotic weights:

- *One non-zero penalization coefficient:*
  - *if $k = 2\alpha$:* $\left(a_0^{(1)}, a_1^{(1)}, a_2^{(1)}, a_3^{(1)}\right) = (0, 1, 0, 0)$,
  - *if $k = 2\alpha + 1$:* $\left(a_0^{(1)}, a_1^{(1)}, a_2^{(1)}, a_3^{(1)}\right) \to_{j\to+\infty} \left(0, L_{-1}^{1,2}(-\frac{1}{2}), L_0^{1,2}(-\frac{1}{2}), L_1^{1,2}(-\frac{1}{2})\right)$.
- *Two non-zero penalization coefficients:*
  - *if $k = 2\alpha$:* $\left(a_0^{(2)}, a_1^{(2)}, a_2^{(2)}, a_3^{(2)}\right) \to_{j\to+\infty} \left(0, 0, L_0^{0,2}(-1), L_1^{0,2}(-1)\right)$,
  - *if $k = 2\alpha + 1$:* $\left(a_0^{(2)}, a_1^{(2)}, a_2^{(2)}, a_3^{(2)}\right) \to_{j\to+\infty} \left(0, 0, L_0^{0,2}(-\frac{1}{2}), L_1^{0,2}(-\frac{1}{2})\right)$.
- *Three non-zero penalization coefficients: if $k \in \{2\alpha, 2\alpha + 1\}$:*
  $\left(a_0^{(3)}, a_1^{(3)}, a_2^{(3)}, a_3^{(3)}\right) \to_{j\to+\infty} (0, 0, 0, 1)$.
- *Four non-zero penalization coefficients: if $k \in \{2\alpha, 2\alpha + 1\}$:*
  $\left(a_0^{(4)}, a_1^{(4)}, a_2^{(4)}, a_3^{(4)}\right) \to_{j\to+\infty} \left(\frac{\Pi_{i=1, i\neq m}^4 c_i}{\sum_{n=1}^4 \Pi_{i=1, i\neq n}^4 c_i}\right)_{1\leq m\leq 4}$

Proof:

The proofs for the existence as well as for the behavior of the weights when introducing one, two and three non-zero penalization coefficients are based on the asymptotical expansion of $\{A_{in}^{(m)}\}_{(m,i,n)\in\{1,2\}\times\{0,\dots,3\}^2}$ that can be obtained by combining (5.9) with (5.18) and (5.21). For four non-zero penalization coefficients, we use that the limit of A_4 is invertible. Therefore, for sake of simplicity, we focus in the sequel on the cases of one and four non-zero penalization coefficient(s). The interested reader can find the full proof for two and three non-zero penalization coefficients in the Annex.

- One non-zero penalization coefficient:

From (5.16), it is straightforward that for any $c_1 \in I\!R^+$, $\det(B_0) \sim_{j\to+\infty} -2^{6j} c_1 \frac{b_0}{288 b_1^2}$. Therefore, for large enough j, B_0 is invertible and the weights exists.

Moreover, according to (5.9), we get:

$$\begin{cases} A_{10}^{(0)} &= -\frac{1}{16b_1}2^{4j} - \frac{b_0}{96b_1^2}2^{6j}, \\ A_{20}^{(0)} &= \frac{1}{24b_1}2^{4j} + \frac{b_0}{96b_1^2}2^{6j}, \\ A_{30}^{(0)} &= \frac{1}{144b_1}2^{4j} - \frac{b_0}{288b_1^2}2^{6j}. \end{cases} \tag{5.24}$$

Plugging the previous expressions in (5.14) leads to $\lim_{j\to+\infty}\left(a_0^{(1)}, a_1^{(1)}, a_2^{(1)}, a_3^{(1)}\right) = \left(0, \frac{3}{8}, \frac{3}{4}, -\frac{1}{8}\right)$, which is the expected expression when $k = 2\alpha + 1$.

- Four non-zero penalization coefficients:

Coming back to the linear equation (5.3), let us first notice that $\lim_{j\to+\infty} A_4 = G$ and $\lim_{j\to+\infty} f = g$ with

$$G = \begin{bmatrix} -c_1 & 0 & 0 & 0 & 1 \\ 0 & -c_2 & 0 & 0 & 1 \\ 0 & 0 & -c_3 & 0 & 1 \\ 0 & 0 & 0 & -c_4 & 1 \\ 1 & 1 & 1 & 1 & 0 \end{bmatrix} \text{ and } g = (0,0,0,0,1)'.$$

Since G is invertible, it comes $\lim_{j\to+\infty}\Lambda^{(4)} = G^{-1}g$ ensuring that the weights exist. One can easily verify that the unique solution of $GU = g$ is $\forall m \in \{1,\dots,4\}$, $U_m = \frac{\Pi_{i=1,i\neq m}^{4} c_i}{\sum_{n=1}^{4}\Pi_{i=1,i\neq n}^{4} c_i}$. That concludes the proof.

■

Note that by symmetry, the previous proposition also provides the asymptotical behavior of the coefficients when the penalization vectors are of types $(0, c_2, c_3, c_4)$, $(0, 0, c_3, c_4)$ and $(0, 0, 0, c_4)$.

The last limit stated by Proposition 5.6.6 provides an important result for practical issue. More precisely, for linear subdivision schemes, the variations of sign of the coefficients in the mask are responsible for the oscillations of the limit functions and, as a consequence, of the oscillations of the reconstructed data in the vicinity of strong gradients (Gibbs phenomenon). The constant sign of the asymptotic weights connected to the four non-zero penalization coefficient scheme implies that, to the limit, the corresponding Lagrange scheme does not suffer from the Gibbs oscillations. We refer to Section 5.8 for an example of this property (Figure 5.6, bottom, right).

Asymptotical behavior with respect to the penalization constants

We now focus on the situation encountered when the penalization vector satisfies $c_i = c, 1 \leq i \leq m$ ($m \in \{1,\dots,4\}$) and study the limit behavior of the weights when c goes to infinity.

From Expressions (5.14) to (5.22), the asymptotical weights depend on $\{A_{nm}^{(m)}\}_{(m,n)\in\{0,\dots,3\}^2}$ and therefore possibly on j. As a result, for a fully exhaustive description of the limits, many configurations have to be taken into account according to the position and the number of zero coefficients in the previous sequence. For the sake of simplicity, in the next proposition, we focus on the case $A_{nm}^{(m)} \neq 0$, $\forall(m,n) \in \{0,\dots,3\}^2$. This is not restrictive to keep the generality of the results since the subset of scales $I_{nm}^{(m)} = \{j \in \mathbb{N}^+ / A_{nm}^{(m)} = 0\}$ is finite. Mimicking what has been done when $j \to +\infty$ and introducing $J^{(m)} = \cup_{n=0}^{3} I_{nm}^{(m)}$, we have:

Proposition 5.6.7

For any $j \in \mathbb{N}^+ \setminus \cup_{m=0}^{3} J^{(m)}$ there exists $c^\star$ such that for all $c \geq c^\star$, the weights associated with the penalized Lagrange system exists. Moreover,when $c \to +\infty$ their limit are the following asymptotic weights, :

- *One non-zero penalization coefficient:*
  - *if* $k = 2\alpha$*:* $\left(a_0^{(1)}, a_1^{(1)}, a_2^{(1)}, a_3^{(1)}\right) = (0, 1, 0, 0)$,
  - *if* $k = 2\alpha + 1$*:* $\left(a_0^{(1)}, a_1^{(1)}, a_2^{(1)}, a_3^{(1)}\right) \to_{c\to+\infty}$
    $\left(0, \frac{9}{16} - \frac{3b_0 2^{2j}+18b_1}{16b_0 2^{2j}+64b_1}, \frac{9}{16} + \frac{3b_0 2^{2j}+12b_1}{16b_0 2^{2j}+64b_1}, -\frac{1}{16} + \frac{-b_0 2^{2j}+2b_1}{16b_0 2^{2j}+64b_1}\right)$.
- *Two non-zero penalization coefficients:*
  - *if* $k = 2\alpha$*:* $\left(a_0^{(2)}, a_1^{(2)}, a_2^{(2)}, a_3^{(2)}\right) \to_{c\to+\infty} \left(0, 0, \frac{2b_0 2^{2j}+8b_1}{b_0 2^{2j}+b_1}, -\frac{b_0 2^{2j}+7b_1}{b_0 2^{2j}+b_1}\right)$,
  - *if* $k = 2\alpha + 1$*:* $\left(a_0^{(2)}, a_1^{(2)}, a_2^{(2)}, a_3^{(2)}\right) \to_{c\to+\infty}$
    $\left(0, 0, \lim_{c\to+\infty} a_2^{(1)} + \frac{2b_0 2^{2j}+8b_1}{b_0 2^{2j}+b_1} \lim_{c\to+\infty} a_1^{(1)}, \lim_{c\to+\infty} a_3^{(1)} - \frac{b_0 2^{2j}+7b_1}{b_0 2^{2j}+b_1} \lim_{c\to+\infty} a_1^{(1)}\right)$.
- *Three non-zero penalization coefficients: if* $k \in \{2\alpha, 2\alpha + 1\}$*:*
  $\left(a_0^{(3)}, a_1^{(3)}, a_2^{(3)}, a_3^{(3)}\right) \to_{c\to+\infty} (0, 0, 0, 1)$.
- *Four non-zero penalization coefficients: if* $k \in \{2\alpha, 2\alpha + 1\}$*:*
  $\left(a_0^{(4)}, a_1^{(4)}, a_2^{(4)}, a_3^{(4)}\right) \to_{c\to+\infty} (\frac{1}{4}, \frac{1}{4}, \frac{1}{4}, \frac{1}{4})$.

Proof:

The asymptotical weights are again based on the asymptotical expansion of $\{A_{in}^{(m)}\}_{(m,i,n)\in\{1,\dots,3\}\times\{0,\dots,3\}^2}$ that can be obtained by combining (5.9) with (5.18), (5.21) and (5.23). For the sake of simplicity, we focus on the cases of one penalization coefficient.

From (5.16), it is straightforward that for any $j \in I\!N^+ \setminus \cup_{m=0}^3 J^{(m)}$, $\det(B_0) \sim_{c\to+\infty} -c(\frac{2^{4j}}{72b_1} + 2^{6j}\frac{b_0}{288b1^2})$. Therefore, for large enough c, B_0 is invertible and the weights exists.

Moreover, plugging the value of $A_{10}^{(0)}, A_{20}^{(0)}, A_{30}^{(0)}$ given by (5.24) into Expression (5.14), it comes out

$$\lim_{c\to+\infty} \left(a_0^{(1)}, a_1^{(1)}, a_2^{(1)}, a_3^{(1)}\right) = \left(0, \frac{9}{16} - \frac{3b_0 2^{2j} + 18b_1}{16b_0 2^{2j} + 64b_1}, \frac{9}{16} + \frac{3b_0 2^{2j} + 12b_1}{16b_0 2^{2j} + 64b_1}, -\frac{1}{16} + \frac{-b_0 2^{2j} + 2b_1}{16b_0 2^{2j} + 64b_1}\right),$$

which is the announced expression when $k = 2\alpha + 1$.

The derivation for two, three and four non-zero penalization coefficients can be worked out following Expressions (5.17), (5.20) and (5.22). ∎

5.6.3 Numerical study

In this numerical study, the polynomial P_j is defined by $P_j(x) = 100 * 2^{-2j}x^2 - 2^{-4j}x^4$. Moreover, we still consider a penalization vector characterized by a single coefficient c which is our assumption in Sections 5.7 and 5.8.

Critical values of the penalization constant

Let us first focus on the critical values of c provided by Propositions 5.6.2 to 5.6.5 that have to be avoided in order to ensure the existence of the weights associated with the 4 penalized schemes. Table 5.1 gives their numerical values for $j \leq 2$ when they are positive.

j	$(c,0,0,0)$	$(c,c,0,0)$	$(c,c,c,0)$	(c,c,c,c)
0	3	0.31	-	0.16
1	$4.5e-2$	$4.6e-3$	-	$2.3e-3$
2	$7e-4$	$7e-5$	-	$3.5e-5$

Table 5.1: Critical values of c. The symbol "-" means that there is no positive value.

As expected, the critical values decrease with respect to the scale. Therefore, when $j \geq 1$, the weights associated with the 4 penalized schemes always exist when $c \in \{0\} \cup [1, \infty[$. This result will be used in Section 5.8.

Behavior of the weights

We numerically investigate the behaviors of the weights with respect to j and c. This study is restricted to the case of a penalization vector with 4 non-zero coefficients that is mainly involved in the zone-dependent subdivision scheme constructed in Section 5.7.

Figure 5.1 displays the weights behaviors from $j = 0$ to $j = 10$ when $c = 2$.

As expected from Proposition 5.6.6, the weights for large enough values of j converge to $\left(\frac{1}{4}, \frac{1}{4}, \frac{1}{4}, \frac{1}{4}\right)$; moreover, they become of constant sign for $j \geq 2$.

Figure 5.2 displays the evolution of the weights from $c = 0$ to $c = 100$ when $j = 0$. In the two plots, the weights slowly move from the interpolatory Lagrange weights corresponding to $c = 0$ towards the asymptotical values for large c. Note that the asymptotical

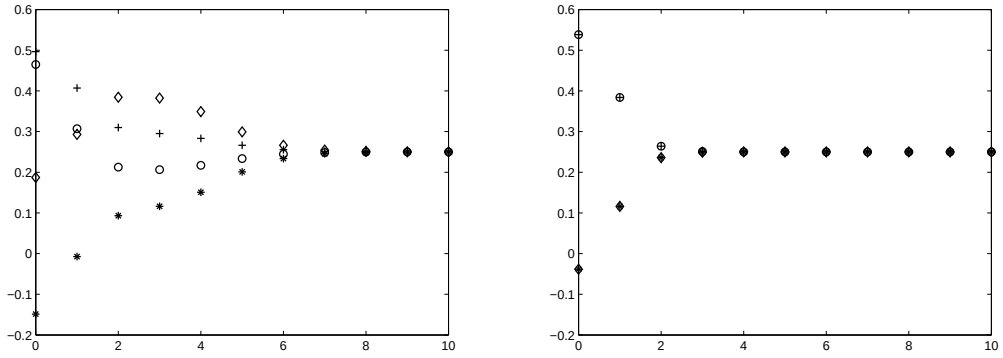

Figure 5.1: Behavior of the weights with respect to j for the prediction of f_k^j ($c = 2$). Left, $k = 2\alpha$, Right, $k = 2\alpha + 1$. $'\diamondsuit'$ represents $a_0^{(4)}$, $'+'$ represents $a_1^{(4)}$, $'o'$ represents $a_2^{(4)}$ and $'*'$ represents $a_3^{(4)}$.

behavior is not yet reached when $c = 100$. Moreover, it appears that the weights become non-negative for $c \geq 38$, resp $c \geq 8$ which is important to keep in mind to reduce the Gibbs phenomenon.

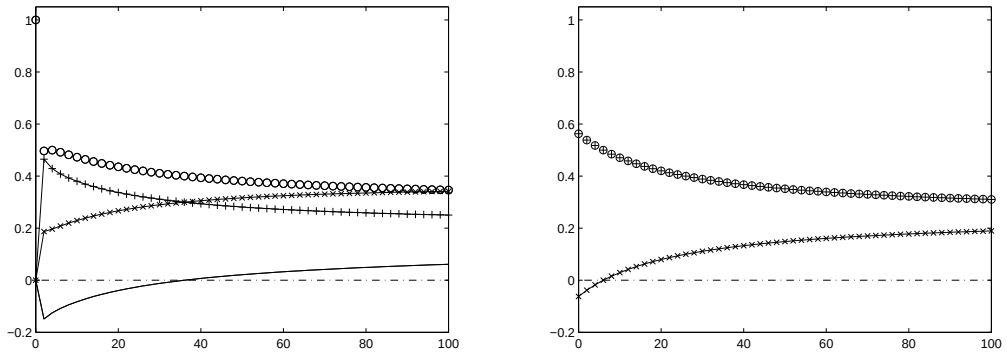

Figure 5.2: Behavior of the weights with respect to c for the prediction of f_k^j ($j = 0$). Left, $k = 2\alpha$, right, $k = 2\alpha + 1$. $'\times'$ represents $a_0^{(4)}$, $'o'$ represents $a_1^{(4)}$, $'+'$ represents $a_2^{(4)}$ and $'-'$ represents $a_3^{(4)}$.

Table 5.2 deals with the asymptotical behavior of the weights. More precisely, it exhibits for each scale the value of c required to obtain the limit $\left(\frac{1}{4}, \frac{1}{4}, \frac{1}{4}, \frac{1}{4}\right)$ up to a l_2-error bounded by 10^{-3}. On one hand it shows that for large j ($j \geq 4$) the weights reach their asymptotical values for very small c. On the other hand, it points out that

for $0 \leq j \leq 3$, there exists a large range of values of c where the weights move from the interpolatory Lagrange weights to the asymptotical ones.

	j=0	j=1	j=2	j=3	j=4	j=5	j=6
c	3726	232.9	14.5	$9.1e-1$	$5.7e-2$	$3.5e-3$	$2.2e-4$

Table 5.2: Inferior bound of c to reach the asymptotical weights up to a l_2-error of 10^{-3}.

5.7 Zone-dependent penalized Lagrange subdivision scheme

The previous penalized Lagrange prediction is here coupled with a zone-dependent strategy in order to derive a new type of subdivision schemes improving the reconstruction of locally non-regular or noisy data. Its definition as well as its convergence analysis are fully specified in what follows.

5.7.1 Construction of the scheme

The scheme is based on the 4-point Lagrange interpolatory scheme associated with a penalization function depending on the position. More precisely:

Definition 5.7.1
The zone-dependent strategy on the real line $\mathbb{R}$ is characterized by:

- *A partition of $\mathbb{R}$ in p zones: $\mathbb{R} = \cup_{0 \leq i \leq p-1} I_i$ where $I_i = [y_i, y_{i+1}]$ with $y_0 = -\infty, y_p = +\infty$ and, for $1 \leq i \leq p-1, y_i < y_{i+1}$.*
- *A penalization function, $\mathcal{P}$, defined piecewise on each interval I_i.*

For each position ($2\alpha 2^{-(j+1)}$ or $(2\alpha+1)2^{-(j+1)}$), the linear system that defines the weights to be used for the prediction is of type (5.3) with a left hand side matrix A_m given by (5.12) and $\mathcal{C} = (\mathcal{P}((\alpha-1)2^{-j}), \mathcal{P}(\alpha 2^{-j}), \mathcal{P}((\alpha+1)2^{-j}), \mathcal{P}((\alpha+2)2^{-j}))$.

For the sake of clarity and without loss of generality, we focus in the remaining of this section on three zones. The penalization function is piecewise constant with a non-zero value, c, only in the interval I_1 (Figure 5.3).

The reconstruction therefore relies on three different kinds of local predictions based on

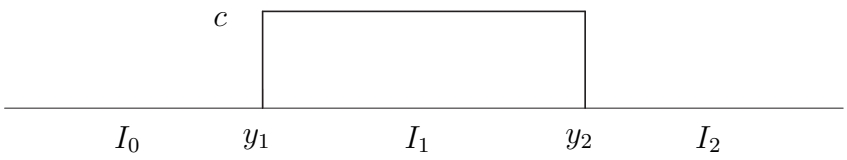

Figure 5.3: Penalization function for the 3-zone-dependent scheme

- an interpolatory Lagrange subdivision scheme in the interior[3] of Zones I_0 and I_2,
- a penalized Lagrange subdivision scheme with four non-zero penalization coefficients in the interior of I_1,
- subdivision schemes mixing non-zero penalization vectors of types $(0,0,0,c)$, $(0,0,c,c)$ and $(0,c,c,c)$ in the vicinity of y_1 and of types $(c,c,c,0)$, $(c,c,0,0)$ and $(c,0,0,0)$ in the vicinity of y_2.

The resulting scheme is position-dependent and moreover non-stationary since the coefficients of the masks depend on the scale j.

5.7.2 Convergence analysis

The convergence of the coefficients of the masks towards those of masks associated with stationary schemes when j goes to infinity can be used to establish the convergence of the non-stationary scheme. This important result is recalled by the theorem below ([1])

Theorem 5.7.1
Let S be a non-stationary subdivision scheme defined by its masks $a_k^j = \{a_{k,m}^j\}_{m\in\mathbb{Z}}$, $(j,k) \in \mathbb{Z}^2$. We suppose that there exists two constants $K < K'$, independent of j and k such that $a_{k,m}^j = 0$ for $m > K'$ or $m < K$. If there exists a convergent stationary subdivision scheme SS of masks $a_k = \{a_{k,m}\}_{m\in\mathbb{Z}}$, $k \in \mathbb{Z}$, with $a_{k,m} = 0$ for $m > K'$ or $m < K$ and such that

$$\lim_{j\to+\infty} \sup_{k\in\mathbb{Z}} ||a_k^j - a_k||_\infty = 0 \ ,$$

then S is convergent.

[3] If (l,r) characterizes the stencil of the subdivision scheme, the interior of the zone I at level j is the set $I_e^j \cup I_o^j$ with $I_e^j = \{x = 2\alpha 2^{-j}$, such that $\exists l$, resp. $r+1$, points of $X_{j-1} \cap I$ on the left, resp. right, of $x\}$ and $I_o^j = \{x = (2\alpha+1)2^{-j}$, such that $\exists l+1$, resp. $r+1$, points of $X_{j-1} \cap I$ on the left, resp. right, of $x\}$

Since the asymptotical masks associated with the penalized Lagrange predictions involved in our zone-dependent scheme has already been identified in Section 5.6, according to Theorem 5.7.1, it is enough to study the convergence of the corresponding zone-dependent stationary subdivision scheme.

The asymptotical scheme in the interior of Zones I_0 and I_2 coincides with the classical 4-point stencil Lagrange interpolatory scheme which convergence property is well known ([19]). Therefore, we focus on the convergence in the interior of I_1 and in the vicinity of y_1 since the analysis around y_2 is similar. Moreover, for simplicity reasons, we suppose that $y_1 = k_j 2^{-j}$ for large enough j.

Convergence in the interior of I_1:

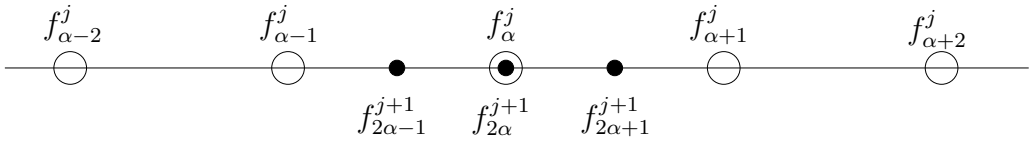

Figure 5.4: Prediction in the interior of I_1: available values at level j (o) and predicted values at the next level ($\bullet$).

Since the scheme is uniform, it is enough to focus on the differences $\delta f^{j+1}_{2\alpha-1} = f^{j+1}_{2\alpha} - f^{j+1}_{2\alpha-1}$ and $\delta f^{j+1}_{2\alpha} = f^{j+1}_{2\alpha+1} - f^{j+1}_{2\alpha}$ (Figure 5.4). According to Proposition 5.6.6, the mask associated with four non-zero penalization coefficients (c, c, c, c) is $(\frac{1}{4}, \frac{1}{4}, \frac{1}{4}, \frac{1}{4})$, therefore $f^{j+1}_{2\alpha-1} = \frac{1}{4}(f^j_{\alpha-2} + f^j_{\alpha-1} + f^j_{\alpha} + f^j_{\alpha+1})$ and $f^{j+1}_{2\alpha+1} = f^{j+1}_{2\alpha} = \frac{1}{4}(f^j_{\alpha-1} + f^j_{\alpha} + f^j_{\alpha+1} + f^j_{\alpha+2})$. It comes that:

$$\begin{cases} \delta f^{j+1}_{2\alpha-1} = \frac{1}{4} \times [(f^j_{\alpha+2} - f^j_{\alpha+1}) + (f^j_{\alpha+1} - f^j_{\alpha}) + (f^j_{\alpha} - f^j_{\alpha-1}) + (f^j_{\alpha-1} - f^j_{\alpha-2})] \ , \\ \delta f^{j+1}_{2\alpha} = 0 \ . \end{cases}$$

As $\forall j, \alpha, \delta f^{j+1}_{2\alpha} = 0$,

- if α is even ($\alpha = 2m$), $f^j_{\alpha+1} - f^j_{\alpha} = f^j_{2m+1} - f^j_{2m} = \delta f^j_{2m} = 0$, $f^j_{\alpha-1} - f^j_{\alpha-2} = f^j_{2m-1} - f^j_{2m-2} = \delta f^j_{2m-2} = 0$. Therefore,
$$\delta f^{j+1}_{2\alpha-1} = \frac{1}{4} \times [(f^j_{\alpha+2} - f^j_{\alpha+1}) + (f^j_{\alpha} - f^j_{\alpha-1})] \ ,$$
- if α is odd ($\alpha = 2m+1$), $f^j_{\alpha+2} - f^j_{\alpha+1} = f^j_{2m+3} - f^j_{2m+2} = \delta f^j_{2m+2} = 0$, $f^j_{\alpha} - f^j_{\alpha-1} = f^j_{2m+1} - f^j_{2m} = \delta f^j_{2m} = 0$. Therefore,
$$\delta f^{j+1}_{2\alpha-1} = \frac{1}{4} \times [(f^j_{\alpha+1} - f^j_{\alpha}) + (f^j_{\alpha-1} - f^j_{\alpha-2})] \ .$$

Since $|\frac{1}{4}| + |\frac{1}{4}| < 1$, $\delta f^{j+1}_{2\alpha-1} \to_{j\to+\infty} 0$.

Convergence at the point y_1:

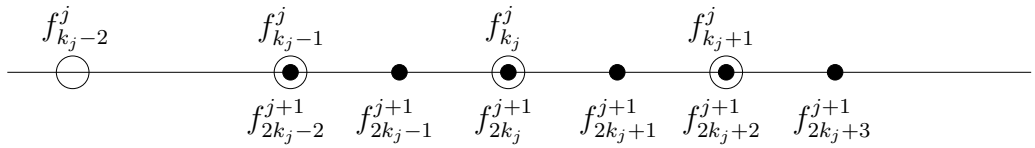

Figure 5.5: Prediction in the vicinity of $y_1 = k_j 2^{-j}$: available values at level j (o) and predicted values at the next level (•).

We first focus on the left side of y_1 and consider the differences $\delta f^{j+1}_{2k_j-2} = f^{j+1}_{2k_j-1} - f^{j+1}_{2k_j-2}$ and $\delta f^{j+1}_{2k_j-1} = f^{j+1}_{2k_j} - f^{j+1}_{2k_j-1}$ (See Figure 5.5). The computation of $f^{j+1}_{2k_j-1}$ is performed using a mask integrating one non-zero penalization coefficient $(0, 0, 0, c)$ which implies, according to Proposition 5.6.6 that $f^{j+1}_{2k_j-1} = -\frac{1}{8} f^j_{k_j-2} + \frac{3}{4} f^j_{k_j-1} + \frac{3}{8} f^j_{k_j}$. Combining $f^{j+1}_{2k_j-2} = f^j_{k_j-1}$ and $f^{j+1}_{2k_j} = f^j_{k_j}$ leads to

$$\begin{cases} \delta f^{j+1}_{2k_j-2} = \frac{1}{8}(f^j_{k_j-1} - f^j_{k_j-2}) + \frac{3}{8}(f^j_{k_j} - f^j_{k_j-1}), \\ \delta f^{j+1}_{2k_j-1} = -\frac{1}{8}(f^j_{k_j-1} - f^j_{k_j-2}) + \frac{5}{8}(f^j_{k_j} - f^j_{k_j-1}). \end{cases}$$

Since $|\frac{1}{8}| + |\frac{3}{8}| < 1$ and $|-\frac{1}{8}| + |\frac{5}{8}| < 1$, $\delta f^{j+1}_{2k_j-2} \to_{j\to+\infty} 0$ and $\delta f^{j+1}_{2k_j-1} \to_{j\to+\infty} 0$.

Considering now the right hand side of y_1, we recall that the penalization vectors associated with the reconstruction of $f^{j+1}_{2k_j+1}$, $f^{j+1}_{2k_j+2}$ and $f^{j+1}_{2k_j+3}$ are $(0, 0, c, c)$ and $(0, c, c, c)$. Therefore, according to Proposition 5.6.6, the asymptotical reconstruction formulas are $f^{j+1}_{2k_j+1} = -\frac{1}{2} f^j_{k_j-1} + \frac{3}{2} f^j_{k_j}$, $f^{j+1}_{2k_j+2} = f^{j+1}_{2k_j+3} = f^j_{k_j}$. The differences $\delta f^{j+1}_{2k_j} = f^{j+1}_{2k_j+1} - f^{j+1}_{2k_j}$, $\delta f^{j+1}_{2k_j+1} = f^{j+1}_{2k_j+2} - f^{j+1}_{2k_j+1}$ and $\delta f^{j+1}_{2k_j+2} = f^{j+1}_{2k_j+3} - f^{j+1}_{2k_j+2}$ can be written as

$$\begin{cases} \delta f^{j+1}_{2k_j} = \frac{1}{2}(f^j_{k_j} - f^j_{k_j-1}) \\ \delta f^{j+1}_{2k_j+1} = -\frac{1}{2}(f^j_{k_j} - f^j_{k_j-1}) \\ \delta f^{j+1}_{2k_j+2} = 0 \end{cases}$$

Since the scheme is convergent on the left side of y_1, $|f^j_{k_j} - f^j_{k_j-1}| \to_{j\to+\infty} 0$, therefore $\delta f^{j+1}_{2k_j} \to_{j\to+\infty} 0$ and $\delta f^{j+1}_{2k_j+1} \to_{j\to+\infty} 0$. This concludes the convergence at y_1 and also the global convergence of the scheme.

5.8 Numerical applications

This section provides several numerical tests in order to evaluate the capability of the zone-dependent penalized Lagrange subdivision scheme. A special attention is devoted to the analysis of the effect on data reconstruction of the local introduction of a penalization vector. The first test is related to the prediction of a discontinuous function while in the second one, noisy data are considered. Finally, in the last example, we focus on curve generation. Again, in all our tests the polynomial model is $P_j(x) = 100 * 2^{-2j}x^2 - 2^{-4j}x^4$.

5.8.1 Step function

In this test, we consider, as initial data ($j = 0$), the sampling of the following step function

$$f(x) = \begin{cases} 10 & x \in [1, 7.3], \\ -10 & x \in]7.3, 13] \end{cases}$$

that exhibits a discontinuity at $x = 7.3$.

According to Figure 5.3, a zone-dependent penalization function is defined, corresponding to $I_1 = [y_1, y_2]$ with $y_1 = 4$ and $y_2 = 11$. Figure 5.6 displays the reconstructed functions starting from a coarse level $j = 0$ for different values of the constant $0 \leq c \leq 100$. As expected, the convergence of the weights towards constant sign weights close to the initial discontinuity implies that the Gibbs oscillations disappear for large enough value of parameter c.

5.8.2 Locally noisy data

In real situations, available data can be perturbated by noise. If nothing is done, the presence of noise strongly deteriorates the reconstruction using linear subdivision schemes. In this example, we assume that the noisy data can be isolated in a known zone that is used to define a penalization function. More precisely, the initial data are first generated by sampling the test function $f(x) = 0.4 * \sin(\frac{x}{3})$ for $1 \leq x \leq 24$. Then a white Gaussian noise (mean 0, variance 0.4) is added in $I_1 = [y_1, y_2]$ with $y_1 = 8$ and $y_2 = 17$.

A zone-dependent penalized Lagrange subdivision scheme based on the above values of (y_1, y_2) is then applied. Figure 5.7 exhibits the reconstructed functions for different values of $0 \leq c \leq 4000$. Moreover, Table 5.3 provides the l_2-error between the reconstructed sequence at $j = 6$ and the sampling of the initial function at the same scale.

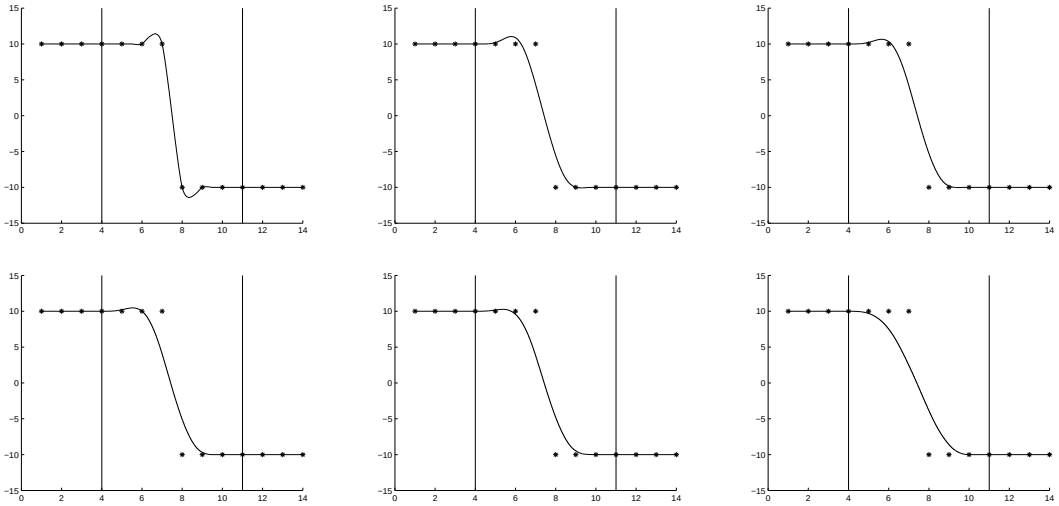

Figure 5.6: Reconstruction of a step function: $*$ is associated with the sampled points, the solid line is the reconstructed function. I_1 is limited by the two straight lines. From top to bottom and left to right, $c = 0$, $c = 2$, $c = 4$, $c = 6$, $c = 10$ and $c = 100$.

It turns out that the introduction of a penalization and its coupling with the zone-dependent strategy lead to a more robust reconstruction in presence of noise. For $c = 100$ (Figure 5.7, bottom, right), the effect of the noisy data is really damped. This strong improvement is quantified in Table 5.3 where a reduction of a factor 7 in the l_2-error between $c = 0$ and $c = 3726$ can be noticed.

	$c = 0$	$c = 1$	$c = 10$	$c = 50$	$c = 100$	$c = 3726$
l_2-err	5.6	2.9	2	1.2	1.05	0.85

Table 5.3: l_2-error between the sampling at level $j = 6$ and the reconstructed sequence for different values of c.

5.8.3 Curve generation

The zone-dependent penalized Lagrange subdivision scheme is here applied to curve generation. More precisely, we evaluate the capability of this approach in presence of noisy control points. Figure 5.8 displays an example of curve reconstruction, where some control points have been polluted by a white noise.

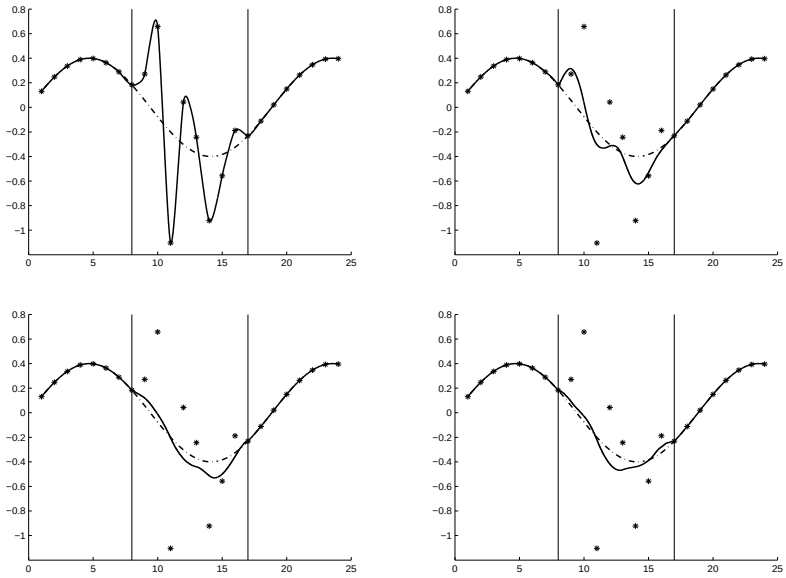

Figure 5.7: Reconstruction from noisy data with different values of c (solid line); $*$ is associated with the initial data while the dashed line represents the original function. I_1 is limited by the two straight lines. From top to bottom and left to right, $c = 0$, $c = 10$, $c = 100$ and $c = 3726$.

Again, it appears that interpolatory subdivision schemes such as Lagrange-based ones are not tailored to adapt to noisy data and leads to undesirable oscillations (Figure 5.8, left). On the contrary, since the penalized strategy allows to combine interpolatory (in the zone without noise) and non-interpolatory (in the noisy zone) schemes, the oscillations are reduced and the reconstructed curve is more satisfactory (Figure 5.8, right).

5.9 Conclusion

A new type of subdivision schemes combining interpolatory and non-interpolatory predictions has been constructed in this article. The starting point is the classical 4-point Lagrange interpolatory scheme. The main ingredient to transform this scheme in an approximating one relies on the connection to Kriging subdivision that offers a more flexible framework to mix interpolatory and non-interpolatory predictions thanks to the introduction of error variances. Plugging the determination of the weights into that framework allows to define a penalized Lagrange scheme that can be either interpolatory or

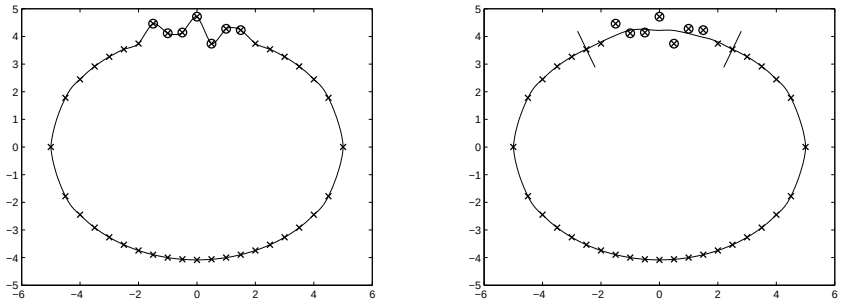

Figure 5.8: Curve generation from a set of control points (cross signs), in which several ones are perturbated by a noise (circled cross signs). I_1 is limited by the two straight lines. Left, reconstruction by a Lagrange interpolatory scheme ; right, reconstruction by our penalized Lagrange subdivision with $c = 100$.

non-interpolatory according to the choice of the penalization constants. After a full theoretical analysis, this original approach is coupled to a zone-dependent strategy in order to derive non-stationary subdivision schemes adapted to the local behavior of the data to reconstruct. The numerical applications have shown a strong improvement compared to classical Lagrange predictions when data exhibit discontinuities or are perturbated by noise.

Appendix: existence and expression of the asymptotical weights (Proof of Proposition 5.6.6)

It requires to study for large j $det(B_1) = 1 - c_2 A_{11}^{(1)}$, $det(B_2) = 1 - c_3 A_{22}^{(2)}$ and the weights given by (5.17) and (5.20).
Exploiting the symmetrical property of A_1 and A_2, it is therefore enough to derive the asymptotical behavior of the subsets $\{A_{01}^{(1)}, A_{02}^{(1)}, A_{03}^{(1)}, A_{11}^{(1)}, A_{12}^{(1)}, A_{13}^{(1)}, A_{22}^{(1)}, A_{23}^{(1)}, A_{33}^{(1)}\}$, and $\{A_{02}^{(2)}, A_{03}^{(2)}, A_{12}^{(2)}, A_{13}^{(2)}, A_{22}^{(2)}, A_{23}^{(2)}, A_{33}^{(2)}\}$.

After a technical calculus one gets

$$\begin{cases} A_{01}^{(1)} \sim_{j\to+\infty} \frac{3}{c_1}, \\ A_{02}^{(1)} \sim_{j\to+\infty} -\frac{3}{c_1}, \\ A_{03}^{(1)} \sim_{j\to+\infty} \frac{1}{c_1}, \\ A_{11}^{(1)} \sim_{j\to+\infty} \frac{1}{24b_1}2^{4j}, \\ A_{12}^{(1)} \sim_{j\to+\infty} -\frac{1}{12b_1}2^{4j}, \\ A_{13}^{(1)} \sim_{j\to+\infty} \frac{1}{24b_1}2^{4j}, \\ A_{22}^{(1)} \sim_{j\to+\infty} \frac{1}{6b_1}2^{4j}, \\ A_{23}^{(1)} \sim_{j\to+\infty} -\frac{1}{12b_1}2^{4j}, \\ A_{33}^{(1)} \sim_{j\to+\infty} \frac{1}{24b_1}2^{4j}, \end{cases}$$

and

$$\begin{cases} A_{02}^{(2)} \sim_{j\to+\infty} \frac{3}{c_1}, \\ A_{03}^{(2)} \sim_{j\to+\infty} -\frac{2}{c_1}, \\ A_{12}^{(2)} \sim_{j\to+\infty} \frac{2}{c_2}, \\ A_{13}^{(2)} \sim_{j\to+\infty} -\frac{1}{c_2}, \\ A_{22}^{(2)} \sim_{j\to+\infty} -\frac{1}{2b_0}2^{2j}, \\ A_{23}^{(2)} \sim_{j\to+\infty} \frac{1}{2b_0}2^{2j}, \\ A_{33}^{(2)} \sim_{j\to+\infty} -\frac{1}{2b_0}2^{2j}, \end{cases}$$

As a result, it is straightforward that for large enough j the determinants are non-zero, ensuring the existence of the weights. Moreover, keeping in mind the limit of the weights in the case of one non-zero penalization coefficient (Proposition 5.6.6), one can deduce that

$$lim_{j\to+\infty}\left(a_0^{(2)}, a_1^{(2)}, a_2^{(2)}, a_3^{(2)}\right)^T = \begin{cases} (0,0,2,-1)^T \text{ if } k = 2\alpha, \\ \left(0,0,\frac{3}{2},-\frac{1}{2}\right)^T \text{ if } k = 2\alpha+1, \end{cases}$$

and $lim_{j\to+\infty}\left(a_0^{(3)}, a_1^{(3)}, a_2^{(3)}, a_3^{(3)}\right)^T = (0,0,0,1)^T$ for any $k \in \{2\alpha, 2\alpha+1\}$, which are the announced results. That concludes the proof.

Conclusion and Perspectives

Conclusion

In this work, three families of new subdivision schemes have been introduced:

1. Zone-dependent Lagrange/B-spline subdivision schemes,
2. Kriging-based subdivision schemes with local error variance,
3. Penalized Lagrange subdivision schemes.

- Zone-dependent Lagrange/B-spline subdivisions schemes use classical Lagrange interpolatory subdivision schemes and B-spline approximating subdivision schemes as two main elements. A zone-dependent implementation, based on an a priori segmentation of the line is used to choose at any position and any scale the stencil involved in the prediction. Lagrange prediction is employed in the interior of zones where the data are supposed to be smooth and not perturbated while B-spline subdivision is applied to those where discontinuities or noise may be present. A special adaption of the prediction stencils at the edges of the zones is performed. This adaption involves prediction with non-centered stencil and extrapolations.

- Kriging-based subdivision schemes are derived from Kriging theory. A semi-variogram is used to define the spatial correlation of the original data. The ordinary Kriging system is constructed. Its solution provides the corresponding mask coefficients of the Kriging subdivision. Thanks to the introduction of an error variance into the system, a non-interpolatory scheme can be generated. This new approach is fully studied for a four point stencil and the convergence is established as well. A zone-dependent implementation of this scheme is then defined, following the same track as the Lagrange/B-spline subdivision scheme. Here it is the error variance that is zone dependent. As previously, adaption at the edges of the zones is performed.

- A new scheme called penalized Lagrange subdivision scheme has then been derived, borrowing many ideas from the Kriging-based schemes analysis. Since the classical Lagrange interpolatory schemes can not overcome the Gibbs phenomenon problem and since the Kriging-based subdivision schemes require large enough datasets to yield a reliable semi-variogram model, the original idea was to combine the advantages of both schemes: simplicity for Lagrange schemes and flexibility (interpolatory, non-interpolatory) for the Kriging schemes, knowing that the link between the two families appeared in the asymptotical analysis of Kriging schemes.

  The resulting scheme is a new scheme including a penalization parameter that allows to evolve smoothly from interpolatory to non interpolatory schemes. A full analysis is performed for the four points scheme. Coupling this approach with a zone dependent implementation (here it is the penalization parameter that becomes zone dependent) leads to a new family of schemes suitable for locally non smooth or noisy data.

These three new schemes and corresponding zone dependent implementation have two main similar elements in common:

- the zone-dependent implementation: for the three schemes key, parameters (type of subdivision for the first family, error variance for the second family, penalization parameter for the last family) can be locally adapted to an a priori segmentation of the data,

- switch between interpolatory and non-interpolatory schemes: The three schemes allow to switch locally between interpolatory and non-interpolatory schemes.

Thanks to these two elements, these subdivision schemes share three main advantages:

- They can significantly overcome the Gibbs phenomenon problem associated to interpolatory subdivision scheme in presence of discontinuous data.

- The zone dependent implementation is more robust than the position dependent implementation as far as the segmentation points are concerned.

- The use of approximation rather than interpolation makes these subdivision schemes attractive to handle noisy data.

Future Work

1. Kriging-based subdivision schemes with error variance as well as penalized Lagrange subdivision schemes have been fully analyzed for four points stencil. Among other reasons, numerical tests have shown that the generalization of the approach, (already performed for Kriging-based subdivision schemes without error variance) is possible. The theoretical analysis of the two families of schemes for any size of the stencil is not yet performed.

2. The multi-resolution decomposition associated to these family of non stationary schemes has not been tested. Various questions on the efficiency of these decompositions or some asymptotical results are unsolved, including for the subdivision as well as the decimation, the reproduction of polynomials of degree larger than 1.

3. In all this work, the segmentation has been considered as granted. Coupling between various schemes could be used to generate the segmentation as well as to evaluate the values of the error variance or the penalization parameter.

4. In the same vein, non linear schemes incorporating in a unique framework the segmentation and the values of the parameters (error variance or the penalization parameter) could be considered and analyzed.

5. Kriging-based and penalization Lagrange schemes have provided promising results for the reconstruction of discontinuous and noisy signals. It is now intended to extend their application to images and to evaluate how the introduction of an error variance or a penalization term can contribute to increase the efficiency of subdivision scheme in the case of real images. Moreover, despite a first attempt to the reconstruction of code response in presence of uncertainties, the use of this kind of scheme for risk analysis will require the generalization of the construction of our scheme on non-regular grid.

Bibliography

[1] J. Baccou and J. Liandrat. Kriging-based interpolatory subdivision schemes. *Appl. and Comp. Harm. Anal.*, page DOI: 10.1016/j.acha.2012.07.008, 2012.

[2] G.M. Chaikin. An algorithm for high speed curve generation. *Computer Graphics and Image Processing*, 3:346–349, 1974.

[3] N.Dyn. Subdivision schemes in computer-aided geometric design. *Advances in Numerical analysis II, Wavelets, Subdivision algorithms and Radial Basis functions*, 20(4):36–104, 1992.

[4] J. Baccou and J. Liandrat. Kriging-based subdivision schemes:application to the reconstruction of non-regular envirionmental data. *Mathematics and Computers in Simulation(MCS)*, 81(10):2033–2050, 2011.

[5] Gottlieb D. and Shu C-W. On the gibbs phenomenon and its resolution. *SIAM Rev.*, 39(4):644–668, 1997.

[6] G. Deslauriers and S. Dubuc. Symmetric iterative interpolation processes. *Constructive approximation*, 5:49–68, 1989.

[7] K. Dadourian. *'Schémas de subdivision, approximation multi-échelles non linéaires et applications*. PhD thesis, Université d'Aix-Marseille I, LATP, UMR7353, October 2008.

[8] J. Baccou and J. Liandrat. Position-dependent lagrange interpolaing multiresolutions. *Int. J. of Wavelets, Multiresol. and Inf.*, 5(4):513–539, 2005.

[9] P. Goovaerts. *Geostatistics for natural resources evaluation*. Oxford University Press, New York, 483 pp, 1997.

[10] N.A. Cressie. *Statistics for spatial data*. Wiley Series in Probability and Mathematical Statistics, New York, 900 pp, 1993.

[11] G. Matheron. The theory of regionalized variables and its applications. *Cahiers du Centre de Morphologie Mathématique*, 5, 1971.

[12] H. Wackernagel. *Multivariate geostatistics*. Springer, Berlin, 291 pp, 1998.

[13] J-P. Chiles and P. Delfiner. *Geostatistics: modelling spatial uncertainty*. Wiley, New York, 695 pp, 1999.

[14] K. Fang, R. Li, and A. Sudjianto. *Design and modeling for computer experiments*. Chapman&Hall/CRC (Univ. Michigan), 2006.

[15] S. Amat, F. Arandiga, A. Cohen, and R. Donat. Tensor product multiresolution analysis with error control for compact image representation. *Signal Processing*, 4:587–608, 2002.

[16] G. Deslauriers and S. Dubuc. Interpolation dyadique. In *Fractals, dimensions non entières et applications*, pages 44–45. Masson, Paris, 1987.

[17] X. Si, J. Baccou, and J. Liandrat. Construction and analysis of zone-dependent interpolatory/non-interpolatory stochastic subdivision schemes for non-regular data. *Lecture Notes in Computer Science*, 2012.

[18] J.P Chiles and P. Delfiner. *Geostatistics: Modeling spatial uncertainty*. Wiley (New York), 1999.

[19] N. Dyn. Subdivision schemes in computer-aided geometric design. In W.A Light, editor, *Advances in Numerical analysis II, Wavelets, Subdivision algorithms and Radial Basis functions*, pages 36–104. Clarendon Press, Oxford, 1992.

[20] A. Cohen, N. Dyn, and B. Matei. Quasilinear subdivision schemes with applications to ENO interpolation. *Appl. Comp. Harm. Anal.*, 15:89–116, 2003.

[21] J. Baccou and J. Liandrat. Position-dependent lagrange interpolating multiresolutions. *Int. J. of Wavelet, Multiresolution and Information*, 5(4):513–539, 2005.

[22] A. Cohen, I. Daubechies, and J.-C. Feauveau. Biorthogonal bases of compactly supported wavelets. *CPAM*, 45(5):485–560, Jun. 1992.

[23] Y. Meyer. *Ondelettes et Opérateurs I : Ondelettes*. Hermann, Paris, 1990.

[24] J.A. Gregory N.Dyn and D. Levin. A four-point interpolatory subdivision scheme for curve design. *Comp. Aid. Geom. Des.*, 4:257–268, 1987.

[25] J.A. Gregory N.Dyn and D. Levin. Analysis of linear binary subdivision schemes for curve design. *Constr. Appr.*, 7(2):127–148, 1991.

[26] G. Delauriers and S. Dubuc. Symmetric iterative interpolation processes. *Constructive Approximation*, 5:49–68, 1989.

[27] W. Dahmen A.S. Cavaretta and C.A. Micchelli. Stationary subdivision. *In Memoirs of the American Mathematics Society*, 93(453), 1991.

[28] M. Doblas F. Arandiga, J. Baccou and J. Liandrat. Near-lossless image compression based on a multi-directional map-dependent algorithm. *ENUMATH Conference, Santiago de Compostela*, 2005.

[29] Jean BACCOU. Analyses multiresolutions et problemes de bords: applications au traitement d'images et a la resolution numerique d'equations aux derivees partielles. *PhD thesis, Universite d'Aix Marseille I; LATP (Marseille)*, December 2004.

[30] S. Amat and J. Liandrat. On the stability of the pph nonlinear multiresolution. *Journal of Applied and Computational Harmonic Analysis*, 18(2):198–206, 2005.

[31] A. Harten. Multiresolution representation of data: a general framework. *SIAM J. Numer. Anal.*, 33(3):1205–1256, 1996.

[32] G. Deslauriers and S. Dubuc. Interpolation dyadique. *In Fractals, dimensions non entieres et applications*, pages 44–45, 1987.

[33] D.L. Donoho. Interpolating wavelet transforms. *Technical report, Department of statistics, Stanford University*, 1992.

[34] I. Daubechies. Ten lectures on wavelets. *SIAM, Philadelphia, PA*, 1992.

[35] F. Arandiga R. Donat and A. Harten. Multiresolution based on weighted averages of the hat function i: linear reconstruction techniques. *SIAM J. Sci. Comput.*, 36(1):160–203, 1999.

[36] F. Arandiga R. Donat and A. Harten. Multiresolution based on weighted averages of the hat function ii: non-linear reconstruction techniques. *SIAM J. Sci. Comput.*, 20(3):1053–1093, 1999.

[37] C.A. Miccheli and H. Prautzsch. Uniform refinement of curves. *Linear Algebra and Applications*, 114(115):841–870, 1989.

[38] S. Amat, F. Arandiga, A. Cohen, R. Donat, G. Garcia, and M. von Oehsen. Data compression with ENO schemes: a case study. *Appl. Comp. Harm. Anal.*, 11:273–288, 2001.

[39] F.Arandiga, J.Baccou, M.Doblas, and J.Liandrat. *Image compression bases on a multidimensional map dependent algorithm.* ACHA, 07.